NOTE TO USERS

Dehydration and Digestion of Magnola Metallurgie Inc. 'Prills' In a Molten Salt

Matthew Kreuh

Department of Metals and Materials Engineering

McGill University, Montréal

August 2003

A thesis submitted to McGill University

in partial fulfilment of the requirements for the degree of

Master of Engineering

Your file Votre référence
ISBN: 0-612-98539-3
Our file Notre référence
ISBN: 0-612-98539-3

ABSTRACT

The digestion (dehydration and dissolving), in a molten salt containing $MgCl_2$, of partially hydrated $MgCl_2$ in the form of 'prills' was visually observed. The 'prills' were prepared by *Magnola Metallurgie Inc.*. Pictures of the digestion are presented and two types of bubbling behaviours were observed.

It was concluded that the digestion process occurred in two steps: (1) dehydration / hydrolysis of prills in the solid state and (2) dissolution of the dehydrated products. Each step was accompanied by a distinctive bubbling behaviour as the gas products of the step were evolved.

The type of bubbling behaviour associated with the first step was termed 'Primary Bubbling' and was due to the release of the waters of hydration, hereinafter termed dehydration. The second type of bubbling behaviour observed was termed 'Secondary Bubbling' and was due to the decomposition of dissolved oxide in the molten salt according to the reaction:

$$MgOHCl_{(diss)} \rightarrow MgO_{(s)} + HCl_{(g)}$$

The solubility of the dissolved oxide was seen to be a function of temperature and $MgCl_2$ activity in the melt. Analysis of the gas evolved during Secondary Bubbling revealed a gas composition of about 51 vol.% HCl and 49 vol.% H_2O, indicating that dissolved oxide was also being chlorinated by the reaction:

$$MgOHCl_{(diss)} + HCl_{(g)} \rightarrow MgCl_{2(l)} + H_2O_{(g)}$$

Injection of Ar decomposed the dissolved oxide by offsetting the first reaction above to the left and injection of HCl chlorinated solid MgO by the reaction:

$$MgO_{(s)} + 2HCl_{(g)} \rightarrow MgCl_{2(l)} + H_2O_{(g)}$$

Surprisingly, it was found the HCl atmosphere in the freeboard of the reactor had no significant effect to suppress the hydrolysis reaction occurring during dehydration.

RÉSUMÉ

Le procédé d`ajout du $MgCl_2$ hydraté en forme de 'prills' dans du sel fusionné contenant du $MgCl_2$ a été observé. Ces 'prills' ont été fabriqués par *Magnola Métallurgie Inc.* Des images du procédé sont présentées dans cette thèse. Deux sortes de bouillonnement ont été remarqués.

Il a été conclu que le procédé est survenu en deux étapes: (1) la déshydratation des 'prills' dans leurs états solides et (2) la dissolution du produit déshydraté. Chaque étape était accompagné d`un bouillonnement propre produit par l`évolution des gaz.

Le type de bouillonnement associé avec la première étape a été nommé 'Primary Bubbling' et est causé par l`évolution de l'eau pendant la déshydratation. Le deuxième type de bouillonnement associé avec la deuxième étape a été nommé 'Secondary Bubbling' et est causé par la décomposition d`oxydes dissous dans le sel en fusion selon la réaction:

$$MgOHCl_{(diss)} \rightarrow MgO_{(s)} + HCl_{(g)}$$

La solubilité de l`oxyde dissout a été fonction de la température et de la concentration du $MgCl_2$ dans la solution liquide. L`analyse de l`évolution du gaz pendant le 'Secondary Bubbling' donne une composition de 51 vol.% HCl et 49 vol.% $H_2O$, indiquant que l`oxyde dissout se transforme aussi par la reaction:

$$MgOHCl_{(diss)} + HCl_{(g)} \rightarrow MgCl_{2(l)} + H_2O_{(g)}$$

L`injection d`Ar a décomposé l`oxyde dissout en poussant la première réaction présentée vers la gauche. L`injection de HCl a transformé le MgO solide par la réaction:

$$MgO_{(s)} + 2HCl_{(g)} \rightarrow MgCl_{2(l)} + H_2O_{(g)}$$

Etonnamment, le HCl ambiant, contenu dans le réacteur, n'a eu aucun impact significatif sur la formation d'oxydes durant la première étape.

ACKNOWLEDGMENTS

I owe my supervisor, Professor Ralph Harris, my prevalent gratefulness for accepting me as an undergraduate research assistant where interest in the project led me to pursue my Master's degree. His strong communication skills have helped me grow into a professional. Needless to say, his financial support and technical expertise throughout my degree was very much appreciated.

A special thanks to Ka Wing Ng, whose initial design of the experimental setup and ideas proved priceless to the work presented in this thesis.

I would also like to thank Sina Kashani Nejad for his shared knowledge and discussions. They helped me deepen my overall knowledge of the project.

The research project could not have been carried out without the financial support of Noranda and NSERC, as well as the supply of partially dehydrated $MgCl_2$ feed from Magnola Metallurgie Inc.

A special thanks to my cousins Patricia Vincent and Sébastien Dakin for helping in the translation of the abstract.

Lastly, I could never find the words to thank my parents, Adolph and Marguerite Kreuh, in a manner that they deserve. They have done everything possible to give me the education I have received.

TABLE OF CONTENTS

LIST OF FIGURES

LIST OF TABLES

NOMENCLATURE

Symbol	Description	Units	S.I. Units
A	Mole fraction in Fact*Sage*™	mole	
A	Cross-sectional area	m^2	
a_i	Activity of species i	unit-less	
a_{Mg}	Activity of magnesium	unit-less	
a_{MgCl2}	Activity of $MgCl_2$	unit-less	
a_{MgOHCl}	Activity of MgOHCl	unit-less	
C_{MgO}	Concentration of MgO	ppm	$mole/m^3$
C^i_{MgO}	Initial concentration of MgO	ppm	$mole/m^3$
E	Electrolytic reduction potential	V	
E^o	Standard electrolytic reduction potential	V	
e^o	Standard half cell reduction potential	V	
ε	Interaction parameter	unit-less	
F	Faraday's constant (96485 c/equiv.)	c / equivalence	
$\Delta G^o_{(i)}$	Standard free energy of formation for reaction i	J / mole	
$\Delta H^o_{(i)}$	Standard enthalpy of formation for reaction i	J / mole	
k_n	Specific reaction rate constant	s^{-1}	
M_i	Moles of species i	mole	
MW_i	Molecular weight of species i	g / mole	
N	Normality	equivalence / l	

n	Number of moles	mole	
Q	Volumetric flowrate	m^3 / s	
R	Ideal gas constant (8.314 J/mol·K)	J / (mole·K)	
T	Temperature	°C	K
t	Time	minute	second
P	Pressure	atm	Pa
P_i	Partial pressure of species i	atm	Pa
ρ_i	Density of species i	g / l	kg / m_3
X_i	Mole fraction	mole	
X_{MgCl2}	Mole fraction of $MgCl_2$	mole	
v	Velocity	m / s	
$\gamma_{(i)}$	Activity coefficient of species i	$mole^{-1}$	
$\gamma^{o}_{(i)}$	Activity coefficient of species i at infinite dilution	$mole^{-1}$	

1 THE THESIS

The preparation of anhydrous $MgCl_2$ is difficult due to the formation of oxides. These oxides are severely detrimental to the electrolysis cells in the electrolytic production of magnesium metal. Magnola Metallurgie Inc. (MMI) is an electrolytic producer of magnesium metal using a novel process to enrich the electrolyte with $MgCl_2$. In MMI's process, partially dehydrated $MgCl_2$ ($MgCl_2 \cdot xH_2O$, where x ~ 2), referred to as 'prills', is produced in a fluidized bed dryer under an HCl containing atmosphere. The prills are fed onto the surface of molten salt electrolyte in which the activity of the $MgCl_2$ is reduced and into which HCl gas is injected. The HCl has a dual function; it suppresses the formation of oxides and it chlorinates the oxides present, if any.

MMI's pilot plant studies were based on the chlorination of MgO as opposed to considering other oxides in the molten electrolyte, as it was believed that only MgO was stable at the desired operating temperature. As a consequence, the digestion of prills into the electrolyte was neither observed nor studied. Essentially, MMI's design team assumed that the partially hydrated $MgCl_2$ instantaneously dissolved into the electrolyte after flashing off its waters of hydration.

The focus of the present thesis was to study the digestion of Magnola Metallurgie Inc prills added onto the surface of molten synthetic electrolyte. Prill digestion under Ar and HCl atmospheres was performed. It was found that significant amounts of dissolved oxide was generated during digestion and entered into the electrolyte as a dissolved species. Factors determining its solubility were determined.

The thesis begins with Chapter Two, which has several components. It commences with a short discussion on the magnesium market followed by current magnesium production processes, of which the electrolytic process is discussed in greater detail. The Magnola Metallurgie Inc.'s flowsheet is described and the reasons for its novelty are explained. Information on the production and behaviour of oxides found in the literature is given.

Chapter Three of the thesis describes the methodology of the experiments as well as the experimental setup. The experimental procedure is also included. The test program was separated into three sections: 1) Observing the digestion of prills and gas injection; 2)

Explain the observed bubbling behaviour; and 3) Determine the effect of atmosphere during prill digestion.

Chapter Four of the thesis presents the experimental results with pictures and observations.

Chapter Five of the thesis presents an interpretation of the experimental results. The tests show that prill digestion produces significant amounts of dissolved oxide. Moreover, the solubility of the dissolved oxide was found to be a function of temperature and $MgCl_2$ content of the melt. Finally, it was found that the bulk atmosphere had no significant effect on the production of oxide.

Chapter Six of the thesis provides conclusions of the research.

Chapter Seven of the thesis provides the recommendations for future work.

2 LITERATURE REVIEW

2.1 Magnesium

Magnesium is the 8th most abundant element in the in the earth's crust[1]. It commonly occurs in nature in the form of silicates (talc, olivine, serpentine), carbonates (magnesite, dolomite), and hydroxide (brucite) or is present in the form of $MgCl_2$ and sulphate in seawater, underground brines, and salt deposits (carnallite, $KCl{\cdot}MgCl_2{\cdot}6H_2O$)[2]. Magnesium is the lightest structural metal, with a density of 0.65 times that of pure aluminium. Due to current lower market costs, existing consumers of magnesium, such as the automotive industry, are utilizing more and more magnesium. In addition, new consumers of magnesium are developing, as magnesium becomes an economically attractive metal.

The world primary magnesium consumption was forecasted to increase significantly in 1995, as shown in Figure 1. However, magnesium consumption in the United States has been decreasing since 1998[3] along with its competitor aluminium. The U.S. primary aluminium production decreased in 2001 due to the energy crisis in California. This greatly affected the magnesium industry as alloying with aluminium plays a major role in the consumption of magnesium[5]. Figure 2 shows the trends of aluminium and magnesium consumption in the U.S.[4,5]. The primary consumption of magnesium in the United States for 2002 was aluminium alloying and represented 46 % of total consumption. Die-casting for the automotive industry placed second with 32 %. The third most important consumption of magnesium was desulfurizing of iron and steel, which used 12 % of the produced magnesium.

There currently exist three magnesium producing plants in North America: Magcorp (Salt Lake City, Utah), Norsk Hydro (Bécancour, Québec), and Magnola Metallurgie Inc. (MMI) (Danville, Québec). MMI is indefinitely shutdown due to technical difficulties and a significant drop in magnesium price from 1.40 USD/lbs (3.08 USD/kg) to 0.85 USD/lbs (1.87 USD/kg) from 1995 to 2002[6]. The drop in price was caused by the rapid growth of magnesium production in China. China produced 5 % of the world's magnesium in 1990 and currently produces 55 % using the Pigeon process.

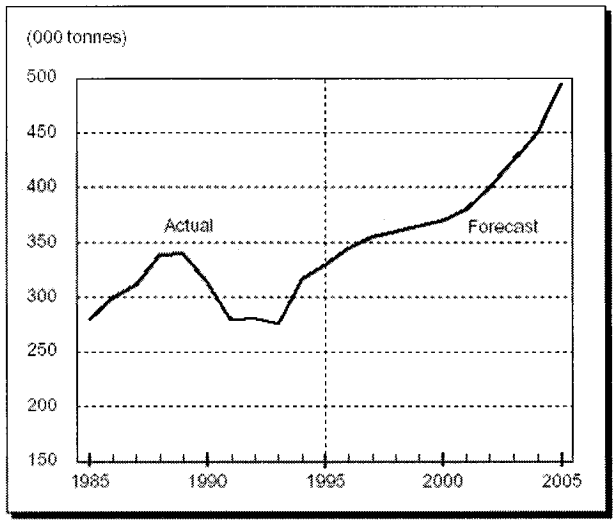

Figure 1 : Forecast in 1995 of world primary magnesium consumption.[7]

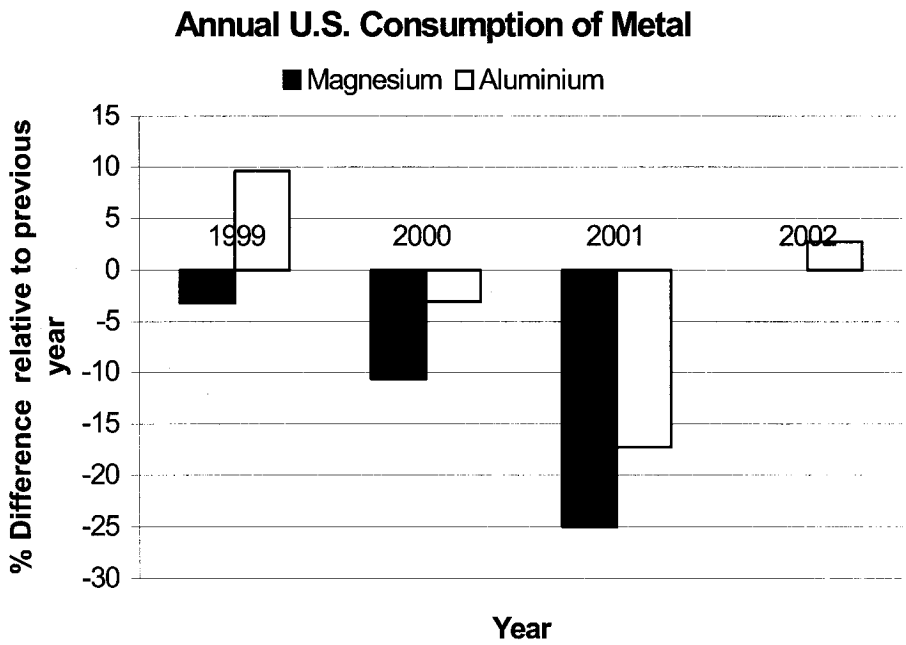

Figure 2 : The U.S. magnesium consumption compared with aluminium consumption.

Metallic magnesium is produced by thermal reduction of MgO or electrolysis of molten $MgCl_2$. The method of production depends on the raw material and location of the particular plant.

2.2 Thermal Reduction Process for the Production of Mg

The thermal reduction process uses high heat with a reducing agent to produce a magnesium vapour and a slag. The vapour is condensed and high purity magnesium metal is recovered. The thermal reduction process can be separated into three steps: preparation of the reducing agent, preparation of raw material, and thermal reduction. If the feed material is magnesite or dolomite, it must also be calcined according to Reactions (1) and (3).

$$MgCO_{3(s)} \rightarrow MgO_{(s)} + CO_{2(g)} \quad (1)$$

$$\Delta G^{o}_{(1)}\Big|^{1400\,K}_{1200\,K} = 98688 - 153T \quad (J)^{8} \quad (2)$$

$$CaCO_3{\cdot}MgCO_{3(s)} \rightarrow CaO{\cdot}MgO_{(s)} + 2CO_{2(g)} \quad (3)$$

$$\Delta G^{o}_{(3)}\Big|^{1400\,K}_{1200\,K} = 271491 - 142.48T \quad (J)^{8} \quad (4)$$

The main advantages of this process over the electrolytic process are the low capital costs and the low (Chinese) operating costs. The disadvantage is the operation is a batch process. The two types of thermal reduction can be used: carbothermic and silicothermic. The oxide Ellingham diagram indicates which reagents can be used to reduce the MgO. However, the cost of producing the reducing reagents must also be taken into consideration for the industrial production of magnesium.

Carbothermic reduction, Reaction (5), is not a commercially used process due to the formation of a two-component gas.

$$MgO_{(s)} + C_{(s)} \rightarrow CO_{(g)} + Mg_{(g)} \quad (5)$$

$$\Delta G^{o}_{(5)}\Big|^{2323\,K}_{2123\,K} = 603653 - 289.69T \quad (J)^{8} \quad (6)$$

Silicothermic reduction, shown in Reaction (7), is most commonly used for thermal reduction processes. The reducing agent is typically silicon-containing iron. The reason for not removing all the iron is to reduce the cost of the reducing agent. The reducing agent is commonly known as ferrosilicon.

$$2MgO_{(s)} + Si{\cdot}xFe_{(s)} \rightarrow 2Mg_{(g)} + SiO_{2(s)} + xFe_{(s)} \quad (7)$$

If the feed is calcined dolomite, then Reaction (7) becomes Reaction (8).

$$2CaO{\cdot}MgO_{(s)} + Si{\cdot}xFe_{(s)} \rightarrow 2Mg_{(g)} + (CaO)_2SiO_{2(s\ or\ l)} + xFe_{(s)} \quad (8)$$

There are two forms of industrial silicothermic reduction[9]; the Pigeon process, which is an externally heated vacuum retort and the Magnetherm process, which is an internally heated vacuum furnace.

2.3 Electrolytic Process for the Production of Magnesium

The largest current magnesium producers use the electrolytic process to manufacture magnesium metal[10]. Two steps are required for the extraction of magnesium by electrolysis: (1) the preparation of $MgCl_2$ feed to the electrolyte and (2) the electrolysis of $MgCl_2$. The preparation of $MgCl_2$ feed varies depending on the raw material and is formed from either aqueous $MgCl_2$ brine that is dehydrated, or by direct chlorination of MgO (not practiced commercially). Electrolysis is carried out in a molten salt system.

2.3.1. Electrowining of Mg: Cell Voltage

Reaction (9) represents the electrowining of $MgCl_2$ from aqueous solution and Reactions (10) and (11) represent the half reactions for the cathode and anode respectively[11]. The standard reduction potential for $MgCl_2$, Reaction (9), is –3.733 volts and for water, Reaction (12), is -1.228 volts, all at 25 °C. Electrolysis of magnesium cannot be carried out in an aqueous system because the water would decompose prior to the reduction of magnesium.

$$MgCl_{2(aq)} \rightarrow Mg_{(s)} + Cl_{2(g)} \qquad E^{\circ} = -3.733\ V \quad (9)$$

$$Mg^{2+} + 2e^{-} \rightarrow Mg_{(s)} \qquad e^{0} = -2.375\ V \quad (10)$$

$2Cl^- \rightarrow Cl_{2(g)} + 2e^-$ $\quad e^0 = -1.358\ V$ (11)

$H_2O_{(l)} \rightarrow \frac{1}{2}\ O_{2(g)} + H_{2(g)}$ $\quad E^0 = -1.228\ V$ (12)

In practice, the system has to operate above the melting point of magnesium and a molten salt is used to replace water as the electrolyte. The electrolytic reaction becomes Reaction (13). The standard reduction potential is calculated using Equations (15) and (16). The reversible reduction potential of Reaction (13) is a function of temperature and composition as is shown in Figure 3 for a cell producing $MgCl_2$. A decrease in $MgCl_2$ concentration increases the measured potential, as does a decrease in temperature[12,13,14]. This observation is described by Equation (16), giving the potential generated when $MgCl_2$ is produced as in Figure 3.

$MgCl_{2(l)} \rightarrow Mg_{(l)} + Cl_{2(g)}$ (13)

$$\Delta G^o_{(13)}\Big|_{823\,K}^{1023\,K} = 598353 - 115.61T \quad (J)^{8} \tag{14}$$

$$\Delta G^o = -nFE^o \tag{15}$$

$$E_{MgCl_2} = E^0{}_{MgCl_2} - \frac{RT}{nF}\ln a_{MgCl_2} \tag{16}$$

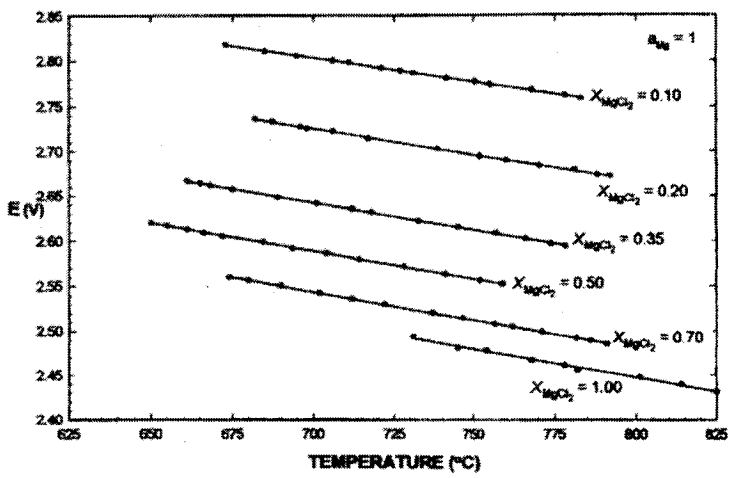

Figure 3 : Experimental reduction potentials of $MgCl_2$ with different a_{MgCl2} in the $MgCl_2$ – KCl – NaCl system.[14]

2.3.2. Structure of Molten Salt

A discussion of the structure of molten salts is in order to better understand the molten salt system. It should be noted that due to their corrosive nature and high temperature, they are much more difficult to study than aqueous systems, solids, or gases.

Models are used to help define the structure of molten salts, but none of these can be deemed perfect. They include the Vacancy model, the Hole model, the Crystalline model, the Polyhedral-Hole model, the Liquid Free-Volume model, and the Significant Structure model. All of the above-mentioned models are explained by Bloom in "The Chemistry of Molten Salts" [15]. Figure 4 shows an example of the NaCl lattice and Figure 5 shows its molten structure using the Hole model. Upon melting, the structure is thought to dissociate into cations and anions, giving rise to the high electrical conductivity of molten salts that is roughly ten times that of aqueous systems. The cations are surrounded by anions, due to columbic forces, and the anions are surrounded by cations. This is in agreement with the short-range order observed when pure molten salts are analyzed with X-ray diffraction[16]. Additionally, the melting of a salt will cause an increase in volume. Figure 5 shows the Hole model that is derived from the solid lattice; it is here the short-range order and the increase in volume can be observed upon melting.

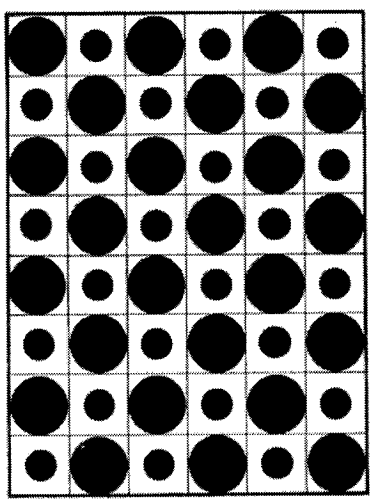

Figure 4 : Lattice of solid NaCl.[15]

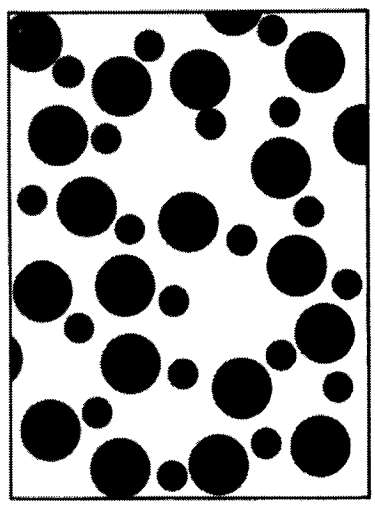

Figure 5 : Liquid NaCl using the hole model.[15]

The electrolyte used for the production of magnesium contains a number of salts. NaCl, KCl, $MgCl_2$, and $CaCl_2$ are used to obtain the desired physical and chemical properties of the electrolyte. A mixture of these compounds forms an electrolyte with unsymmetrical charge, meaning that all the anions have only one negative valence charge (Cl^-) but the cations can have one or two valence charges (Na^+, Ca^{2+}). A monovalent molten salt with a common anion charge is identified as a symmetric binary system, e.g. NaCl–KCl, and will generally follow ideal behaviour (activity equals mole fraction), because the quantity of anions and cations are equal[13]. Blander[17] has shown that small negative deviation from ideal behaviour in monovalent systems can be explained by the difference in the size of the cations.

Moreover, the molten salts used in the production of magnesium are characterized by an unsymmetric charge system, e.g. NaCl and $MgCl_2$, resulting with the quantity of anions and cations being different. This causes complexations (formation of complex systems in the electrolyte) that creates large negative deviation from ideal behaviour at low concentrations. Furthermore, it has been shown that increasing the size of the alkali ion or decreasing the size of the alkali-earth ion will increase the extent of the negative behaviour[13]. These variations make the ion interactions more complicated and difficult to determine equilibrium quantities of species and thermodynamic properties of the electrolyte due to complexations.

The electrolytic magnesium industry is acutely interested in the activity of $MgCl_2$ in the molten salt since this is the component being decomposed. The activity of $MgCl_2$ can be experimentally measured by using Equation (16). Complexation of $MgCl_2$ decreases the activity of $MgCl_2$ and requires a larger reduction potential.

One of the reasons alkali-earth ionic liquids are not fully understood is because of the formation of complexes. A system of pure alkali-earth halides, MX_2, is thought to disassociate to produce the complexes shown in Reactions (17) and (18)[15].

$$M^{2+} + 2X^- \leftrightarrow MX^+ + X^- \quad (17)$$

$$MX^+ + X^- \leftrightarrow MX_2 \quad (18)$$

Also, there have been several experiments that have shown the existence of a magnesium complex, $MgCl_4^{2-}$, in $MgCl_2$ –alkali chloride systems[15,18,19,20]. In addition, Karakaya[20] et al. have shown that $CaCl_4^{2-}$ might be present in $MgCl_2$–NaCl–$CaCl_2$ melts.

The composition of the molten salt electrolyte for magnesium production varies between companies. Pure $MgCl_2$ is not favoured due to its high melting point (714 °C), its low conductivity, and its high volatility[21]. The salts chosen for the electrolyte must have a reduction potential that is more negative than $MgCl_2$. The chloride Ellingham diagram presented in Figure 6 presents some possible chloride salts. As previously mentioned, the electrolyte typically contains $MgCl_2$, NaCl, $CaCl_2$, and KCl. Composition of the salt changes the physical and chemical properties of the electrolyte. The NaCl and KCl increases the conductivity and $CaCl_2$ increases the density of the electrolyte to promote the buoyancy of magnesium and increase the separation between the magnesium and the electrolyte[12,21]. LiCl can also be added to increase conductivity, however, it is expensive and reduces the density significantly. Other physical properties that concern the industry include the viscosity for magnesium–electrolyte separation and surface tension for the wettability of the cathode.

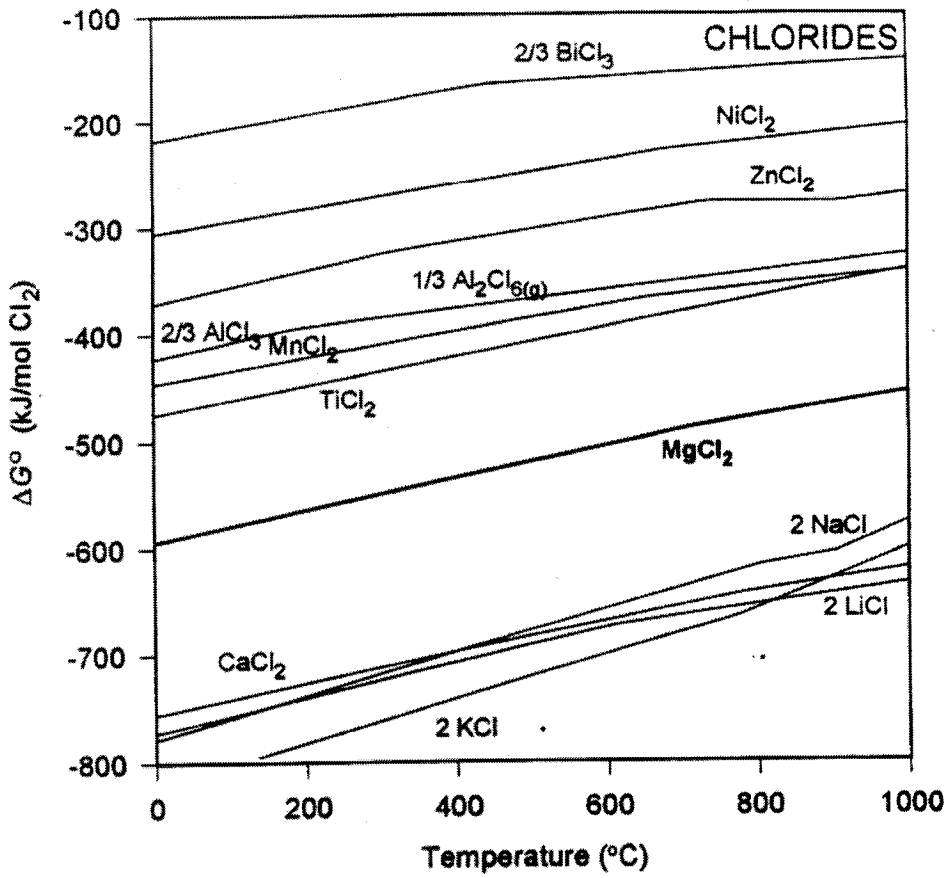

Figure 6 : Chloride Ellingham Diagram.[9]

There are two main methods for the preparation of $MgCl_2$ feed. They are brine dehydration and direct chlorination.

2.3.3. Dehydration of $MgCl_2$ brine

In commercial production of magnesium, a purified aqueous brine containing $MgCl_2$ is prepared and then dried in a fluidized bed dryer. The $MgCl_2$ fed to the electrolyte can be either partially dehydrated or completely dehydrated. Partial dehydration produces hydrous $MgCl_2$ ($MgCl_2 \cdot xH_2O$) and when added to the electrolyte, it flashes its waters of hydration to produce $MgCl_2$ and oxides. Complete dehydration of the brine produces anhydrous $MgCl_2$ and oxides. The quantity of oxides are controlled by maintaining a high

ratio of partial pressure of HCl gas (P_{HCl}) to water vapour (P_{H2O}). The dehydration to two molecules of water is industrially feasible[12,21]. Dehydrating beyond two molecules of water requires a substantial amount of HCl gas and this is not viable as the chlorine balance cannot be reached, i.e. the HCl required to dilute the H_2O evolved exceeds the HCl that can be produced from the $Cl_{2(g)}$ generated during electrolysis. The advantage of using partially dehydrated feed is lower dehydration cost, however, this comes at the expense of added oxides. Furthermore, dehydration is dependent on the design of the plant in order to minimize the hydrolysis reaction.

2.3.4. Dehydration of carnallite

An alternative method to feeding $MgCl_2$ to an electrolysis cell is by the dehydration of carnallite ($KCl{\cdot}MgCl_2{\cdot}6H_2O$). The former U.S.S.R. used this salt on industrial scale[12,21] and currently, Dead Sea Magnesium is the only producer of magnesium using carnallite[6]. The feed material to the electrolysis cell becomes dehydrated carnallite ($KCl{\cdot}MgCl_2$). The dehydration reactions are similar to the dehydration of $MgCl_2$ brine. During the last stages of dehydration, the hydrolysis of $MgCl_2$ also occurs to form a solid solution of $MgCl_2$ and MgOHCl. The main advantage of this process is that the $MgCl_{2(s)}$ activity is less than one; therefore, less hydrolysis occurs. A disadvantage with this process is that there is accumulation of KCl in the electrolyte, which is continuously changing its composition. It is because of this detrimental effect that the electrolyte cannot be recycled indefinitely.

2.3.5. Direct chlorination

Anhydrous $MgCl_2$ can also be produced by the direct chlorination of MgO (although not currently practiced commercially) and the overall reaction is presented in Reaction (19).

$$MgO_{(s)} + Cl_{2(g)} \rightarrow MgCl_{2(l)} + \tfrac{1}{2}\, O_{2(g)} \qquad (19)$$

$$\Delta G^{o}_{(19)}\Big|_{1300\,K}^{1400\,K} = 5877 + 12T - 7.3\times10^{-3}T^{2} \quad (J)^{8} \qquad (20)$$

However, an acceptable chlorination rate in industrial practice increases the partial pressure of oxygen above the equilibrium value resulting in back reaction. Carbochlorination has been used for industrial practices and follow Reactions (21) and (23). The reactions are highly exothermic and self-sustaining once initiated[12].

$$MgO_{(s)} + Cl_{2(g)} + C_{(s)} \rightarrow MgCl_{2(l)} + CO_{(g)} \quad (21)$$

$$\Delta G^{o}_{(21)}\Big|^{1400\,K}_{1300\,K} = 95100 - 93.95T \quad (J)^{8} \quad (22)$$

$$MgO_{(s)} + Cl_{2(g)} + CO_{(g)} \rightarrow MgCl_{2(l)} + CO_{2(g)} \quad (23)$$

$$\Delta G^{o}_{(23)}\Big|^{1400\,K}_{1300\,K} = 262052 + 77.98T \quad (J)^{8} \quad (24)$$

Even so, this process also has the disadvantage that the liquid $MgCl_2$ formed on the surface of the MgO particles impedes further chlorination[22].

The $MgCl_2$ produced by the various methods mentioned above is then fed onto the surface of the electrolyte.

2.3.6. Oxides in the electrolysis cell

The preparation of oxide-free anhydrous $MgCl_2$ represents one of the most costly operations in the production of electrolytic magnesium. Oxides are not desired for several reasons. Firstly, they represent a loss of magnesium. Secondly, MgO is not soluble in the molten salt electrolyte and forms a sludge deposit at the bottom of the cell[12,21,23,24].

Moreover, oxides are detrimental to the electrolysis cell. The reason for this is that anodes in a molten salt electrolyte are generally made of graphite. The MgO reacts with the chlorine gas and graphite to produce $MgCl_2$ and carbon oxide gases. The consumption of graphite increases the anode-to-cathode distance. Oxides dissolved in the electrolyte react at the cathode, i.e. Reaction (25), producing MgO[21]. The MgO deposits on the steel cathode and results in the decrease of magnesium wettability. Moreover, passivation occurs resulting in a larger potential difference across the electrodes.

$$MgOH^{+} + 2e^{-} \rightarrow MgO_{(s)} + H_{2(g)} \quad (25)$$

MgO also coats the surface of magnesium droplets and prevents their coalescence. Furthermore, MgO coated droplets will not have sufficient buoyancy to rise to the surface of the electrolyte.

2.4 Magnola Metallurgie Inc.

The following information is taken from Ficara[25] explaining the Magnola Metallurgie Inc. (MMI) process. Designed to be the lowest cost producer of magnesium metal in the western world (Chinese plants built on the Pigeon process have the lowest cost), MMI received the environmental approval in the spring of 1998 and construction began that spring. Reasons for the low cost production included free serpentine tailing feed from a nearby asbestos mine that averaged 24 wt.% magnesium. A second reason was the availability of an inexpensive source of electricity. Located in Danville, Québec, the MMI plant cost about 900 million $ and was expected to have a production capacity of 58,000 tones per year of magnesium, approximately 20 % of the worlds production prior to the Chinese magnesium markets' growth.

Figure 7 is a diagram of the MMI flowsheet. The process comprises six steps: 1) feed preparation, 2) leaching, purification and ion exchange, 3) brine dehydration, 4) melt chlorination, 5) electrolysis, and 6) casting.

2.4.1. Feed Preparation

The MMI plant was designed to accept serpentine ($3MgO{\cdot}2SiO_2{\cdot}2H_2O$) as the raw material, after it had been processed from the asbestos mine operations. As a result, no communition was needed and the mineralogy, chemistry, and size distribution were considered constant. Typical feed composition was 40% MgO, 38% SiO_2, 13% H_2O, 5% Fe compounds (Fe_2O_3 and $Fe(OH)_2$), varying amounts of Al_2O_3 and CaO, and traces of nickel, manganese, and boron. The tailings from the asbestos mine were scooped up with a front end loader and passed through an initial screening stage to remove oversized material. The oversized was rejected and the undersized was sent to a magnetic separator.

Due to the elevated iron content in the feed, a magnetic separator was used to increase the magnesium-iron separation. This also increased the efficiency of latter filtering steps. The magnetic separator required the media to be a slurry. Hence, process water was added to the feed prior to the magnetic separation step. The magnetic material was rejected and the demagnetized material was sent to the leaching circuit.

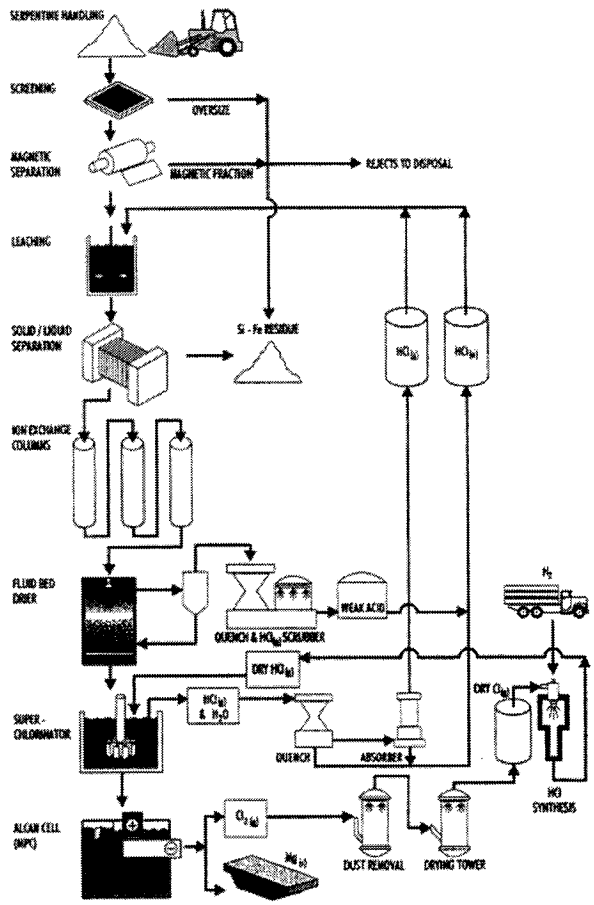

Figure 7 : MMI Flowsheet.[25]

2.4.2. Leaching, Purifying, and Ion Exchange

The slurry medium was leached in a continuous process with hydrochloric acid and HCl gas recycled from the fluidized bed dryer and the "Super Chlorinator". To neutralize the chlorinated solution, MgO was added and the un-leached residue was filtered using belt filters. The residue was sent to the tailings pond and the brine was sent to the purification step.

The purification step injected recycled chlorine gas to oxidize impurities such as iron, manganese, and nickel. Following this, MgO and 50 % caustic (NaOH) were added in order to precipitate the impurities as hydroxides and neutralize the solution. The solution was filtered again, the residue was rejected, and the filtrate was sent to ion exchange columns.

The ion exchange was to ensure all traces of undesired ions; such as iron, boron, nickel, and manganese were removed from the brine. These ions were detrimental to the electrolysis cell. With the unwanted ions removed, the brine was now a purified $MgCl_2$ solution containing 350 g per litre $MgCl_2$ (27 wt.% $MgCl_2$). The solution was pumped to storage tanks.

The off-gases from leaching and purification were sent to HCl gas scrubbers and 7 wt.% hydrochloric acid was produced which was reused in the leaching section.

2.4.3. Brine Drying

The $MgCl_2$ rich brine was dehydrated by evaporation using a fluidized bed dryer (FBD). The product was free flowing granules of hydrated $MgCl_2$ ($MgCl_2 \cdot \sim 2H_2O$) called prills; see Figure 8, which contained some oxides and traces of NaCl and $CaCl_2$. The prills were sent to the "Super Chlorinator".

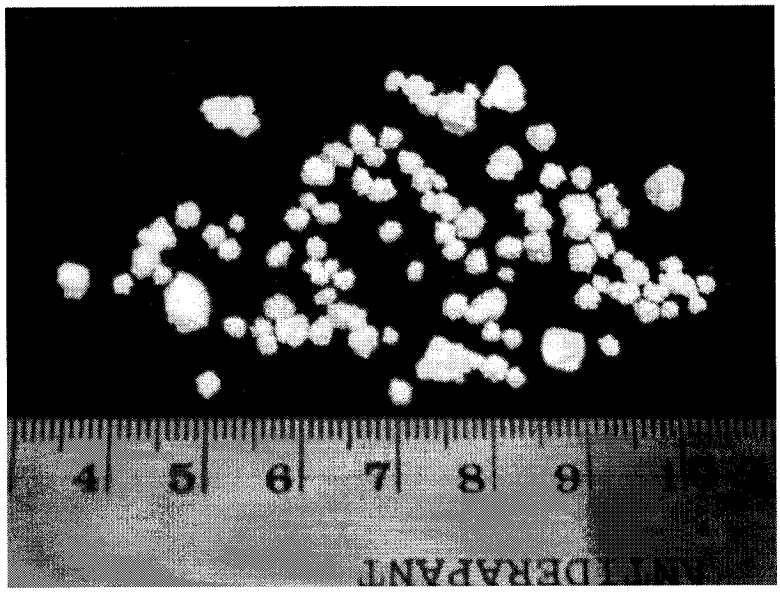

Figure 8 : Magnola Metallurgie Inc. 'Prills'. Scale is in cm.

The FBD off-gases were passed through a cyclone where the dust was recycled back to the FBD and the gases were sent to a water scrubber to produce hydrochloric acid.

2.4.4. Melt Chlorination

The "Super Chlorinator" was a three phase reacor; solid (prills), liquid (electrolyte), and gas (HCl/H_2O). The reactor was heated using a.c. electrical heating. Prills were added on the surface of the electrolyte and HCl gas was injected via agitators. The prills flashed off the waters of hydration and dissolved into the electrolyte. Having a $HCl_{(g)}/H_2O_{(g)}$ greater than 0.5[9] was necessary to suppress the hydrolysis reaction and produced anhydrous $MgCl_2$. The oxides that did form were chlorinated according to Reaction (26) by the HCl gas. The cell operated at under a slight draft for safety reasons. The oxide-free electrolyte was sent to the electrolysis cell via overflow launder.

$$MgO_{(s)} + 2HCl_{(g)} \rightarrow MgCl_{2(l)} + H_2O_{(g)} \quad (26)$$

$$\Delta G^{o}_{(26)}\Big|_{823\,K}^{1023\,K} = 57492 + 87.4T - 1.05\times10^{-2}T^{2} \quad (J)^{8} \quad (27)$$

The off-gases were collected and sent to the thermal quench unit where the gas was cooled to produce hydrochloric acid and HCl gas.

2.4.5. Electrolysis

Alcan's Multi-Polar Cells (MPCs) were used to electrowin the magnesium. The cell was divided in two compartments: the metal compartment (where the $MgCl_2$ rich electrolyte was added and the magnesium metal was tapped) and the electrolysis compartment (where the electrowining of magnesium and the generation of chlorine occurred). MMI electrolyte was composed of NaCl, $CaCl_2$, $MgCl_2$, KCl, and CaF_2 with graphite anodes, graphite bipolar electrodes, and steel cathodes. There were two regulating devices in the cell. Heat was controlled using heat exchangers and a "submarine" was used for level control of the electrolyte / metal layer in the metal compartment.

The off-gases, mainly chlorine, were treated to obtain dry chlorine gas and were then reacted, burnt, with pure hydrogen to form dry HCl gas that was recycled in the process.

2.4.6. Casting

When the magnesium metal reached a desired volume in the metal compartment of the MPC, it was removed from the electrolysis cell via a preheated vacuum ladle. The

magnesium was cast in three continuous ingot casting machines for pure and alloyed products[6].

2.5 Why is Magnola Metallurgie Inc a Novel Process

The MMI process was designed with three original practices, two that lay in the "Super Chlorinator"[9]. This was the first plant to use asbestos tailings (serpentine) as the raw feed material. In the Super Chlorinator, a novel aspect was the use of an electrolyte in which the activity of $MgCl_2$ has been greatly reduced due to the electrolyte composition forming magnesium complexes. The low activity reduced the hydrolysis of the molten $MgCl_2$, Reaction (28). The final novel aspect was the injection of HCl gas into the electrolyte in order to suppress hydrolysis of the electrolyte during prill digestion. Because of the reduced $MgCl_2$ activity, less HCl was required to suppress the hydrolysis of the $MgCl_2$ in the electrolyte and MMI was able to close the chlorine balance for the operation.

$$MgCl_{2(l)} + H_2O_{(g)} \rightarrow MgO_{(s)} + 2HCl_{(g)} \quad (28)$$

$$\Delta G^{o}_{(28)}\Big|_{823\,K}^{1023\,K} = 57492 - 87.4T + 1.05\times10^{-2}T^{2} \quad (J)^{8} \quad (29)$$

The injection of HCl gas through an impeller was assumed to evenly disperse the gas in order to contact the $MgCl_2$ in the electrolyte. The HCl had a dual effect being that it suppressed hydrolysis during prill digestion and also chlorinated any oxides present in the electrolyte, thus ensuring that the feed to the electrolysis cell was an oxide free $MgCl_2$ rich molten salt. Lowering the $MgCl_2$ activity further helped chlorination, Reaction (28).

Earlier in the chapter it was mentioned that NaCl caused the activity of $MgCl_2$ to deviate negatively from ideal behaviour (unsymmetric charge) at low concentrations of $MgCl_2$ and $CaCl_2$ did not (i.e. followed ideal behaviour). To illustrate, Figures 9 and 10 were generated using Fact*Sage*™, a thermodynamic software developed by CRCT[8]. KCl also caused the activity of $MgCl_2$ to deviate negatively from ideality, however, it is not shown here.

<A> $MgCl_2$ + <1-A> NaCl at 800 °C
Activity of $MgCl_2$ shows negative ideal behaviour at low concentration

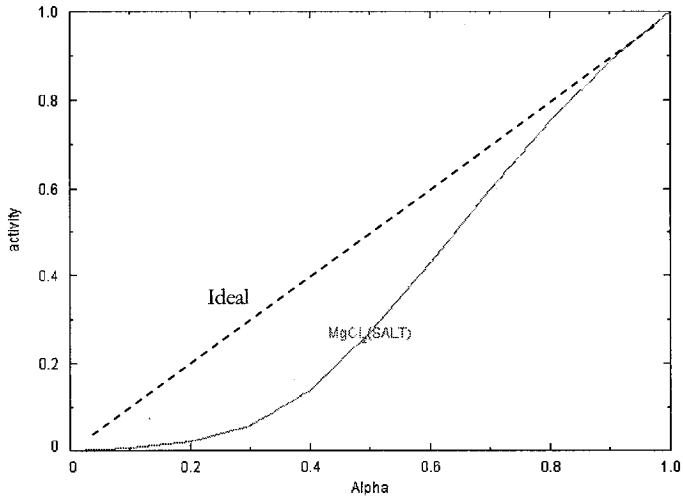

Figure 9 : Fact*Sage*™ prediction showing the behaviour of $MgCl_2$ activity with increasing $MgCl_2$ content in a binary $MgCl_2$-NaCl system. The temperature was arbitrarily chosen to ensure the materials were liquid.

<A> $MgCl_2$ + <1-A> $CaCl_2$ at 800 °C
Activity of $MgCl_2$ shows ideal behaviour

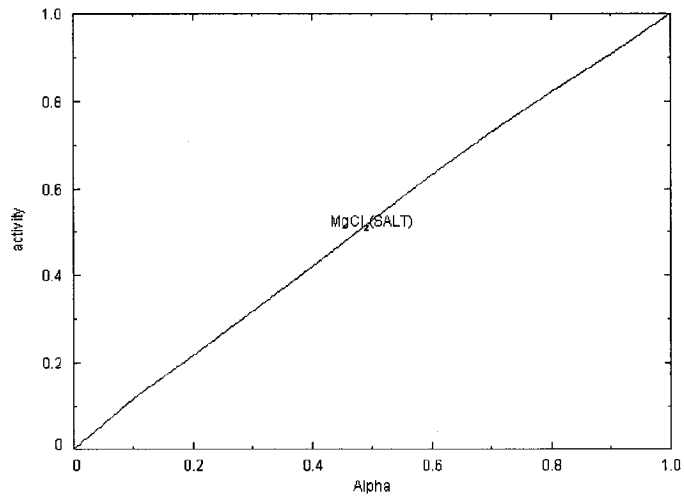

Figure 10 : Fact*Sage*™ prediction showing the behaviour of $MgCl_2$ activity with increasing $MgCl_2$ content in a binary $MgCl_2$-$CaCl_2$ system. The temperature was arbitrarily chosen to ensure the materials were liquid.

Figure 11 was generated to show the effect of the NaCl-$CaCl_2$ ratio on $MgCl_2$ activity. The amount of $MgCl_2$ was arbitrarily chosen to be 0.3 mole fraction, which was typical to the industrial electrolyte in magnesium production, and the remainder of the molten salt was a

molar ratio of NaCl and $CaCl_2$. The temperature was also arbitrarily chosen to be 800 °C. It is observed that increasing the NaCl content decreased the activity of $MgCl_2$, as expected.

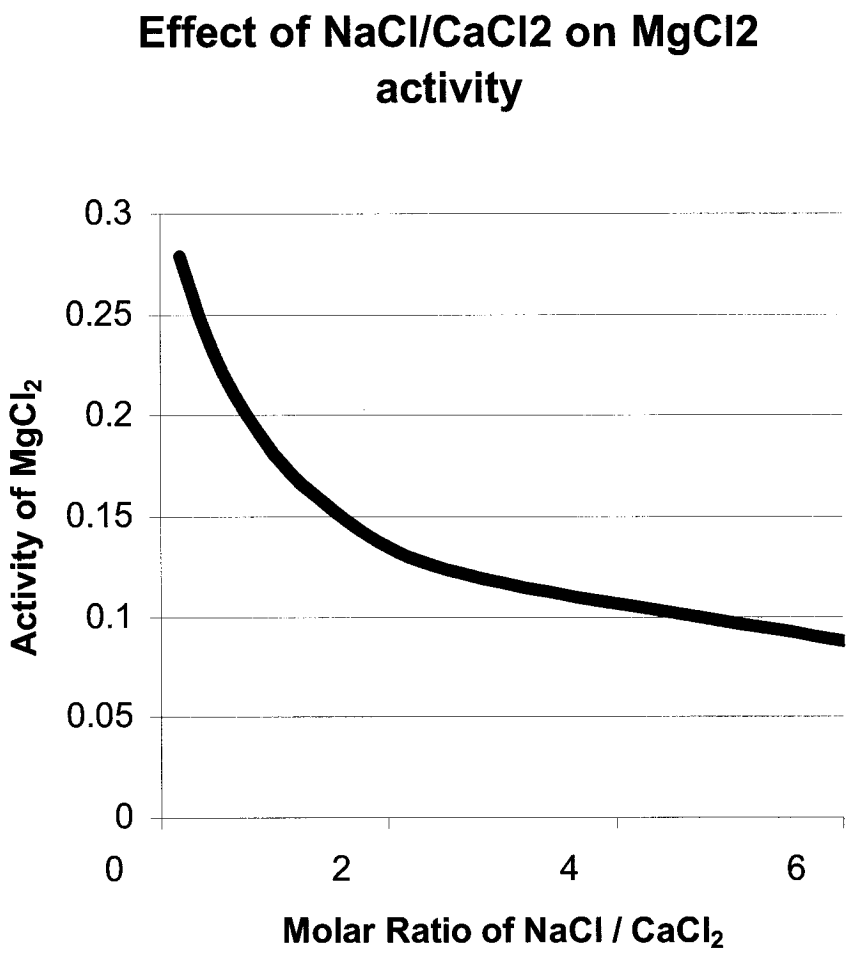

Figure 11 : Fact*Sage*™ computation showing the effect of $NaCl/CaCl_2$ ratio containing a fixed amount of $MgCl_2$ (0.3 mole fraction).

2.6 Production & Behaviour of Oxides

2.6.1. Dehydration of $MgCl_2$

Figure 12 shows the possible number of waters of hydration associated with $MgCl_2$ in its various forms. Depending on the temperature range, the numbers of water molecules of hydration in decreasing order are 12, 8, 6, 4, 2, and 1. Above 0 °C, only 6 molecules of

water or less appear in the crystalline phases and these are of commercial importance for the production of $MgCl_2$.

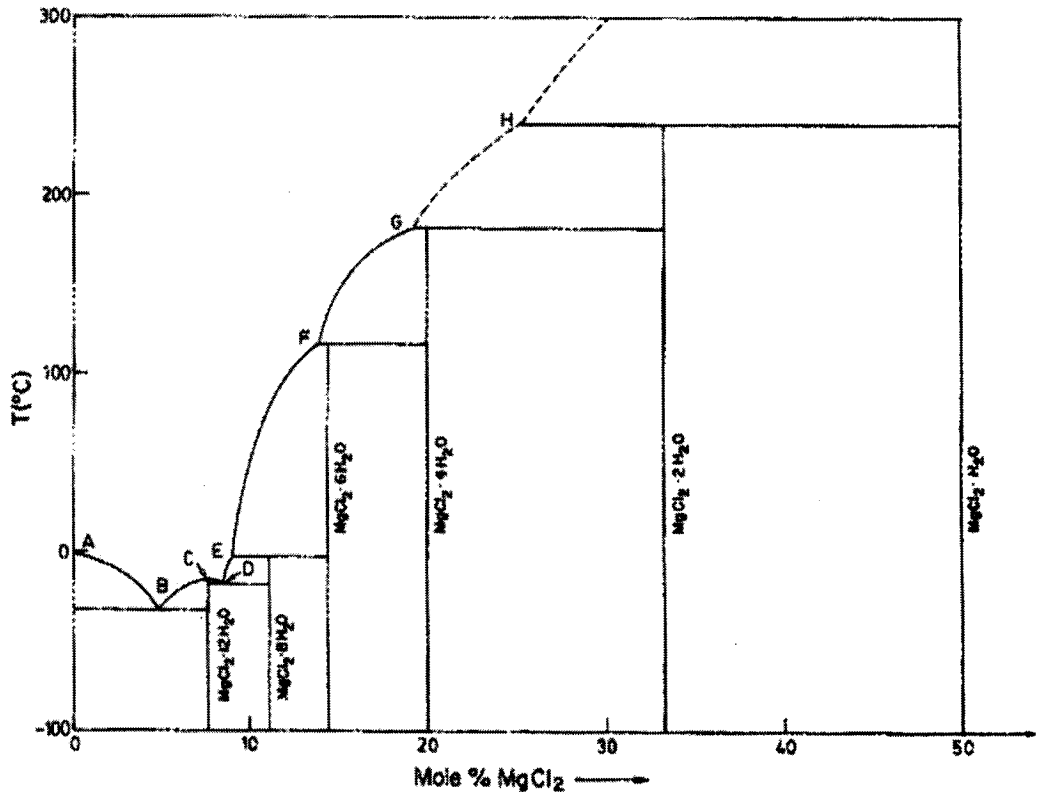

Figure 12 : Water-rich portion of the $MgCl_2 - H_2O$ Phase Diagram.[12]

Kelley[26] was the first to perform a complete thermodynamic study on the dehydration and hydrolysis of $MgCl_2$. Thermodynamic calculations were performed and compared with experimental data. At a given temperature, there was a vapour pressure of water (P_{H2O}) for which the coexistence of two hydrates occurred. The dehydration of $MgCl_2$ hexahydrate to dihydrate is shown in Reactions (30) and (32). Figures 13 and 14 display the equilibrium partial pressure needed for the hydrates to co-exist.

$$½\ MgCl_2{\cdot}6H_2O_{(s)} \leftrightarrow ½\ MgCl_2{\cdot}4H_2O_{(s)} + H_2O_{(g)} \qquad (30)$$

$$\Delta G^{o}_{(30)}\Big|_{298\,K}^{390\,K} = 116079 - 274.46T \quad (J)^{8} \qquad (31)$$

$$\tfrac{1}{2}\,MgCl_2{\cdot}4H_2O_{(s)} \leftrightarrow \tfrac{1}{2}\,MgCl_2{\cdot}2H_2O_{(s)} + H_2O_{(g)} \quad (32)$$

$$\Delta G^{o}_{(32)}\Big|_{298\,K}^{455\,K} = 134531 - 290T \quad (J)^{8} \quad (33)$$

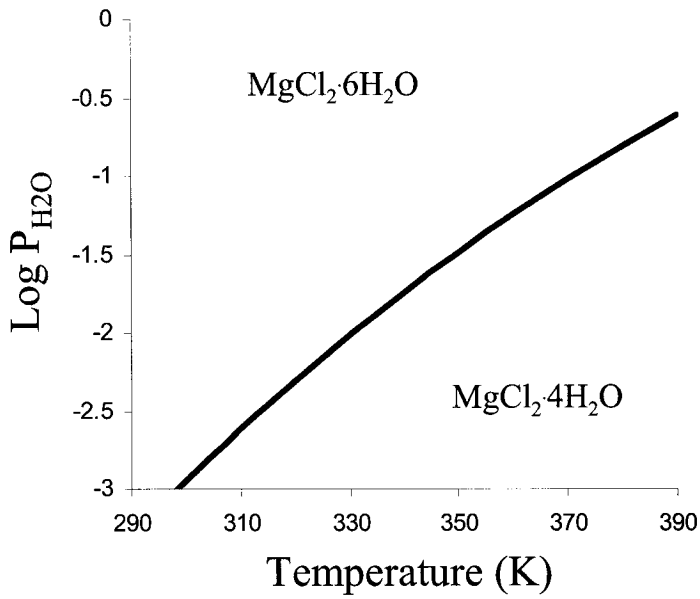

Figure 13 : Water vapour equilibrium for Reaction (30) as a function of temperature[26].

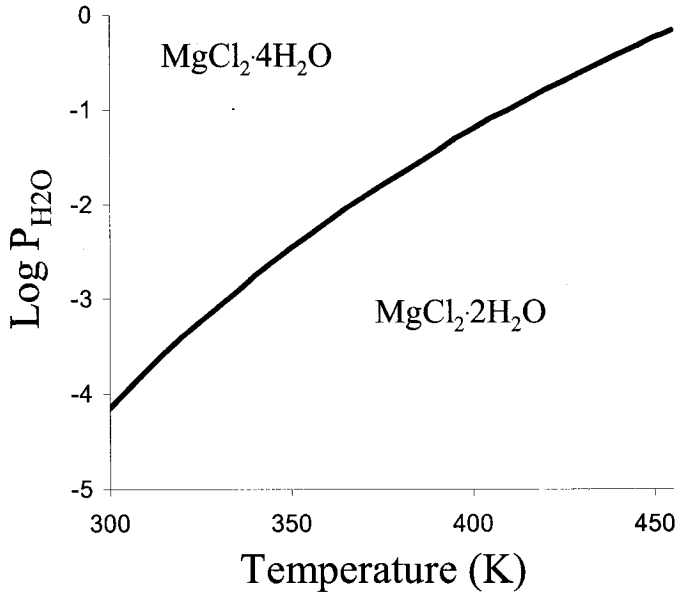

Figure 14 : Water vapour equilibrium for Reaction (32) as a function of temperature.[26]

For dehydration to occur, the P_{H2O} surrounding the hydrate must be less than the equilibrium P_{H2O}. This was accomplished by increasing the temperature, which increased the equilibrium P_{H2O}. However, one must be careful not to increase the temperature above the melting point of the hydrate or the latter melts congruently in its own waters of crystallization, rendering any additional dehydration difficult.[21]

Dehydration to less than two molecules of water without a HCl atmosphere was not possible without significant hydrolysis. There are some discrepancies between researchers at this level of dehydration regarding the composition of the products. Figure 15 presents the Gibbs energy change for the dehydration of the dihydrate, the hydrolysis of the $MgCl_2$ and the decomposition of the MgOHCl as a function of temperature. The figure does not clearly show the thermodynamic conditions necessary to suppress hydrolysis while permitting dehydration.

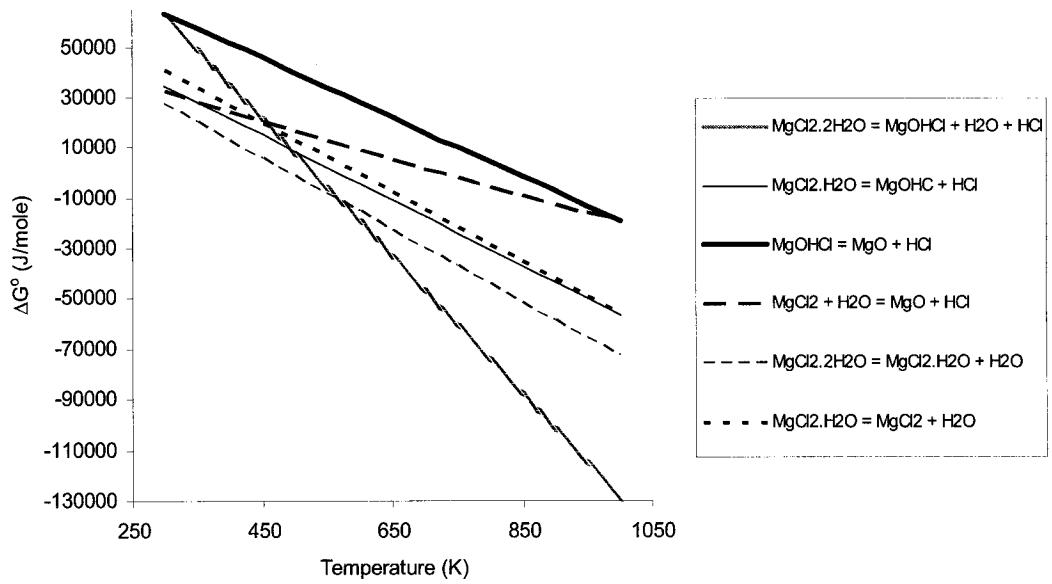

Figure 15 : Gibbs Energy Change for Reactions that can occur during $MgCl_2 \cdot 2H_2O$ dehydration.

Kelley[26] claimed that the dihydrate reduces to the monohydrate prior to complete dehydration as shown in Reaction (34). In addition, the hydrolysis reaction occurred at the same time. Reaction (36) presents the hydrolysis reaction during the dehydration of the dihydrate[12,21,26]. Figures 16 and 17 displays the equilibrium partial pressure needed for Reactions (34) and (36) to occur.

$$MgCl_2 \cdot 2H_2O_{(s)} \leftrightarrow MgCl_2 \cdot H_2O_{(s)} + H_2O_{(g)} \quad (34)$$

$$\Delta G^o_{(34)}\Big|_{298\,K}^{513\,K} = 70256 - 143.02T \quad (J)^{8} \quad (35)$$

$$MgCl_2 \cdot 2H_2O_{(s)} \leftrightarrow MgOHCl_{(s)} + H_2O_{(g)} + HCl_{(g)} \quad (36)$$

$$\Delta G^o_{(36)}\Big|_{298\,K}^{823\,K} = 143764 - 272.88T \quad (J)^{8} \quad (37)$$

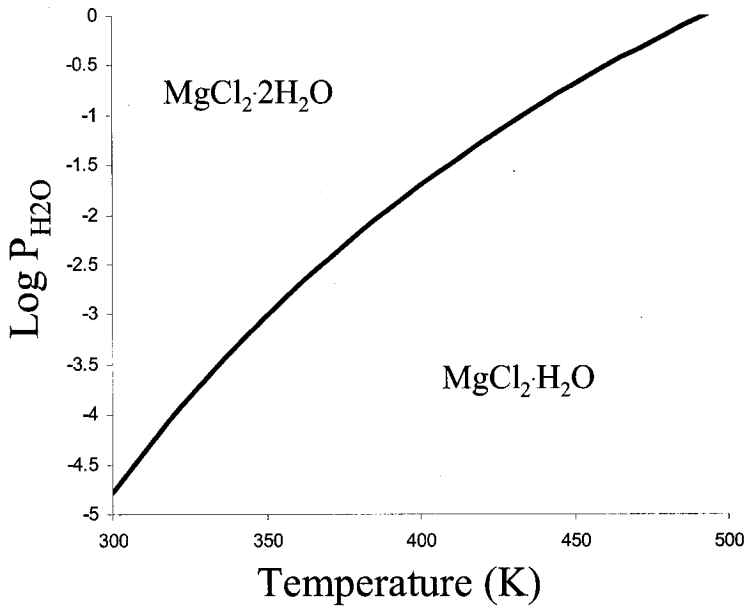

Figure 16 : The dependence on gas composition for Reaction (34) as a function of temperature.[26]

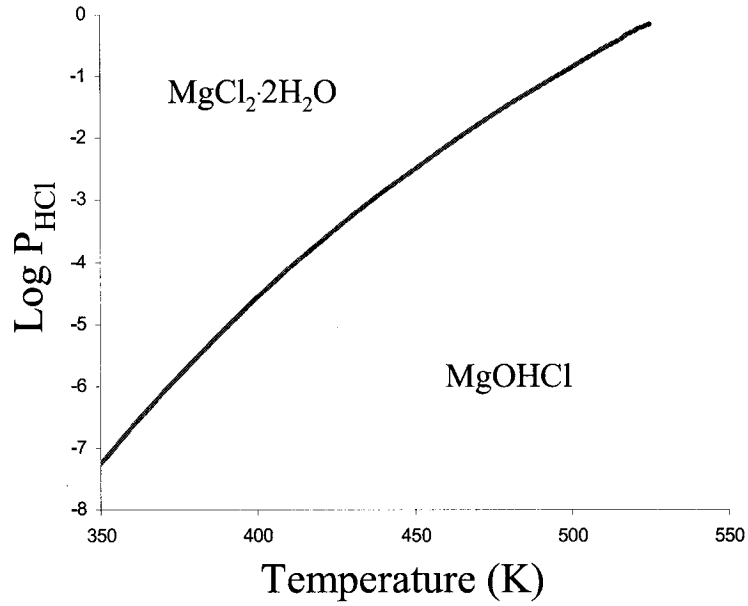

Figure 17 : The dependence on gas composition for Reaction (36) as a function of temperature.[26]

It is obvious, thermodynamically speaking, that the monohydrate can be produced without hydrolysis provided that the gas composition is maintained sufficiently concentrated in HCl.

The final stage of dehydration was Reaction (38). The hydrolysis of the monohydrate Reaction (40) occurred at a higher P_{HCl} as compared to the dihydrate. This was explained by the greater vapour pressure of water generated by Reaction (34), which inhibited reaction (36)[26]. Figures 18 and 19 displays the equilibrium partial pressure needed for the hydrates to co-exist. It becomes obvious that a high P_{HCl} is required to prevent the hydrolysis Reaction (40).

$$MgCl_2 \cdot H_2O_{(s)} \leftrightarrow MgCl_{2(s)} + H_2O_{(g)} \quad (38)$$

$$\Delta G^{o}_{(38)}\Big|_{298\,K}^{823\,K} = 82235 - 138.35T \quad (J)^{8} \quad (39)$$

$$MgCl_2 \cdot H_2O_{(s)} \leftrightarrow MgOHCl_{(s)} + HCl_{(g)} \quad (40)$$

$$\Delta G^{o}_{(40)}\Big|_{298\,K}^{823\,K} = 73650 - 130.13T \quad (J)^{8} \quad (41)$$

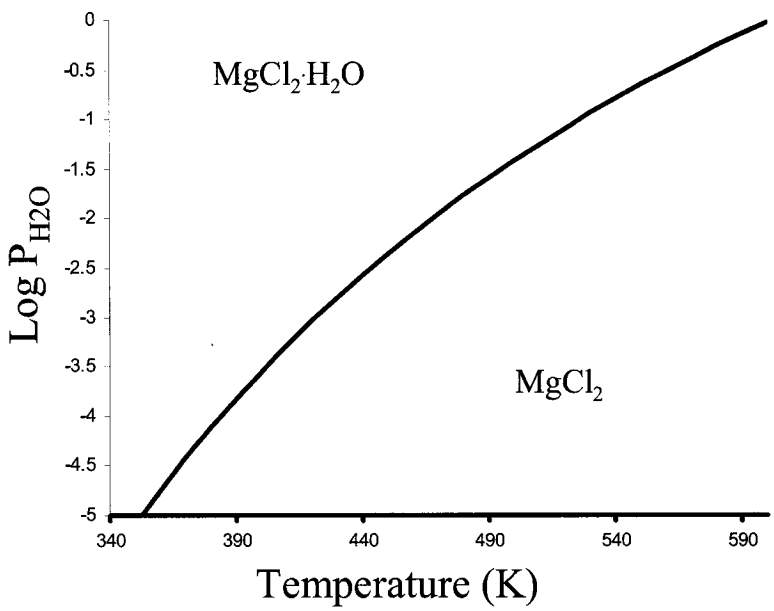

Figure 18 : The dependence on gas composition for Reaction (38) as a function of temperature.[26]

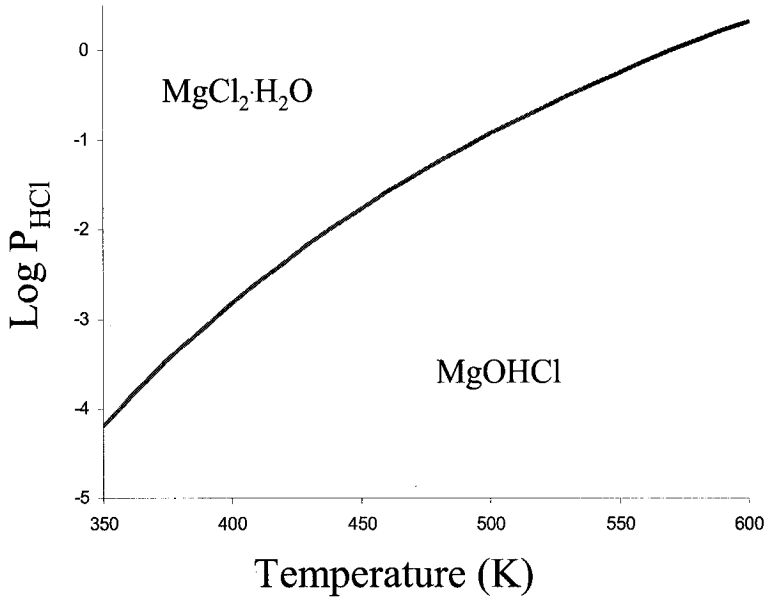

Figure 19 : The dependence on gas composition for Reaction (40) as a function of temperature.[26]

Reaction (42) was the thermal decomposition of the MgOHCl.

$$MgOHCl_{(s)} \rightarrow MgO_{(s)} + HCl_{(g)} \quad (42)$$

$$\Delta G^{o}_{(42)}\Big|_{723\,K}^{923\,K} = 98581 - 117.63T \quad (J)^{8} \quad (43)$$

The decomposition temperature of Reaction (42) has been studied by several investigators. Kelley[26] calculated that above 555 °C, the P_{HCl} was 1 atmosphere (atm) and that MgOHCl was unstable above that temperature. He mentioned that Moldenhauer[27] experimentally reported that above 524 °C, the hydrolysis reaction yielded MgO.

The temperature of operation for the electrolyte in magnesium electrolysis is above the melting temperature of magnesium, 650 °C. Ficara[9] mentions on page 31 that the MgOHCl formed decomposed to MgO at elevated temperatures, which allowed him to ignore the presence of the other oxides. The claim was referenced to Quintero[28] who stated on page 11 that at the "*temperature of interest in the electrolysis of $MgCl_2$*", decomposition of MgOHCl to MgO occurs. Quintero's[28] conclusions were drawn from the work of Glasner et

al.[29], who studied the dehydration and hydrolysis of $MgCl_2$. Therefore; the oxide feed to the electrolysis cell was believed to be MgO.

The dehydration to two molecules of water without significant hydrolysis was industrially feasible by maintaining an HCl atmosphere. The reason for this was that the formation of oxides during the dehydration stages was suppressed by maintaining a high partial pressure of HCl gas, P_{HCl}, surrounding the $MgCl_2$. Dehydrating beyond two molecules of water required a substantially higher P_{HCl} to prevent the hydrolysis reaction and this was not economically viable.

Vil'Nyanskii and Savinkova[30] have provided evidence that the complete dehydration yields a mixture of $MgCl_2$ and MgOHCl at equilibrium in solid solution depending on the gas composition and the temperature. Results were acquired with their alkalimetric speciation technique. They showed that increasing the temperature increased the MgOHCl content. In addition, at a specified temperature, the amount of MgOHCl present was directly dependent on the gas composition. The starting material was both $MgCl_2$ and MgO, and they reached the same end results. Table 1 presents the MgOHCl content in a solid solution of MgOHCl in $MgCl_2$. Reaction (44) presents how the gas phase affects the solid solution.

$$MgCl_{2(ss)} + H_2O_{(g)} \leftrightarrow MgOHCl_{(ss)} + HCl_{(g)} \qquad (44)$$

$$\Delta G^{o}_{(44)} = -2170 - 33.9T + 14.07T\log T - 5.8\times10^{-3}T^{2} - 1.03\times10^{5}T^{-1} \quad (J)^{30} \qquad (45)$$

Table 1 : Solubility of MgOHCl in $MgCl_2$ with mixtures of HCl and H_2O[30]

Temperature (°C)	310	342	350	385	420	450	467	480
MgOHCl content (mole %)	12	15	16	20	25	30	35	40
HCl content (vol.%)	75.4	70.6	69.4	64.4	60.0	56.3	54.2	52.9
H_2O content (vol.%)	24.6	29.4	30.6	35.6	40.0	43.7	45.8	47.1

Glasner et al.[29] have developed a method to measure the extent of hydrolysis by capturing HCl gas in water and measuring its conductivity as a function of time. By dehydrating hexahydrate, they identified the main hydrolytic reaction to be Reaction (40), involving only the monohydrate. Moreover, they saw that some of the monohydrate was dehydrated

without hydrolysis, Reaction (38). They claimed that the hydrolysis reaction has a lower activation energy compared to the dehydration reaction. Their final product was a solid solution of $MgCl_2$ in MgOHCl. They also hydrolyzed anhydrous $MgCl_2$ at low temperature and concluded that the hydrolysis occurred on the exposed surface, thereby inhibiting any further hydrolysis. At elevated temperatures (400 to 500 °C), the MgOHCl formed first and then slowly decomposed to form MgO. The rate of decomposition increased with increasing temperatures.

Dutt et al. [31] have studied the dehydration of $MgCl_2$ hexahydrate using thermo-gravimetric analysis (TGA). They supported the finding of the formation of MgOHCl below 500 °C and they performed minor kinetic studies. They concluded that the MgOHCl that formed was completely decomposed at 550 °C.

Quintero[28] dehydrated $MgCl_2$ hexahydrate equilibrated under different P_{HCl} / P_{H2O} atmospheres during TGA. He found that hydrolysis could be suppressed with increasing P_{HCl}. However, due to corrosion, he was only able to study the water-rich side of the $MgCl_2$-H_2O phase diagram. Stepwise dehydration was observed but the samples were never analysed for oxides. Kelley[26] mentioned that dehydrating the monohydrate without hydrolysis can be accomplished in an enriched HCl atmosphere below 284 °C. Vil'nyanskii's work[30] claimed that it was impossible to fully dehydrate the monohydrate without hydrolysis, regardless of the P_{HCl} in the atmosphere.

Herbstein et al.[32] have also done some kinetic studies on the thermal decomposition of $MgCl_2 \cdot 6H_2O$ using X-ray diffraction. They claimed that further dehydration of the dihydrate followed Reactions (46)-(48) in dry air or nitrogen and formed non-stoichiometric oxides. The non-stoichiometric oxides can be represented as solid solution of $MgCl_2$ and MgOHCl (e.g Mg_2OHCl_2).

$$MgCl_2 \cdot 2H_2O \rightarrow MgCl_{1.5}(OH)_{0.5} \cdot H_2O + \tfrac{1}{2} HCl + \tfrac{1}{2} H_2O \quad (46)$$

$$MgCl_{1.5}(OH)_{0.5} \cdot H_2O \rightarrow Mg(OH)Cl \cdot 0.3H_2O + \tfrac{1}{2} HCl + 0.2\ H_2O \quad (47)$$

$$Mg(OH)Cl \cdot 0.3H_2O \rightarrow MgO + HCl + 0.3H_2O \quad (48)$$

Furthermore, the temperature of decomposition of MgOHCl was found to be 470 °C. They found evidence that the hydroxyl ions can easily interchange with the chloride in MgOHCl

compounds, depending on P_{HCl}. This idea of interchanging the chlorine ion with the hydroxyl ions was first mention by Vil'Nyanskii et al[30].

Galwey et al. [33] have studied the thermal decomposition of $MgCl_2$ dihydrate by alkalimetric titration of the capture HCl gas. Tests were carried out in dry nitrogen and nitrogen gas containing 10 torr (0.013 atm) water vapour. The temperature varied between 350 °C and 430 °C for both experiments, well within the range of MgOHCl formation. Their results showed that MgO was the main product of hydrolysis, not MgOHCl as expected. They claimed that the reaction was controlled by an "*interface advance mechanism*". The presence of water vapour accelerated the hydrolysis reaction. Furthermore, they claimed that the decomposition of MgOHCl to MgO was slow as compared to the hydrolysis of $MgCl_2$.

The hydrolysis of $MgCl_2$ can be suppressed if its activity is reduced. One example is the dehydration of carnallite. Orekhova[34] also displayed this fact when dehydrating $MgCl_2$ containing NaCl.

2.6.2. MgO in Molten Salts Containing $MgCl_2$

The hydrolysis of molten salts containing $MgCl_2$ is known to produce two oxides: solid MgO and dissolved oxide[12,21,35,36,37,38]. Melts containing $CaCl_2$ might form CaO, but Reaction (49) occurs[39].

$$CaO_{(s)} + MgCl_{2(l)} \rightarrow MgO_{(s)} + CaCl_{2(l)} \quad (49)$$

$$\Delta G^{o}_{(49)}\Big|_{823\,K}^{1023\,K} = -143188 + 26.7T - 4.3\times10^{-3}T^{2} \quad (J)^{8} \quad (50)$$

MgO is insoluble in molten salts. An explanation of MgO precipitation has been attempted by Combes[40]. Reaction (51) expresses the dissolved form of MgO as a complex and has an equilibrium constant associated with it. Measurements were performed by potentiometric titration of O^{2-} ions by Mg^{2+} ions using barium oxide. Their results confirmed that Reaction (52) represents the precipitation of MgO.

$$2Mg^{2+} + O^{2-} \leftrightarrow Mg_2O^{2+} \quad (51)$$

$$Mg_2O^{2+} + O^{2-} \leftrightarrow 2MgO_{(s)} \quad (52)$$

Boghosian et al.[39] have studied the oxide complexes in alkali-alkaline-earth chloride melts by means of alkalimetric titrations. They claim that the solubility of MgO was not affected by temperature between 730-830 °C. Results have shown that it was reasonable to assume that the oxide present in NaCl-$MgCl_2$-MgO system was in the form of Mg_2OCl_2, as shown in Reaction (53). This finding was in good agreement with Combes, who suggested that the oxide was in the form of Mg_2O^{2+}. This relationship was based on the results that MgO solubility was dependent on $MgCl_2$ activity.

$$MgO_{(s)} + MgCl_{2(l)} \leftrightarrow Mg_2OCl_{2(diss)} \quad (53)$$

2.6.3. Hydrolysis of $MgCl_2$ in Molten Salts

The only hydrolysis products believed to occur in a molten salt are $MgO_{(s)}$ and dissolved oxides. Ivanov et al.[35] have studied the equilibrium hydrolysis of $MgCl_2$-contaning molten salts. They assumed that MgOHCl disassociated in the molten salt as $MgOH^{+}$ and Cl^{-} ions. Other states of hydroxychlorides were improbable for the following reasons. Firstly, a melt of KCl-NaCl does not undergo hydrolysis, therefore Reaction (54) does not occur and the

OH^- does not form an independent ion. For hydrolysis, they argue that the OH^- must be bonded to a Mg^{2+} ion. Secondly, hydroxyl complexes, $MgOHCl_2^-$ or $MgOHCl_3^{2-}$, were though to be unstable due to the counter polarization of chlorine by protons (sic) of the hydroxyl group and the difference in the chlorine-magnesium and oxygen-magnesium bonds.

$$Cl^- + H_2O \leftrightarrow OH^- + HCl \quad (54)$$

Vindstad et al.'s[37] experimental observations concluded that the Raoultian activity coefficient of MgOHCl decreased as the activity of $MgCl_2$ increased. Interpretations of their result led to several possibilities. Referring back to Combes[40], Vindstad[37] noticed similar trends in the relationship of $MgCl_2$ activity with changing MgO and MgOHCl activity coefficients. Reaction (55) is simply a variation of Reaction (53). The dimmer, $(MgOHCl)_2$, from Reaction (56), was shown not to be an important complex at low MgOHCl concentrations but could be a factor at higher concentrations. The oxide analysis technique was by means of carbothermal reduction.

$$MgOHCl_{(diss)} + MgCl_{2(l)} \leftrightarrow Mg_2OHCl_{3(diss)} \quad (55)$$

$$2MgCl_{2(l)} + 2H_2O_{(g)} \leftrightarrow (MgOHCl)_{2(diss)} + 2HCl_{(g)} \quad (56)$$

Savinkova et al.[41] have studied the effect of temperature and $MgCl_2$ content on dissolved oxide in a molten salt as is illustrated in Figure 20. Solid MgOHCl decomposed above 550 °C, however, dissolved oxide survived at higher temperatures. Eventually, the dissolved oxide decomposed according to Reaction (57), depending on temperature and $MgCl_2$ activity. The experiment was carried out in a hydrated $MgCl_2$ – KCl – NaCl melt. The oxide content was determined via alkalimetric titration.

$$MgOHCl_{(diss)} \rightarrow MgO_{(s)} + HCl_{(g)} \quad (57)$$

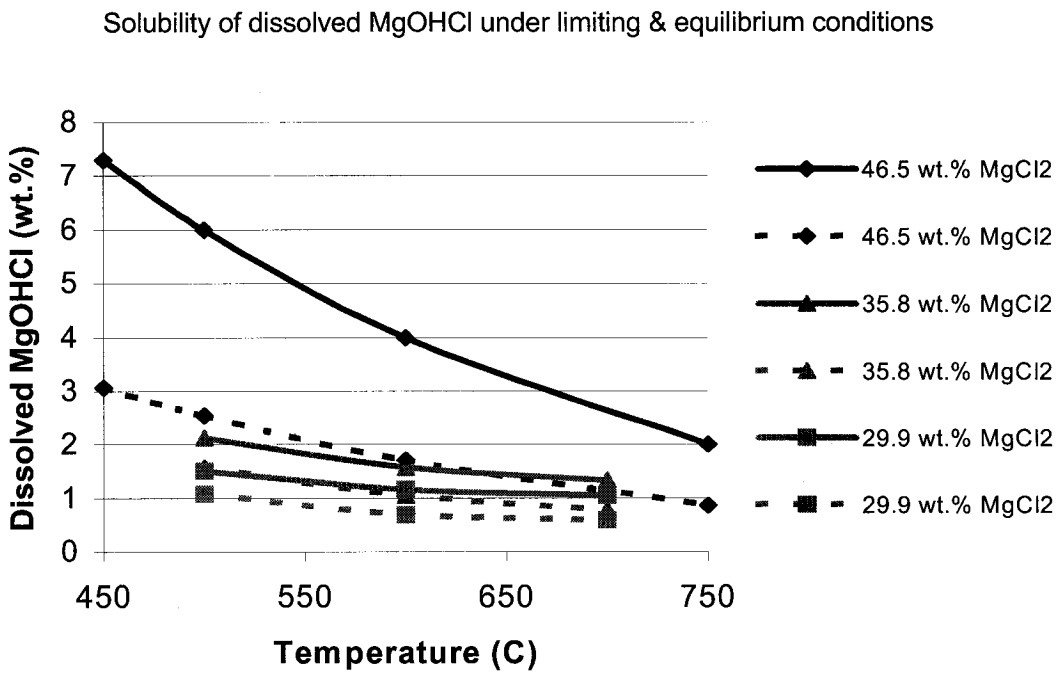

Figure 20 : Experimental data shows the MgOHCl dissolved in a $MgCl_2$ – KCl melt depend on melt temperature and $MgCl_2$ activity[41]. The solid lines represent the limiting conditions where MgO nucleates homogenously. The broken lines represent the equilibrium conditions where MgO nucleates heterogeneously.

The limiting and equilibrium conditions were referenced to homogenous and heterogeneous nucleation, respectively, of MgO from Reaction (57). This implied that if MgOHCl was present above equilibrium conditions but below limiting conditions, it decomposed and the MgO produced nucleated heterogeneously on existing particles, thus less activation energy was required for this type of nucleation. However, if the MgOHCl was present above the limiting value, then MgOHCl decomposed and the MgO spontaneously nucleated homogenously. The large difference in concentration between equilibrium and limiting value represents the necessary energy to overcome the activation barrier for homogenous nucleation. Savinkova[41] was able to study this phenomenon by analysis the size of the MgO particles. Speciation was performed with an alkalimetric titration technique that he developed[42].

Savinkova's[41] graph, Figure 20, is one of the tools used in the present work to determine the presence of dissolved oxides in the electrolyte.

Savinkova et al.[38] have also performed experiments on the hydrolysis of $MgCl_2$ in ternary molten salts. The system studied was $MgCl_2$ – KCL – NaCl – MgOHCl. The oxide content was determined alkalimetrically. Figures 21 and 22 represent the ternary phase diagrams with corresponding activities of $MgCl_2$. The activity of $MgCl_2$ increased with increasing temperature and there was a sharp increase in activity when the mole fraction of $MgCl_2$ was greater than 0.3. It was also noted that maintaining the $MgCl_2$ concentration fixed and adding NaCl increased (sic) the activity of $MgCl_2$. The dissolved oxide content increased with increasing $MgCl_2$ and / or decreasing temperature. A melt composition of $MgCl_2$-NaCl-MgOHCl had more dissolved oxide than a melt of $MgCl_2$-KCl-MgOHCl. In a hydrolyzed melt, the activity of $MgCl_2$ exhibited less negative Raoultian behaviour compared to an anhydrous melt.

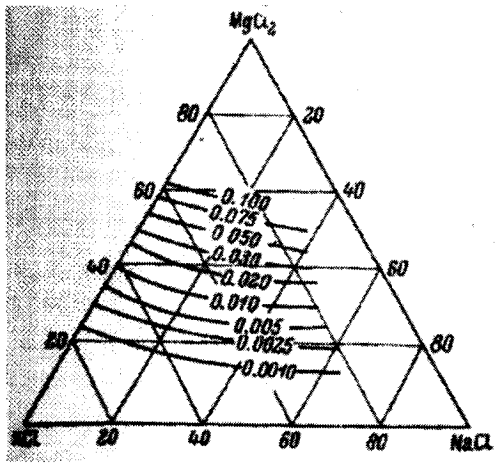

Figure 21 : $MgCl_2$ activity in a $MgCl_2$ – KCl – NaCl melt at 500 °C.[38]

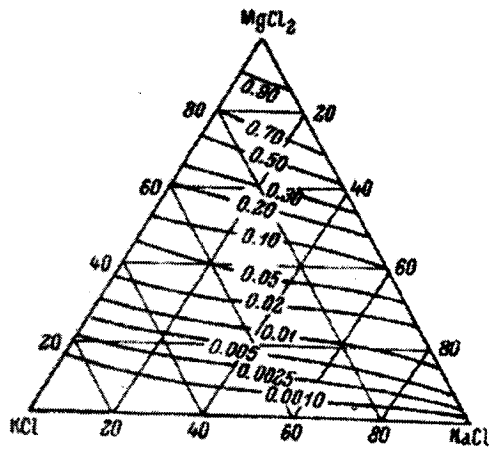

Figure 22 : $MgCl_2$ activity in a $MgCl_2$ – KCl – NaCl melt at 700 °C.[38]

2.7 Chlorination

Lamy[43] has shown that the chlorination of solid MgO particles to dissolved $MgCl_2$ in a molten salt may proceed through an intermediate step as shown by Reactions (58) and (59). His literature review also indicated that the chlorination of carnallite also proceeded the same way. Lukmanova et al.'s[44] article that Lamy[43] referenced proved the presence of dissolved oxides by decomposing it via injecting nitrogen into the melt. The decomposition reaction was Reaction (57), the reverse of Reaction (58).

$$MgO_{(s)} + HCl_{(g)} \rightarrow MgOHCl_{(diss)} \quad (58)$$

$$MgOHCl_{(diss)} + HCl_{(g)} \rightarrow MgCl_{2(l)} + H_2O_{(g)} \quad (59)$$

The reaction mechanism of the chlorination of MgO into MgOHCl was also studied by Lamy[43], who obtained the following rate law:

$$\left(\frac{C_{MgO}}{C^{i}_{MgO}}\right)^{1/3} = 1 - K_n t \quad (60)$$

This relationship fitted the early stages of chlorination because it was assumed that only dissolved MgOHCl was produced and not $MgCl_2$ (i.e. MgO was only partially chlorinated).

There has been no study of the chlorination of dissolved oxides, Reaction (59), and current chlorination models ignore the presence of this reaction. The kinetics of chlorination must include this reaction in order to properly determine the reaction mechanisms.

2.8 Decomposition of Dissolved Oxide by Ar Gas Injection

Prior to undertaking the present Master's degree, the author completed an investigation of the decomposition of dissolved oxide by Ar injection.

The idea of injecting inert gas to decompose dissolved oxide originated from Lukmanova et al.[44] and was also presented in Lamy's thesis[43]. Following this, experiments were performed by Lamy who injected Ar into a hydrolyzed melt to generate a speciation technique. These experiments are discussed here as they promoted my understanding of the prill digestion process.

The speciation technique required two molten salt samples; one melt sample containing both oxides and one melt sample having been treated to cause complete decomposition of the dissolved oxides by inert gas injection. Alkalimetric titrations were done on the two samples. The difference in amount of acid consumed represented the amount of dissolved oxide present in the molten salt prior to inert gas injection. Figure 23 represents the theoretical conversion of $MgOHCl_{(diss)}$ to $MgO_{(s)}$ measured as moles of acid consumed per gram of sample.

A report has been prepared on the experiments[45] performed by the present author. The melt, hydrolyzed using prills, was continuously injected with Ar and samples of the melt were taken every 15 minutes. Alkalimetric titrations determined the level of MgO_{eq}. The amount of $MgO_{(eq)}$ was expected to increase as the dissolved oxide was decomposed following the Reaction (57). The Ar decomposed MgOHCl because the P_{HCl} in the melt decreased.

Experimental difficulties included the solid MgO settling at the bottom of the melt, resulting in unrepresentative samples. However, qualitatively, it was observed that after Ar injection there was a significant increase in the deposit.

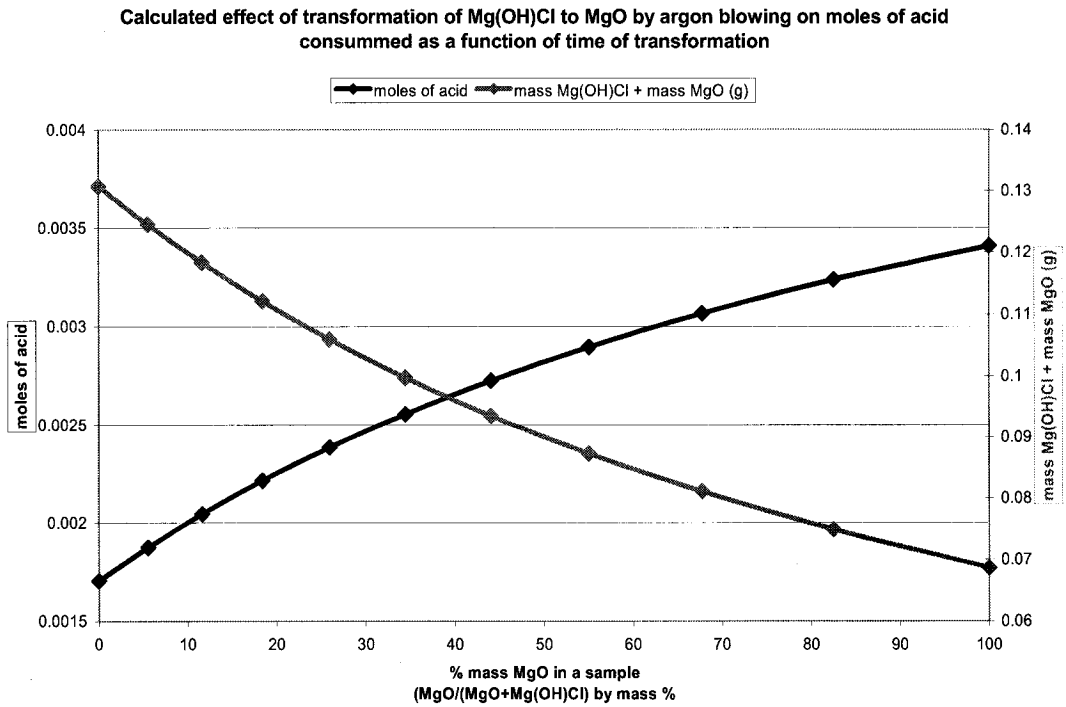

Figure 23 : Theoretical results of alkalimetric titration measuring MgOHCl decomposition.

2.9 Unreliable Mass Balance

The molten salt system is difficult to analyse for its oxide content. Lamy[43] presented a list of possible techniques but all have shortcomings. The shortcomings has been shown by the large variation in previous researchers' works and current experimental analysis has

found that samples are not representative of the melt, particularly for the insoluble $MgO_{(s)}$ that would settle at the bottom of the crucible.

The two most popular methods used to determine the oxide content in molten salts were alkalimetric titrations of molten salt or measurements of the HCl in the off-gas. Uncertainties arise for both methods. Moreover, they are unreliable for the following reasons.

The samples collected from the molten were not necessarily representative of the melt. Firstly, during the cooling and freezing of the melt in the sample tube, the structure of the dissolved oxide changes and there is likely to be segregation. Secondly, in the particular setup, the settling of $MgO_{(s)}$ was unavoidable, which led to samples that were not representative of the melt.

Another method for oxide determination involves the collection of off-gas, which can also introduce large errors. Firstly, collecting all of the gas phase was difficult. Secondly, using the amount of HCl collected and calculating the amount of oxides present was an indirect method of measuring oxide content, presenting large experimental errors. A good example of this fact was given when Galwey & Laverty[33] incorrectly concluded using off-gas analysis that MgOHCl was not formed when dehydrating dihydrate.

2.10 Comments on Novelty

The MMI process does not take into account the solid-state hydrolysis of $MgCl_2$ occurring in the prills when they are fed into the "Super Chlorinator". There is twice the amount of water required to hydrolyze $MgCl_2$ in the $MgCl_2{\cdot}2H_2O$ compound. The literature indicated that dehydrating beyond the dihydrate produced substantial amount of oxides. In addition, it is difficult to imagine that the $HCl_{(g)}$ contacts the fast dehydrating prill as water vapour is rapidly flashing off. The time window that is available for the $HCl_{(g)}$ to penetrate the dehydrating prill, a mass transfer step, is just a few seconds.

The "Super Chlorinator" was said to operate as an equilibrium reactor[9], but to date, the kinetics of dehydration and hydrolysis have not been studied. The fast dehydrating prills are not thermodynamically controlled, as the partial pressure surrounding a prill is not constant. Quintero[28] wrote on p.20 of his thesis: "*When a particle of hydrate is undergoing dehydration a porous structure is developed to accommodate a flux of water vapour to the*

surroundings (9). This changes the local ratio of P_{H2O}/P_{HCl} in such a way that hydrolysis can proceed even if the bulk atmosphere has a composition where MgOHCl is not a stable phase." The reference (9) was a French patent from Nadler[46].

The only oxide present in the electrolyte was assumed to be MgO, the presence of dissolved oxides was discounted. The reason for this was that solid MgOHCl was not stable at the operating temperature of the electrolyte and decomposed into $MgO_{(s)}$ and $HCl_{(g)}$. However, prill digestion is an endothermic reaction (dehydration) and the temperature of the melt surrounding the prill can be lowered. In addition, the dissolution of solid MgOHCl into the molten salt and its stability therein has never been studied.

3 METHODOLOGY & EXPERIMENTAL PROCEDURES

3.1 Methodology

The heating and dissolving (digestion) of prills on molten salt has never been visually studied in detail, perhaps due to misplaced safety concerns or due to a misunderstanding of potential importance of the mechanisms in the overall process performance. It is reasonable to say that the designers of MMI believed that the prills would instantaneously transform from solid to liquid when they touched the molten salt. This belief follows from the hypothesis that the prills melt in their own waters of crystallization.

Upon heating, the mechanisms of prill digestion have been difficult to study because quantitative results, such as $MgCl_2$ and oxide contents, were accompanied by large experimental error. Furthermore, $MgCl_2$ is very hygroscopic and there are no reliable speciation techniques for the oxides produced in the melt by hydrolysis. Most of the experiments performed were qualitative in nature. It should also be mentioned that the present author believes the dissolved species in the electrolyte are in the form of ions as opposed to compounds.

In the present work, synthetic electrolyte was prepared from a mixture of NaCl (99+ %, Sigma Aldrich), $MgCl_2$ (98 %, Sigma Aldrich), $CaCl_2$ (97 %, Sigma Aldrich), and KCl (99 %, Sigma Aldrich) solid salts similar to MMI's electrolyte composition but the exact electrolyte composition is proprietary. The solid chemicals were mixed and charged into a 54 mm ID quartz tube. When $HCl_{(g)}$ was used, the quartz tube was covered by a water-cooled stainless steel (SS) cap connected via a graphite adapter to form a gas-tight reactor. The off-gas from the reactor was directed to a gas scrubbing system to capture the HCl and H_2O gases generated in the tests. The reactor, loaded with the solid charge, was placed in a glowbar furnace. The top of the reactor with the water-cooled cap extended out of the furnace. A window was opened in one of the sidewalls of the furnace, as shown in Figure 24, to allow visual observation and video recording of the molten salt bath. The molten salt bath temperature was monitored continuously throughout the experiments by an immersed thermocouple.

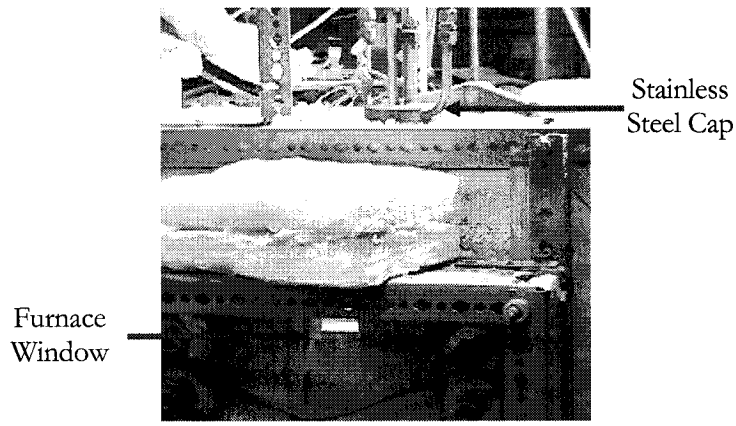

Figure 24 : Configuration of sidewall viewing port in the glow bar furnace used to heat the reaction vessel.

3.1.1. Experimental Setup

A transparent crucible was required for the visual observation of prill digestion. Due to the high operating temperature, quartz was chosen as the crucible material. The quartz crucible, custom made by Chemglass Inc[47], was a 54 mm ID quartz tube, was closed at one end and was 10.5" (26.67 cm) long with 2 mm thick walls. The video camera used to record the experiments was a JVC, model GR-DVL-310, digital video camera.

The circumference of the SS cap was water cooled to increase the life of the o-ring cap seal due to the corrosive environment. The SS cap is shown in Figure 25. It was equipped with openings for insertion of a thermocouple for temperature measurement and a lance for gas injection. A port that allowed material addition without disturbing the gas atmosphere in the reactor was also available (not shown). The ID of the cap was 3" (7.62 cm). A graphite adapter was used between the cap and the crucible. The ID of the adapter was 54 mm and the OD was 3" (7.62 cm). Dow Corning® high temperature vacuum grease and Dow Corning® RTV sealant (732 Multi-purpose sealant) were used to ensure a hermetic seal.

Two thermocouples were used. A K-type thermocouple immersed in the melt was used to monitor the bath temperature. It was 14 AWG (2.0 mm^2) and 24" (60.96 cm) long and was sheathed with a ceramic thermocouple protection tube. The ceramic sheath was 99.8 % alumina. The dimensions of the sheath were ¼" (6.35 mm) ID, 3/8" (9.53 mm) OD and 12"

(304.8 mm) in length. A R-type thermocouple was used to monitor the furnace temperature. The two-thermocouple furnace control system was designed in house[48].

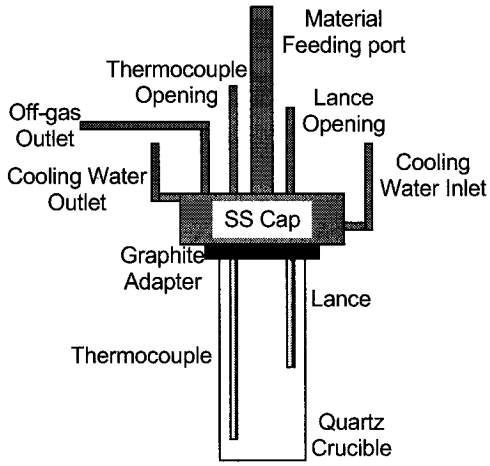

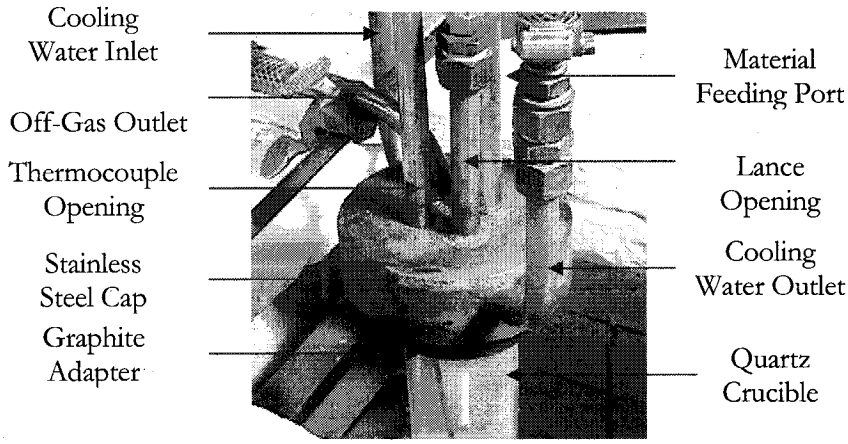

Figure 25 : Crucible with cap installed inside glow bar the furnace.

The gas injection lance was a single bore tube made with 99.8 % alumina. The dimensions were ¼" (6.35 mm) OD, 0.125" (3.18 mm) ID and 500 mm in length. The gas supply system allowed switching between Ar and HCl. A schematic is shown in Figure 26. A purging unit was designed to prevent the corrosion of the regulator. The $HCl_{(g)}$ flowrate was determined using the Ar calibration curve by comparing the flowrates of the two gases at the same flowmeter position. Having the same flowmeter position implied that the momentum of the gas was the same, Equation (61). Using Equations (61) and (62) gives Equation (63) and because the area was the same at the same flowmeter position, rearranging the terms leads to Equation (64). Equation (65) demonstrates the small

difference in volumetric flowrate. It should be noted that the density of HCl was slightly less than Ar.

$$\frac{1}{2}\rho_{Ar}v_{Ar}^2 = \frac{1}{2}\rho_{HCl}v_{HCl}^2 \tag{61}$$

where ρ is density and v is velocity

$$v = \frac{Q}{A} \tag{62}$$

where Q is volumetric gas flowrate and A is cross-sectional area of the flowmeter tube

$$\frac{1}{2}\rho_{Ar}\left(\frac{Q_{Ar}}{A}\right)^2 = \frac{1}{2}\rho_{HCl}\left(\frac{Q_{HCl}}{A}\right)^2 \tag{63}$$

$$Q_{HCl} = \sqrt{\frac{\rho_{Ar}}{\rho_{HCl}}}Q_{Ar} \tag{64}$$

$$\rho_i = \frac{P}{RT} \times MW_i$$

$$\sqrt{\frac{\rho_{Ar}}{\rho_{HCl}}} = \sqrt{\frac{39.948}{36.461}} = 1.047$$

$$Q_{HCl} = 1.047Q_{Ar} \tag{65}$$

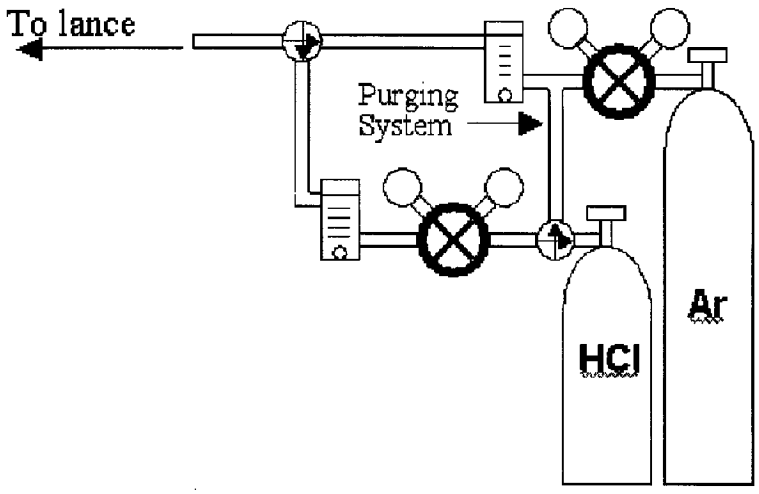

Figure 26 : Gas system.

The off-gas was passed through a series of water scrubbers, as shown in Figure 27, to capture any $HCl_{(g)}$ before being exhausted into the laboratory fume system. The scrubbers were made with six one-litre Erlenmeyer flasks connected in series. About 500 ml of tap water was used in each of Flasks 2 to 5. Flask 1 and 6 were empty to prevent any water from leaving the scrubbing system. The gas was injected into Flask 2 through Flask 4 using a ½" (1.27 cm) OD Teflon hose. Flask 5 was equipped with a gas dispersion tube made of a sintered glass frit.

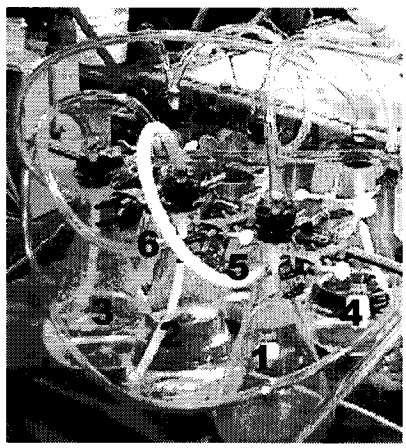

Figure 27 : Water-scrubber system.

The glow bar furnace was built in house at McGill University and Roumeliotis[48] gave specifications. Essentially, it is a resistance furnace using six silicon carbide heating elements with an interior volume of 0.11 m^3. The temperature was controlled using two PID controllers, Omega model CN911A, connected in series. One PID controller monitored the bath temperature and is referred from now on as the "bath temperature controller". The other PID controller was used to monitor the furnace temperature and is referred from now on as the "furnace temperature controller".

3.2 Experimental Procedures

The present work comprised a number of simple experiments, the design of which followed from one to the next as observations were made, conclusions were drawn and hypothesis were tested. The various tests that were performed are sequentially described below.

3.2.1. Digestion of MMI Prills

Objective:

The objective of the present experiment was to visualize prill digestion and to this end a melt of synthetic MMI electrolyte was prepared and prills were added to the surface of the melt. The experiment was recorded and observations were made.

Procedures:

Preparation of the molten salt

- Charge: 150 g of synthetic electrolyte (nominal MMI composition with 35 wt.% $MgCl_2$) in the quartz crucible, without the SS cap.
- Ar atmosphere maintained during heating and melting by keeping a flow of Ar through the lance opening that was positioned approximately 3 cm above the solid charge. The flowrate was 0.75 SLPM.
- Furnace and bath temperature controllers set to 750 °C and 650 °C, respectively.

- Bubbling behaviour and deposit that formed was noted and recorded on occasion.

- Once melted, furnace and bath temperature controller set points were adjusted to 650 °C and 550 °C, respectively.

Digestion of prills

- The melt temperature was allowed to stabilize while the Ar flow was maintained at 0.75 SLPM.

- 10 g of prills were added onto the surface of the melt.

- The digestion and bubbling behaviours were visually recorded.

3.2.2. Injecting Ar and HCl Into a Molten Salt Containing Oxides

Objective:

The objectives of the present experiment were to observe the decomposition of the dissolved oxide by injecting Ar and to observe the chlorination of the solid oxide by injecting HCl. As mentioned in the literature review, injecting Ar into the melt was believed to decompose the dissolved oxide into $MgO_{(s)}$. The solid MgO would precipitate and should be observed as it settles. Moreover, the solid MgO was chlorinated by injecting HCl. Thus injecting either of these gases was though to "clean" the melt of dissolved oxides. The present experiment allowed visual observation of these phenomena. A melt of synthetic MMI electrolyte was prepared and prills were added to the surface of the melt. Ar and HCl were injected. The experiment was recorded and observations were made.

Procedures:

Preparation of the molten salt

- Charge: 150 g of synthetic electrolyte (nominal MMI composition with 35 wt.% $MgCl_2$) in the quartz crucible using the SS cap to create a gas tight reactor.

- Ar atmosphere was maintained during heating and melting by keeping a flow of Ar through the lance opening that was position approximately 3 cm above the solid charge. The Ar flowrate was 0.75 SLPM.

- Furnace and bath temperature controllers were set to 750 °C and 650 °C respectively.

- The bubbling behaviour and deposit that formed was noted and recorded on occasion.

- Once melted, furnace and bath temperature controller set points were adjusted to 650 °C and 550 °C, respectively.

Ar injection

- The melt temperature was allowed to stabilize while the Ar flow was maintained at 0.75 SLPM. The gas flowrate remained constant throughout the tests.

- The lance was lowered and submerged into the melt, positioned approximately 3 cm beneath the surface. Injection time was 15 minutes.

- The lance was then raised approximately 5 cm above the melt surface. Ar flow was maintained.

- The deposit was recorded and noted.

- A batch of 10 g of prills was added onto the surface of the melt via the material feeding port on the water-cooled gas tight reactor. The digestion process and bubbling behaviour were visually recorded.

- Once reactions were complete, the lance was again lowered and submerged into the melt, positioned approximately 3 cm beneath the surface. Injection time was 15 minutes.

- The lance was then raised approximately 5 cm above the melt surface. Ar flow was maintained.

- The deposit was recorded and compared to the deposit after melting.

HCl injection

- The gas supplied to the lance held above the melt was changed to HCl and an HCl atmosphere was maintained with a flowrate of 0.75 SLPM. The gas flowrate was constant throughout the test. The change in the appearance of the melt and the deposit on the reactor wall above the melt under the new atmosphere was noted.

- The lance was lowered and was submerged into the melt, approximately 3 cm from the surface. Injection time was 15 minutes.

- The lance was then raised approximately 5 cm above the melt surface and an HCl flow was maintained.

- The deposit was recorded and compared to the deposit after prill digestion.

During the above-mentioned experiments, intense bubbling was observed after the prills were digested. The terms "Primary Bubbling" and "Secondary Bubbling" are used to describe the bubbling observed when the prills were first added and after the prills were dissolved, respectively. A detailed discussion about this observation and nomenclature is presented in the following chapter. The experiments that follow were designed to further explore these observations.

3.2.3. Effect of Temperature on Secondary Bubbling

Objective:

The objective of the present experiment was to validate the hypothesis that Secondary Bubbling was due to the decomposition of a dissolved oxide in the molten salt. Following Savinkova's results[41], Figure 20, the dissolved oxide was believed to be MgOHCl and was thought to decompose according to Reaction (57), as melt temperature was increased. Assuming that the dissolved oxide in synthetic MMI electrolyte behaved the same way as

the dissolved MgOHCl in the literature, the solubility of dissolved oxides decreased as the temperature increased. Thus, Secondary Bubbling occurred when the temperature was increased. For this reason, the solid charge was melted slowly, not exceeding 550 °C, to determine if any dissolved oxides were generated during melting.

Procedures:

Secondary Bubbling prior to prill addition

- Charge: 150 g of synthetic electrolyte (nominal MMI composition with 35 wt.% $MgCl_2$) in the quartz crucible, without the SS cap.
- Ar atmosphere was maintained during heating and melting by keeping a flow of Ar through the lance opening that was approximately 3 cm above the solid charge. The flowrate was constant 0.75 SLPM.
- Furnace and bath temperature controllers were both set to 550 °C.
- Once the solid charge was completely melted, the furnace and bath temperature controllers were both adjusted to 675 °C.
- Bubbling behaviour and deposit that formed upon the temperature increase was noted.
- The furnace and bath temperature controllers were both adjusted to 550 °C.
- Once the melt temperature stabilized and immediately prior to prill addition, the furnace temperature controller was adjusted to 300 °C (to prevent the activation of the heating elements).
- A batch of 10 g of prills was added onto the surface of the melt. The temperature drop was noted.
- Once digestion was complete, the furnace and bath temperature controllers were both adjusted to 675 °C.

- Bubbling behaviour and deposit that formed upon the temperature increase were noted.

- The test was repeated several times; i.e., the temperature was reduced, prills were added, and the temperature was increased. Observations were made.

3.2.4. Effect of $MgCl_2$ Activity on Secondary Bubbling

Objective:

The objective of the present experiment was to validate the hypothesis that Secondary Bubbling was due to the decomposition of dissolved oxides in the molten salt. The experiment compared the Secondary Bubbling behaviour in two molten salt baths: one with low $MgCl_2$ content and the other with high $MgCl_2$ content. Savinkova's results[41], Figure 20, showed that the solubility of the dissolved oxide, believed to be dissolved MgOHCl, was a function of $MgCl_2$ activity. Assuming that the dissolved oxide in synthetic MMI electrolyte behaved the same way as in the literature, the solubility of the dissolved oxide should decrease as the $MgCl_2$ activity decreases.

The rational for the experimental design was as follows. A molten salt with low $MgCl_2$ activity contained less dissolved oxide and should more readily reach saturation when oxides were added. Assuming that adding the same amount of prills in both baths introduced the same amount of water and produced the same amount of solid MgOHCl, it was expected that a melt with low $MgCl_2$ content reached saturation by adding fewer prills than a bath with a high $MgCl_2$ content. The saturation led to the decomposition of dissolved oxides according to Reaction (57), whereby HCl gas evolved and led to the observation of the onset of "Secondary Bubbling" as a function of the experimental parameters.

As can be seen in Figure 20, the solubility of dissolved MgOHCl in the melt was negligible at high temperatures (> 700 ^{0}C), regardless of the $MgCl_2$ content in the bath. Therefore, complete decomposition of dissolved oxide was assumed to occur by increasing the temperature to 900 ^{0}C.

Since the bath with a high $MgCl_2$ content was initially though to contain more dissolved MgOHCl, it was expected that more HCl gas be evolved during Secondary Bubbling as compared to that in the molten salt bath with low $MgCl_2$ content.

Procedures:

Preparation of the molten salts

- The experiment was carried out under ambient atmosphere and the molten salt baths were filmed continuously.

- Two molten salt baths were prepared. The bath with low $MgCl_2$ content was termed "Bath 1" and the bath with a high $MgCl_2$ content was termed "Bath 2". The composition of the two baths is summarized in Table 2.

Table 2 : Molten salt composition used in experiment to study the effect of $MgCl_2$ activity on Secondary Bubbling. (activities from Fact*Sage*™ FACT-SALT solution model[8])

	Bath 1	**Bath 2**
Wt.% NaCl	36.20	34.40
Wt.% $CaCl_2$	44.95	13.61
Wt.% $MgCl_2$ (activity)	15.88 (0.0203)	49.04 (0.146)
Wt.% KCl	2.98	2.94
mass ratio NaCl:$CaCl_2$	0.8	2.5
Total mass (g)	100.75	101.95

- The solid chemicals for each bath were mixed and charged into two separate quartz crucibles. The two quartz crucibles were placed adjacent to each other in the furnace to allow direct visual observation. The setup is shown in Figure 28.

Figure 28 : Photograph of the two melts used in experiments to study the effect of $MgCl_2$ activity on Secondary Bubbling.

- The K-type bath thermocouple was arbitrarily placed in Bath 2. Due to the configuration of the setup, it was assumed that the temperature of the two baths was the same. It was also assumed that the amount of heat absorbed by the reaction during decomposition did not affect the results, although Fact*Sage*™ shows that Reaction (42) has:

$$\Delta H^{o}_{(42)}\Big|_{823\,K} \approx 100 \quad kJ/mol$$ [8]

- The furnace and bath temperature controllers were set to 900 °C to melt the solid charge and to decompose all the dissolved oxides. The melt was assumed to be clean of dissolved oxide once Secondary Bubbling stopped.

- Once Secondary Bubbling stopped, the furnace and bath temperature controllers were both adjusted to 550 °C.

- Batches of prills, 2 g each, were added to both molten salts to increase the concentration of dissolved oxides. Secondary Bubbling was expected in Bath 1 with fewer batches of prill additions, as the dissolved oxide concentration, sufficient to drive decomposition, was expected to be reached sooner than in Bath 2.

- When sufficient batches of prills had been added to both baths, it was expected that Secondary Bubbling would occur in both baths.

- Upon completion of Secondary Bubbling in both baths, it was assumed that the baths were still saturated with dissolved MgOHCl (Bath 2 containing more dissolved oxide than bath 1). The furnace and bath temperature controller set points were both adjusted to 900 °C

3.2.5. Identifying the Gas Phase During Secondary Bubbling

Objective:

The solid deposit generated upon addition of prills to the molten salt or due to the decomposition of dissolved oxide was shown to be MgO via EDX and XRD (discussed in section 3.2.1). Still, the composition of the off-gas during Secondary Bubbling needed to be determined. The decomposition of the dissolved oxide occurred according to Reaction (57). However, there is another reaction that can determine the equilibrium activity of MgOHCl, Reaction (59).

$$MgOHCl_{(diss)} \rightarrow MgO_{(s)} + HCl_{(g)} \quad (57)$$

$$MgOHCl_{(diss)} + HCl_{(g)} \leftrightarrow MgCl_{2(diss)} + H_2O_{(g)} \quad (59)$$

Therefore, the off-gas could be a mixture HCl and water vapour. Consequently, a condenser was attached at the beginning of the off-gas line, prior to the HCl scrubbing to capture the water vapour that evolved. With this particular setup, it was possible to determine the extent of Reaction (59).

A melt of synthetic MMI electrolyte was prepared and prills were added to the molten salt. The temperature was increased to promote Secondary Bubbling and the off-gas was collected. Alkalimetric titrations were performed to determine the composition of the condensate and the liquor in the HCl trap.

Procedures:

Preparation of the molten salt

- Charge: 150 g of synthetic electrolyte (nominal MMI composition with 35 wt.% $MgCl_2$) in the quartz crucible using the SS cap to create a gas tight reactor.

- Ar atmosphere was maintained during heating and melting by keeping a flow of Ar through the lance opening that was positioned approximately 3 cm above the solid charge. The flowrate was constant throughout the experiment at 0.75 SLPM.

- Furnace and bath temperature controllers were set to 750 °C and 650 °C, respectively.

- Bubbling behaviour and deposit that formed was noted and recorded on occasion.

- Once melted, the furnace and bath temperature controller set points were adjusted to 650 °C and 550 °C, respectively.

- The gas supplied to the lance was changed to HCl with a flowrate of 0.75 SLPM.

- The lance was lowered and was submerged into the melt positioned approximately 3 cm beneath the surface. Injection time was 15 minutes. (This procedure 'cleaned' the melt of oxides.)

- The lance was then raised approximately 5 cm above the melt surface and the gas supplied to the lance was changed to Ar with a flowrate of 0.75 SLPM.

- The lance was again lowered and was submerge into the melt positioned approximately 3 cm beneath the surface. Injection time was 15 minutes. (This procedure removed any residual HCl from the melt).

- The lance was then raised again approximately 5 cm above the melt surface.

- The furnace temperature controller was adjusted to 300 °C to prevent the activation of the heating elements. The cooling water to the SS cap was temporarily closed so that the temperature of the cap raised somewhat and lessened the condensation on it, if any.

- Soon after the adjustment of the furnace temperature controller, 10 g of prills were added onto the surface of the melt via the material feeding port on the SS cap

- Once digestion was complete, the off-gas line was switched as shown in Figure 29 so that a condenser and a single water scrubber were included in to the off-gas system prior to the water scrubbers.

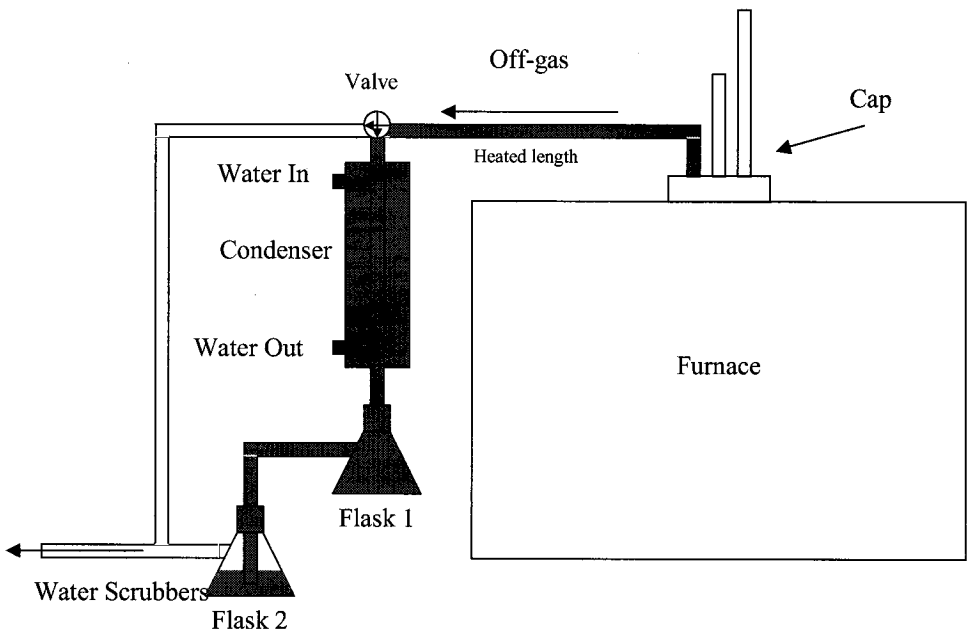

Figure 29 : Experimental setup for capturing water vapour and HCl gas.

- Both temperature controllers were then adjusted to 900 °C to heat the melt and decompose the dissolved oxide. The off-gas line was gently heated

with a blowtorch to prevent condensation along its length ahead of the condenser.

- Water vapour was condensed in the water-cooled condenser and collected in a 250 ml flask, from now on referred to as "Flask 1", as shown in Figure 29.

- The balance of the gas went to a second 250 ml flask, from now on referred to as "Flask 2", containing 100.00 ml (2 X 50.00ml pipette) of distilled water to capture any HCl gas. The residual gas, now considered to be only Ar, went to the water scrubbers.

- The mass of the condensed liquor in Flask 1 was determine using a Sartorius™ scale model LP2200S.

- Alkalimetric titrations of the liquor in Flasks 1 and 2 were performed using a Schott Titroline Easy™ automatic titrator equipped with a magnetic stirrer and Schott Blueline 17 pH electrode. The titrating parameters were preset and the "pH fast weak" was used as the results were found to be reproducible compared to the other presets. The condensed water from Flask 1 was diluted with distilled water using a 250.00 ml volumetric flask. Three independent measurements of 20.00 ml solution were titrated with 0.0485 (± 0.0015) N NaOH. Additionally, 20.00 ml of solution from Flask 2 was titrated against 0.0485 (± 0.0015) N NaOH.

3.2.6. Effect of Atmosphere During Prill Digestion

Objective:

The objective of the present experiment was to determine if the bulk atmosphere had a significant effect on the production of oxides during prill digestion. In these tests, two baths of identical composition were prepared and placed adjacent to one another. The temperature was assumed to be the same in both baths and direct visual observations were made. One bath had a bulk atmosphere of Ar and the other of HCl. The amount of the oxide produced was determined by measuring the change in the thickness of the settled oxide formed by decomposing the dissolved oxide after the digestion of prills was

complete using Ar injection. Although the measurements were not particularly precise, differences were large enough to clearly show trends.

In addition to varying the atmosphere, the prill feeding rate was also studied. Prills were fed onto the surface of the molten baths in two ways. The first was by adding 5 batches of prills weighing 2 g each for a total of 10 g in both baths. This was to allow the atmosphere surrounding the prill to be close to the bulk atmosphere as the rate of water vapour evolution was lower and hence less diluting of the bulk HCl atmosphere. The second feeding method was by adding 10 g of prills in one shot. This feeding method lessened the effect of the bulk atmosphere, by having more local vapour dilution.

Procedures:

Preparation of the molten salts

- Charge: two 150 g synthetic electrolyte baths (nominal MMI electrolyte composition with 30 wt.% $MgCl_2$). The bath under HCl atmosphere was called "HCl Bath" and the bath under Ar atmosphere was called "Ar Bath". The HCl Bath was equipped with the SS cap and the Ar Bath was covered with a piece of malleable refractory material.

- The bath thermocouple was arbitrarily placed in the HCl Bath during heating and melting. However, the bath thermocouple was moved to the Ar Bath during prill digestion when the Ar Bath was subject to the slow feeding rate.

- Both baths were held under Ar during heating and melting of the solid charges.

- The furnace and bath temperature controllers were set to 750 °C and 650 °C, respectively, during heating and melting of the solid charges.

- Once molten, both lances were submerged into the molten salt. Ar was injected for 15 minutes at a flowrate of 0.75 SLPM.

- After 15 minutes of Ar injection, the lances were raised approximately 5 cm above the melt surface and the solids in the baths were allowed to settle.

- Once settled, the bath temperature controller was adjusted to 550 °C.

- The deposit thickness was recorded prior to prill addition and digestion.

- The gas supplied to the HCl Bath lance was switched to HCl and a flowrate of 0.75 SLPM was maintained. The cooling water to the SS cap was temporarily turned off.

- When the atmosphere in the reactor was HCl, after approximately 3 minutes of HCl purging, a batch of 2 g of prills was added onto the surface of the melt in the HCl bath. Once the prills disappeared, another batch of prills was added. These additions were repeated until a total of 10 g was added.

- The cooling water for the SS cap was turned on.

- The bath thermocouple was moved to the Ar Bath.

- A batch of 2 g of prills was added onto the surface of the melt of the Ar Bath. Once the prills disappeared, another batch of prills was added. These additions were repeated until a total of 10 g was added.

- The bath thermocouple was moved back to the HCl Bath.

- The gas supplied to the HCl Bath lance was switched to Ar and once both baths were being supplied with Ar gas, both lances were submerged into the molten baths a second time. Ar was injected for 15 minutes at a flowrate of 0.75 SLPM.

- After the Ar injection, the bath temperature controller was adjusted to 650 °C to increase the settling rate of the solid oxide. Increasing the temperature was believed to render the molten salt less viscous, helping

the fine particles settle. Once settled, the bath temperature controller was adjusted again to 550 °C.

- The deposit thickness, after prill digestion with the slow feeding rate, was recorded in both baths.

- The gas supplied to the HCl Bath lance was switched back, a second time, to HCl and a flowrate of 0.75 SLPM was maintained. The cooling water to the SS cap was temporarily turned off a second time.

- When the atmosphere in the reactor was HCl after 3 minutes of HCl purging, 10 g of prills were added onto each of the surfaces of the melts.

- Once prill digestion was complete, the cooling water supplied to the SS cap was turned on a second time.

- The gas supplied to the HCl Bath lance was switched to Ar a second time. When both baths were being supplied with Ar gas, both lances were submerged into the molten salt a third time. Ar was injected for 15 minutes at a flowrate of 0.75 SLPM.

- After the Ar injection, the bath temperature controller was increased a third time to 650 °C to increase the settling rate of the solid oxide, as increasing the temperature is believed to decrease the viscosity of the molten salt.

- The deposit thickness was recorded in both baths.

4 RESULTS

4.1 Digestion of MMI Prills

Melting of the salt bath

During the melting of the nominally anhydrous solid components used to create the charges for the tests, it was observed that bubbles evolved from the solid portion of the partially melted bath, Figure 30. These bubbles were believed to be H_2O that evolved from hydrated components in the salts upon heating. These observations were corroborated by the chemical assay provided by the supplier that indicated, for example, the nominally anhydrous $MgCl_2$ contained 1.5 wt.% water.

It can be foreseen that such moisture present could hydrolyse the $MgCl_2$ with the result that some of the gas that evolved could have been HCl.

Small (approximately 0.5 mm) black particles were seen dispersed in the bath upon melting and originated from the $MgCl_2$ feedstock. The analysis of these particles is presented in Appendix 1. These particles are hereafter referred to as "inert particles".

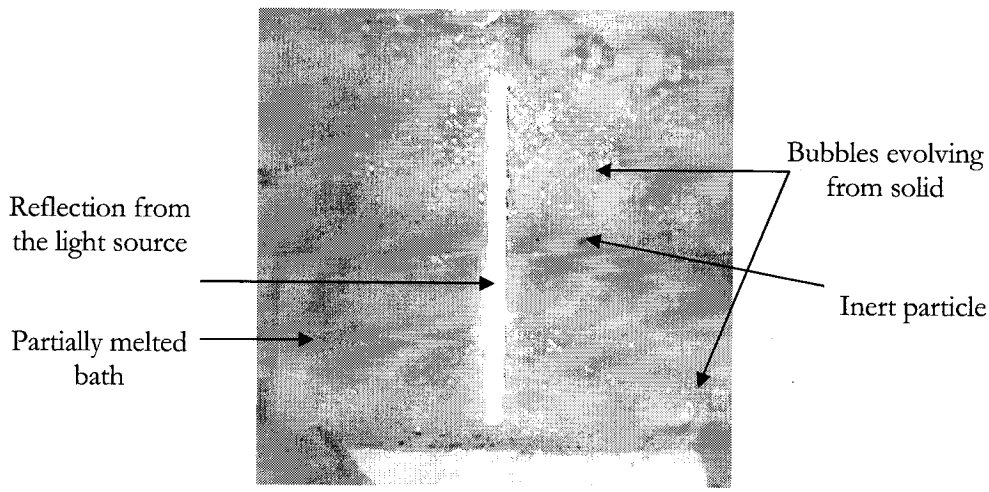

Figure 30 : Bubbles evolving during melting of the solid salt charge to form synthetic electrolyte melts.

Towards the end of melting, a different type of bubbling was observed and as this bubbling progressed, a layer of solid deposit accumulated at the bottom of the reactor. In order to distinguish the different types of bubbling behaviour, this type of bubbling behaviour was termed "Secondary Bubbling", whereas the bubbling due to evolution of H_2O was called "Primary Bubbling".

The average size of the bubbles evolving during Secondary Bubbling (less than 1 mm in diameter) was much smaller than those observed during Primary Bubbling (3 to 10 mm in diameter). Also, the bubbles during Secondary Bubbling were seen to mostly form on the surface of the solid particles at the bottom of the reactor or particles dispersed in the melt. This suggested that these small bubbles required a nucleation site. The bubbles were also seen to congregate at the surface of the bath and eventually collapse. There was a peak in the intensity of the Secondary Bubbling with the most intense bubbling appearing similar to rapidly boiling water.

The intense bubbling behaviour lasted for about 3.5 minutes after which the melt gradually calmed and Secondary Bubbling ceased. A picture of the foamy layer is shown in Figure 31. Figure 32 represents the calm melt after Secondary Bubbling.

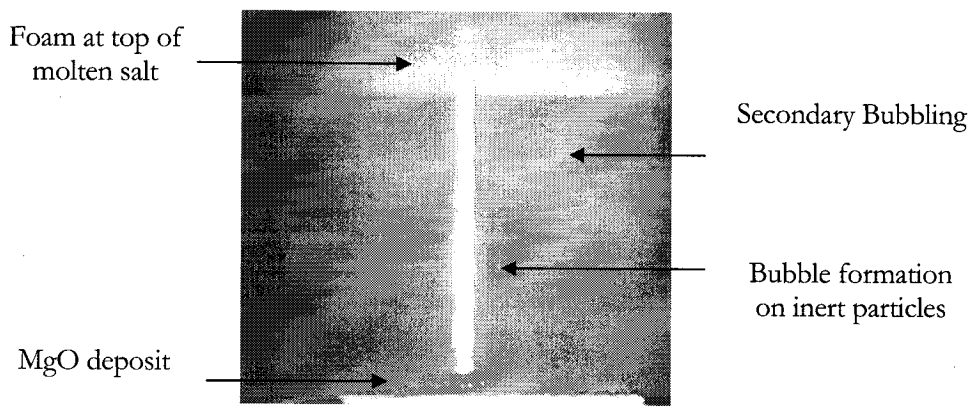

Figure 31 : Secondary Bubbling that was observed during melting for about 3.5 minutes duration.

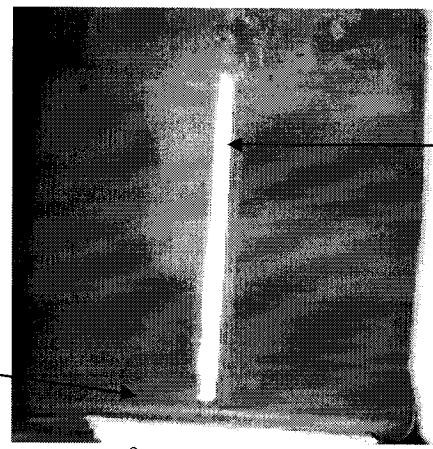

Figure 32 : Calm molten salt at 550 °C after melting and after the cessation of Secondary Bubbling.

Prill Digestion

A series of pictures that illustrate the digestion process and that were extracted from the videotape is presented in Figure 33. In this test, 10 g of prills were added onto the surface of the synthetic electrolyte. Initially, the prills did not submerge into the molten salt and consequently, heating and dehydration occurred on the surface of the melt. The bubbling behaviour observed upon contact of prills with the molten salt was also called "Primary Bubbling" due to the similarity of the bubbling behaviour; i.e. its amount, vigorousness, and bubble size with that seen during the heating and melting, and due to the belief that this bubbling was also H_2O evolution. Characteristically, Primary Bubbling occurred only at the melt surface and resulted in a foamy layer on the surface of the bath. The foam layer during Primary Bubbling, when compared to Secondary Bubbling, differed due to the presences of prills in Primary Bubbling and the bubbles generated within the melt in Secondary Bubbling. The term "effervescent carpet" was coined to describe the Primary Bubbling layer that lasted for about 15 seconds.

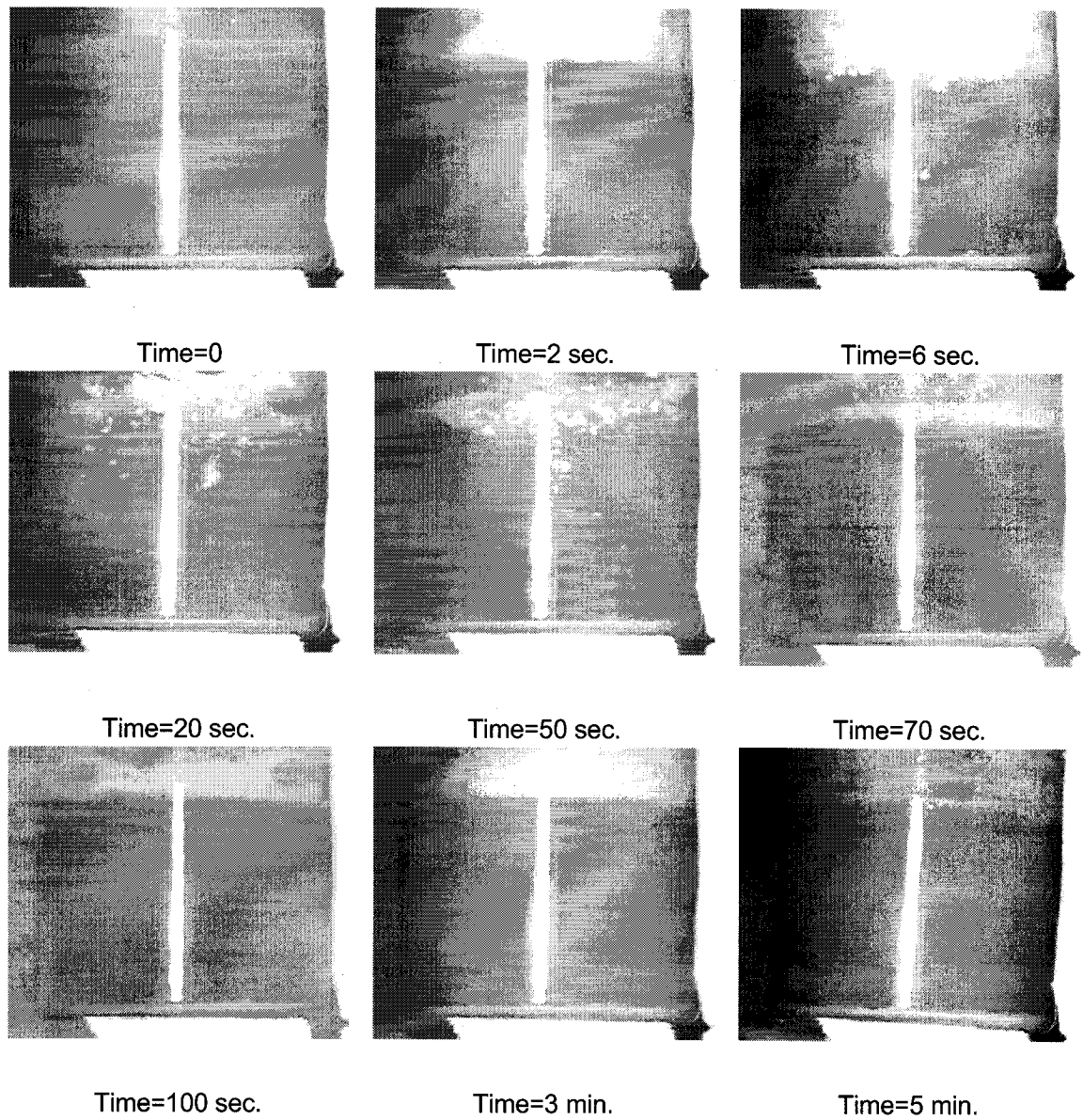

Figure 33 : A series of pictures videotape frames illustrating 10 g of prills added to the surface of the bath and digesting at 550 °C.

It was seen that a single prill ceased evolving its waters of hydration in approximately four seconds, after which, the dehydrated prill was seen to submerge into the melt and then slowly dissolve. A single prill was found to be completely dissolved about twenty seconds after submerging.

The 10 g of prills required roughly 90 seconds to completely dissolve and caused the melt temperature to drop. Due to the design of the furnace temperature control logic, heating elements activated as a result of this melt temperature drop. With the increase in temperature due to the activation of the heating elements, intense bubbling commenced and continued for about 3.5 minutes; a duration that corresponded to the heating elements being active. This bubbling behaviour was also called "Secondary Bubbling" due to the similarity in the appearance to the Secondary Bubbling during heating and melting of the charge. A deposit was also seen to settle after Secondary Bubbling. EDX and XRD analysis of the solid deposit found it to be MgO, Figure 34.

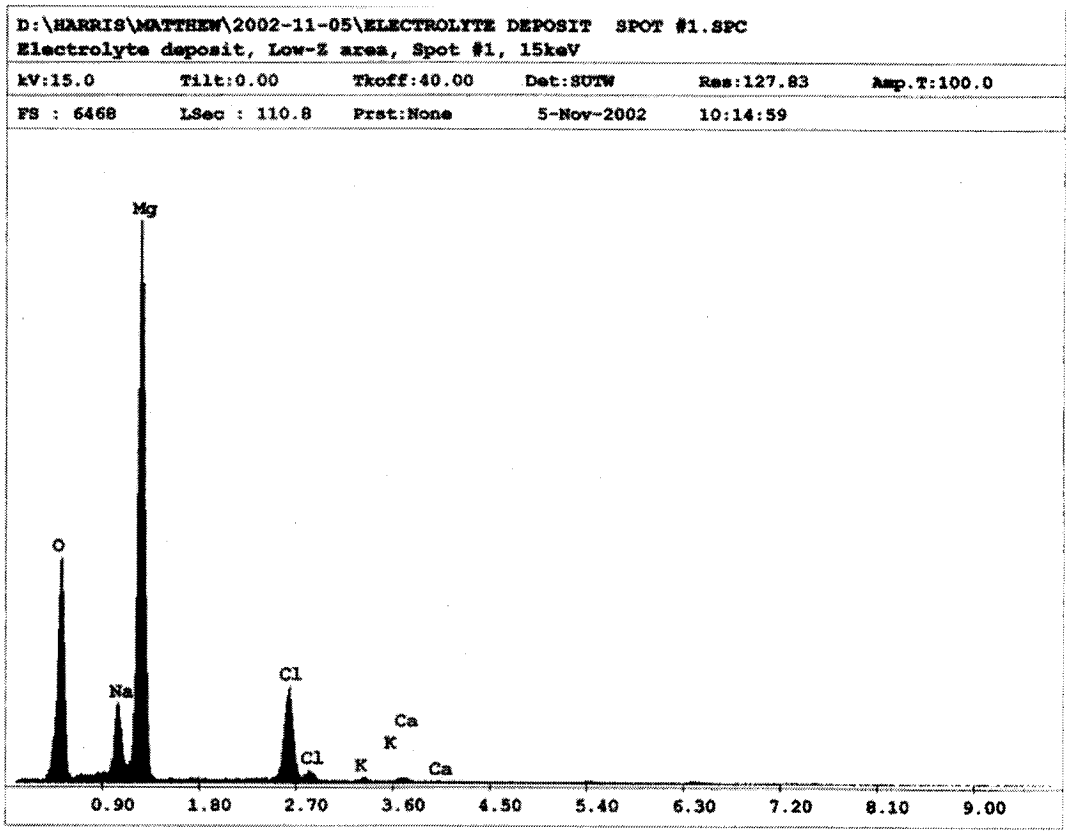

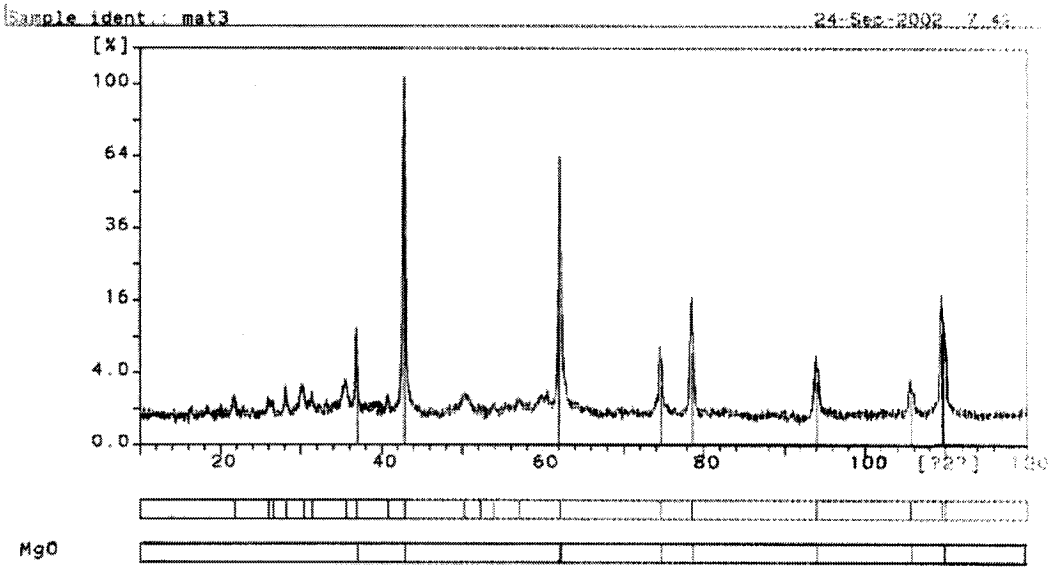

Figure 34 : Typical EDX and XRD spectra of deposit formed in synthetic electrolyte during Secondary Bubbling.

During prill digestion, it was found that prills on the top of the melt agglomerated to form buoyant, gas evolving, liquid impregnated clusters, Figure 35. "Prillbergs" was the colloquial parlance to give the impression of the extent to its buoyancy and submergence. The agglomerated mass was violently thrown about as gas evolved, broke up, and reformed, usually as a smaller mass. By this process, the mass eventually ceased to evolve gas, broke up, submerged in the melt, and was digested.

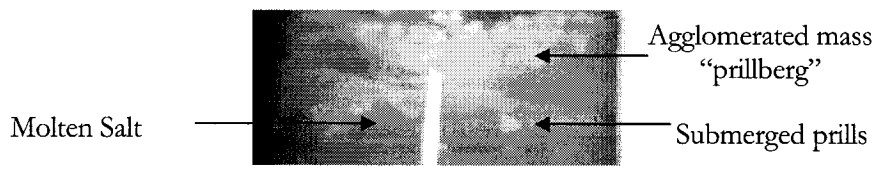

Figure 35 : Agglomerated mass of prills digesting on the surface of synthetic electrolyte.

4.2 Injection of Ar and HCl Into a Molten Salt Containing Oxides

The preparation of the melt followed the procedure presented above and Primary Bubbling and intense Secondary Bubbling were again observed. An MgO deposit again settled after Secondary Bubbling, as presented in Figure 36. Once the melt temperature had stabilized, Ar or HCl was injected into it.

1st Ar injection

In this test, Ar was injected into the bath for 15 minutes following the end of Secondary Bubbling. During Ar injection, the HCl activity in the melt was lowered by dilution with the Ar, and resulted in the dissolved oxides, that were present, decomposing into MgO due to the offset of equilibrium described by Reaction (57). The decomposition was evidenced by the fact that the thickness of the MgO layer at the bottom of the reactor increased to above 6% of the total depth of the bath after Ar injection, as shown in Figures 36 and 37. The melt was thought to be free of dissolved oxide after 15 minutes of Ar injection.

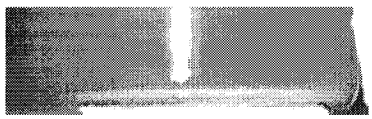

Figure 36 : MgO deposit after melting and before Ar injection.

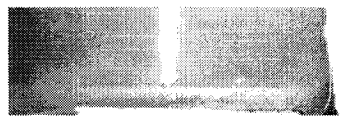

Figure 37 : MgO deposit after melting and after Ar injection.

2nd Ar injection

Once the MgO deposit thickness had been determined, 10 g of prills were added onto the surface of the molten salt. After the digestion of the prills, the nominal $MgCl_2$ content in the bath was increased to about 40 wt.%. The system behaviour during the digestion of the prills was identical to that described above. Primary and intense Secondary Bubbling was observed.

Upon completion of Secondary Bubbling, Ar was injected into the melt for another 15 minutes. The purpose of Ar gas injection at this stage was to decompose the dissolved oxide that might have formed during prill digestion. After Ar injection, the thickness of the MgO layer at the bottom had significantly increased to 11 % of the total depth of the bath as compared to 6 % prior to prills being added. Figures 38 and 39 compares the thickness

of the MgO deposit after prill addition, before and after Ar injection. After Ar injection, the melt was believed to be free of dissolved oxides, see Section 2.7.

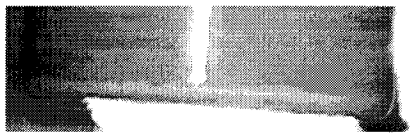

Figure 38 : MgO deposit after prill addition, before Ar injection.

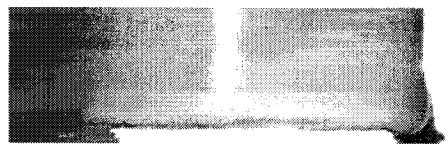

Figure 39 : MgO deposit after prill addition, after Ar injection.

It was also observed that the walls of the quartz crucible accumulated a solid deposit during Secondary bubbling, Figure 40.

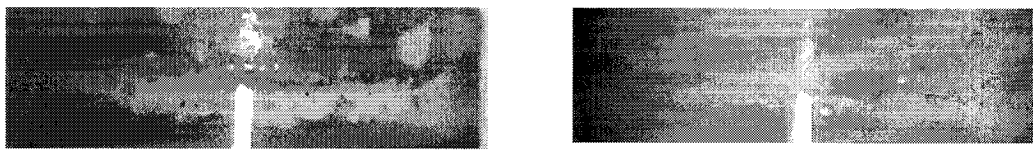

Figure 40 : Walls of quartz crucible before and after Secondary Bubbling.

HCl injection

After the Ar injection tests, the gas supply was switched to HCl and it was observed that the white solid adhering to the wall of the quartz tube started to liquefy and fall back into the melt, Figure 41. The white solid was believed to be frozen electrolyte heavily loaded with oxides that had adhered to the wall of the tube after splashing due to the bubbling. When the gas atmosphere was switched to HCl, the oxides in the frozen layer adhering on the wall were thought to be chlorinated or at least partially chlorinated, perhaps to dissolved oxides and resulted in liquefaction.

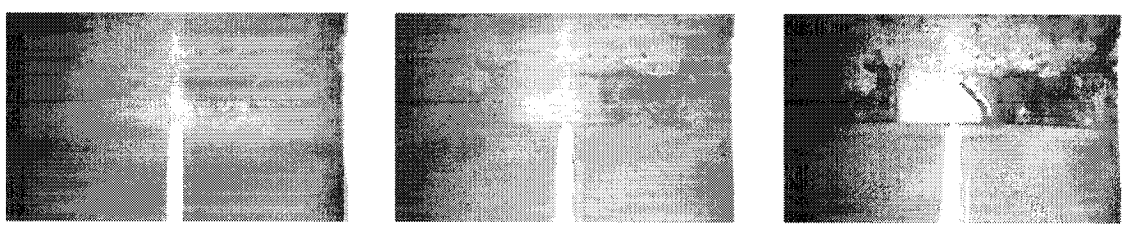

Time=0 sec. Time=20 sec. Time=90 sec.

Figure 41 : Liquefaction of solid deposit on the reactor wall by HCl gas.

10 g of prills were added to produce dissolved oxides. The digestion was identical to that described above. Towards the end of complete dissolution of the prills, Secondary Bubbling occurred. Small bubbles were found generated on the inert particles surfaces and the solid deposit. The Secondary Bubbling lasted for about 3 minutes.

HCl gas was then injected into the melt for 15 minutes. The MgO layer at the bottom of the reactor was found to be reduced significantly by injection of HCl gas as shown by comparison of Figure 42 to Figure 43.

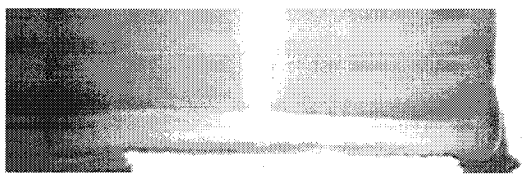

Figure 42 : MgO deposit before HCl gas injection.

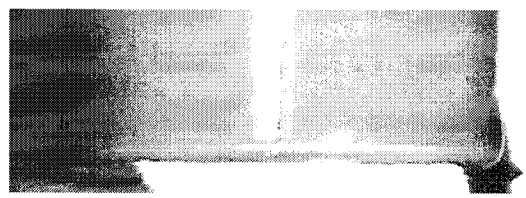

Figure 43 : MgO deposit after 15 min. HCl gas injection.

4.3 Effect of Temperature on Secondary Bubbling.

Previous charges were heated and melted under Ar atmosphere but this was not the case for the present experiment, as the charge was heated and melted under ambient air. The only difference observed when melting the salts under Ar atmosphere as compared to under ambient air was that under ambient air, a thin solid layer was formed on the surface of the molten salt.

For the present experiment, the solid charge was slowly heated and melted to preserve any dissolved oxides present. Primary Bubbling without significant Secondary Bubbling was observed due to the slow heating rate. Once the solid charge was melted and the temperature was stabilized at 550 °C, the temperature was increased to 675 °C and intense Secondary Bubbling occurred, Figure 44. A solid deposit was formed at the end of Secondary Bubbling.

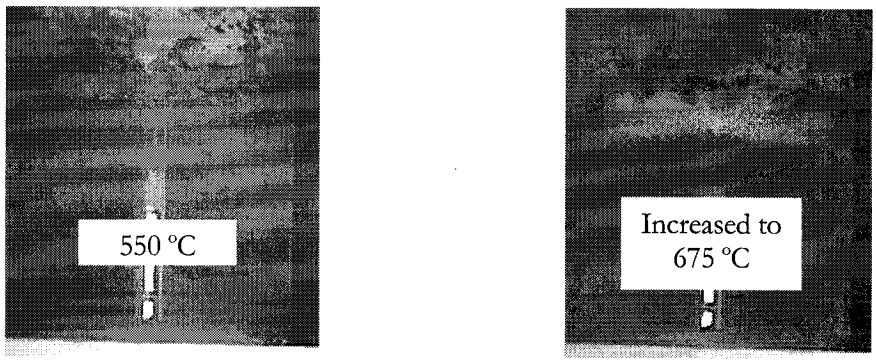

Figure 44 : Secondary Bubbling taking place after melting when temperature of melt was increased from 550 °C to 675 °C.

The melt temperature was reduced back to 550 °C and 10 g of prills were added to the surface of the molten salt, at which time Primary Bubbling was observed again. Because the activation of the heating elements was prevented, by design, the temperature dropped to about 470 °C and Secondary Bubbling was not seen. Once the heating elements were permitted to activate, the melt temperature rose, intense Secondary Bubbling was observed and continued for several minutes until it eventually ceased. The MgO deposit was seen to have increased at the bottom of the crucible. Once again the temperature was reduced, the experiment repeated and the behaviour was seen to repeat itself.

4.4 Effect of $MgCl_2$ Activity on Secondary Bubbling

Melting and Increasing Temperature to 900 °C

In these tests, two melts of different $MgCl_2$ contents were used. Once the solid charge was melted and stabilized at 550 °C, the set points of the furnace and bath temperature controllers were both adjusted to 900 °C and the bubbling behaviour was visually recorded.

It was found that intense Secondary Bubbling occurred in Bath 1 as soon as the temperature of the bath started to increase, as shown in Figure 45. This observation indicated that Bath 1 was close to saturation with the dissolved oxide upon melting at 550

°C. In other words, the dissolved oxide started to decompose as soon as the temperature of the bath was increased, which lead to Secondary Bubbling.

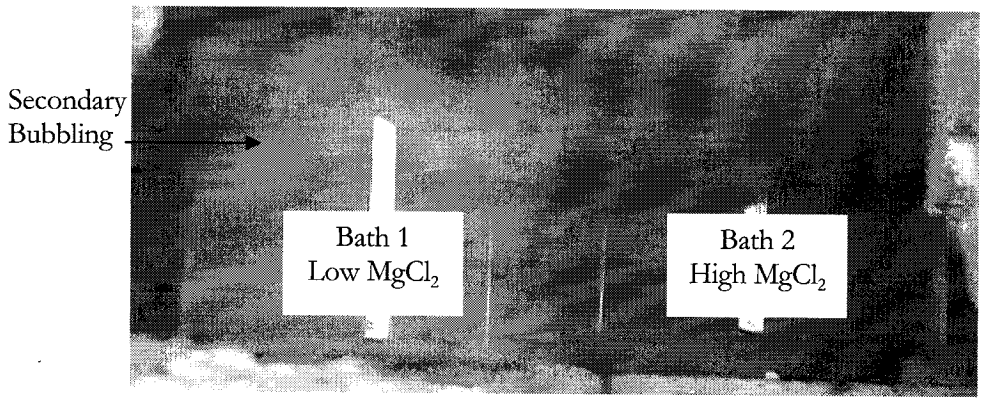

Figure 45 : Secondary Bubbling observed only in the bath with low $MgCl_2$ content subsequent to melting, immediately after the temperature of the melt was increasing.

Bath 2 behaved differently from Bath 1. Bath 2 was found to be quiescent in the early stage of the heating following melting but after this static period, gas began to evolve. The delay of bubbling in Bath 2, as compared with Bath 1, was due to the fact that Bath 2 was not saturated with dissolved oxides upon melting at 550 °C. This observation can be explained by the higher solubility of dissolved oxides in Bath 2 due to Bath 2's higher $MgCl_2$ content as compared to Bath 1.

The size and source of the bubbles in Secondary Bubbling in both baths were analogous to that described in the previous experiments. An MgO layer was formed at the bottom of the crucible after Secondary Bubbling in both instances. Bath 1 had a deposit that settled much faster as compared to Bath 2. The explanation is as follows. Bath 1 decomposed dissolved oxides at a slower rate and allowed the MgO to nucleate heterogeneously, whereas Bath 2 decomposed at a faster rate, due to the larger increase in temperature prior to decomposition, and caused the MgO to nucleate homogenously, which led to very fine solids and slowed the settling rate. It can be observed in Figure 46 that Bath 2 has finer MgO particles and has a milky color compared to Bath 1 with coarse MgO particles. Such a finding was quite surprising and warrants further study in the opinion of the author.

Figure 46 : Bath with low $MgCl_2$ has coarser MgO deposit compared to bath with high $MgCl_2$ after melting and Secondary Bubbling.

As mentioned before, Savinkova[42] showed that the dissolved oxide solubility in the molten salt was almost zero at high temperature (> 700 °C), regardless of $MgCl_2$ content in the bath. Thus the dissolved oxide content of both baths was assumed to be negligible (~0 wt.%) after heating the melts to 900 °C and Secondary Bubbling stopped. The temperature of the melt was then reduced to 550 °C by design.

Adding prills and increasing temperature to 900 °C

A batch of prills, 2 g, was added to each of the baths after cooling them to 550 °C. Figure 47 presents a picture of the baths after the first batch was added. Secondary Bubbling was observed in Bath 1 as the prills digested. However, Bath 2 remained calm, even after the prills were completely digested. This observation suggested that the dissolved oxide produced by the digestion of 2 g of prills was sufficient to saturate Bath 1 but insufficient to saturate Bath 2. Because there was no apparent Secondary Bubbling in Bath 2, two more batches of prills, 2 g per batch, were added to it. It was observed that there were small amounts of gas nucleating on the inert particles but bubbling was not as intense as in Bath 1.

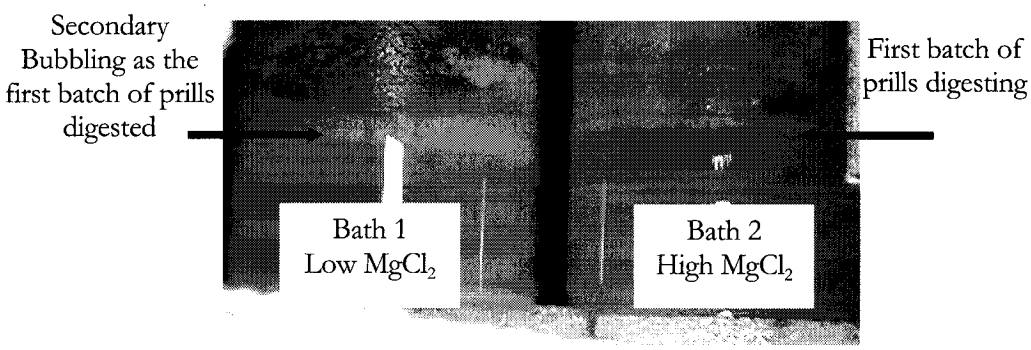

Figure 47 : Digestion of 2 g of prills.

Once the bubbling in both baths had ceased, temperature of both baths was increased a second time to 900 °C to completely decompose the dissolved oxide in the baths. It was observed that Secondary Bubbling occurred in both baths. It was also noted that Bath 2 produced a larger volume of gas as shown in Figure 48.

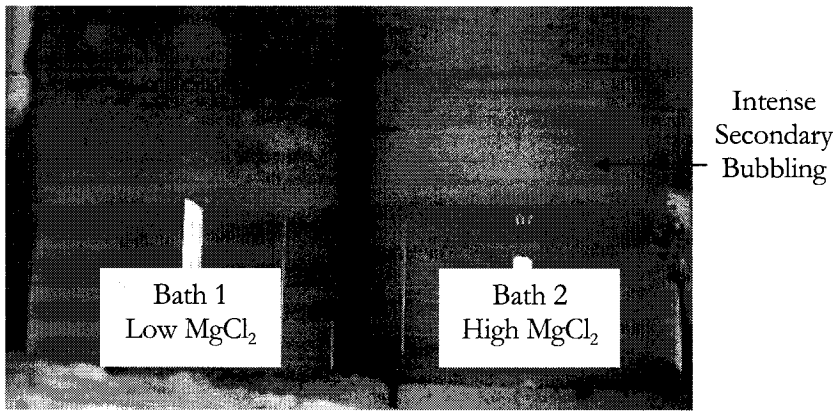

Figure 48 : Intense Secondary Bubbling, as temperature was increased, observed in the bath with high $MgCl_2$.

The amount of gas produced was not measured, but the difference in quantity was readily distinguished by the visual observations. The reason for the greater amount of gas was that more oxide could have been dissolved in Bath 2 (i.e. more prills added prior to the onset of Secondary bubbling) because of its higher $MgCl_2$ content as compared to Bath 1.

Therefore, upon complete decomposition of dissolved oxides, as a result of the temperature increase, more HCl gas was generated in Bath 2 than in Bath 1. The temperature of the melt was then reduced back to 550 °C a second time.

Adding 10 g of prills in one shot and increasing the temperature to 900 °C

After the second cooling to 550 °C, 10 g of prills were added to both baths in one shot. This test allowed direct comparison of the bubbling behaviour in both baths when the same amount of solid MgOHCl was produced and the same amount of water was introduced. Similar to the observation in the previous test, intense Secondary Bubbling occurred in Bath 1 as the prills digested, while no strong Secondary Bubbling was observed in Bath 2, but rather only some bubbles were found nucleating on the surfaces of the inert particles, Figure 49.

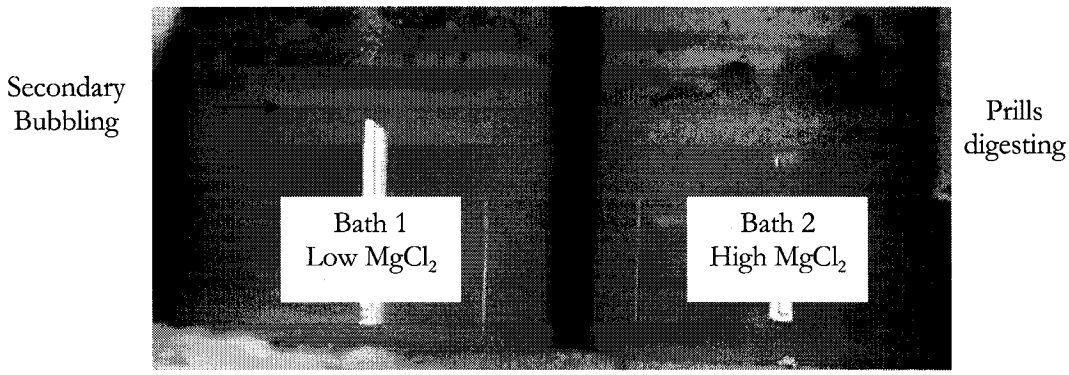

Figure 49 : Secondary Bubbling observed in bath with low $MgCl_2$ but not in bath with high $MgCl_2$ after 10 g of prills were added to both baths.

The temperature of the melt was increased to 900 °C for a third time to completely decompose the dissolved oxides in the baths and the bubbling behaviour was visually recorded. Intensive Secondary Bubbling was observed in both baths as the temperature of the baths increased. Moreover, it was obvious again that Bath 2 generated more gas than Bath 1.

4.5 Identifying the Gas Composition During Secondary Bubbling

The mass gain of Flask 1 due to the collection of the condensed solution was 0.25 ± 0.02 g. A small quantity of the condensed solution also remained in the condenser and was neither collected nor weighed. The titration results of the condensed solution collected in Flask 1 are presented in Table 3.

Table 3 : Flask 1 Titration results of 20 ml of the diluted condensed solution.

	Titration 1	Titration 2	Titration 3	Average
ml 0.485N NaOH (± 0.1 ml)	16.74	16.77	16.73	16.75
End pH	7.20	7.53	7.19	7.31

From Flask 2, 20.00 ml of the 250.00 ml that was originally added was titrated against 0.0485 (± 0.0015) N NaOH. 1.83 ± 0.1 ml of titrant was required to reach an end pH of 7.00.

The mass of HCl in the samples were calculated as follows:

$$16.75\,ml\,(NaOH)\times\frac{0.0485 mol(NaOH)}{1000 ml\,(NaOH)}\times\frac{mol(HCl)}{mol(NaOH)}\times\frac{36.45\,g\,(HCl)}{mol(HCl)}\times\frac{100 ml}{20 ml}=0.15\,g\,(HCl)$$

$$1.83\,ml\,(NaOH)\times\frac{0.0485 mol(NaOH)}{1000 ml\,(NaOH)}\times\frac{mol(HCl)}{mol(NaOH)}\times\frac{36.45\,g\,(HCl)}{mol(HCl)}\times\frac{250 ml}{20 ml}=0.04\,g\,(HCl)$$

Error calculations:

Mass gain error for Flask 1 $\quad\frac{0.02\,g}{0.25\,g}*100=8.0\%$

Titration error for Flask 1 $\quad\frac{0.1\,ml}{16.75\,ml}*100=0.6\%$

Error of titrant concentration $\quad\frac{0.0015\,N}{0.0485\,N}*100=3.1\%$

Titration error for Flask 2 $\frac{0.1\ ml}{1.83\ ml} * 100 = 5.5\ \%$

From the calculations above, there were 0.15 ± 0.02 g of HCl in 0.25 ± 0.02 g of solution from Flask 1, the remainder was assumed to be water, i.e., 0.10 ± 0.04 g. Flask 2 contained 0.04 ± 0.003 g of HCl.

The samples collected yielded a total of 0.19 ± 0.02 g of HCl and 0.10 ± 0.04 g of H_2O. Therefore, the overall gas composition during Secondary Bubbling was estimated to be 66 wt.% HCl and 34 wt.% H_2O. Assuming that all the mass was collected and that the sample was representative. The calculations of the partial pressures are as follows:

$$M_{HCl} = \frac{Vol_{condensate} \times \rho_{condensate} \times wt.\%\ HCl}{MW_{HCl}}$$

$$M_{H_2O} = \frac{Vol_{condensate} \times \rho_{condensate} \times wt.\%\ H_2O}{MW_{H_2O}}$$

$$\frac{M_{HCl}}{M_{H_2O}} = \frac{wt.\%\ HCl}{wt.\%\ H_2O} \times \frac{MW_{H_2O}}{MW_{HCl}} = \frac{66}{34} \times \frac{18}{36.45} = 0.959 = \frac{p_{HCl}}{p_{H_2O}}$$

assuming $p_{HCl} + p_{H_2O} = 1\ atm$

$p_{HCl} = 0.51\ atm$ $\qquad$ $p_{H_2O} = 0.49\ atm$

Using the mass of sample collected, 0.19 ± 0.02 g HCl, and 0.10 ± 0.04 g of H_2O, we can back calculate how much MgOHCl was decomposed using Reactions (57) and (59).

MgOHCl consumed by Reaction (57):

$$0.19 g \left(\frac{1\ mol}{36.46\ g}\right)\left(\frac{1\ mol\ MgOHCl}{1\ mol\ HCl}\right)\left(\frac{76.76\ g}{1\ mol}\right) = 0.40\ g\ MgOHCl$$

$$\frac{\pm 0.02\ g}{0.19\ g} * 0.40\ g = \pm 0.04\ g$$

MgOHCl consumed by Reaction (59):

$$0.10\ g\left(\frac{1\ mol}{18\ g}\right)\left(\frac{1\ mol\ MgOHCl}{1\ mol\ H_2O}\right)\left(\frac{76.76\ g}{1\ mol}\right)=0.43\ g\ MgOHCl$$

$$\frac{\pm 0.04\ g}{0.10\ g} * 0.43\ g = \pm 0.17\ g$$

The total calculated decomposed MgOHCl is 0.83 ± 0.21 g.

4.6 Effect of Atmosphere During Prill Digestion

The deposit thickness was used to determine if the production of oxides was significantly increased or decreased by changing the feeding rate and / or digesting prills under different atmospheres. The thickness was measured from pictures that were twice the actual size. Therefore, measurements from the pictures were divided by two in order to represent the actual deposit thickness, i.e. the values presented represent actual thickness.

All things being equal, the solid MgO deposit was seen to settle at a faster rate when the temperature of the melt was higher. A series of pictures showing the settling of the fine MgO particles after Secondary Bubbling as the temperature increased is presented in Figure 50.

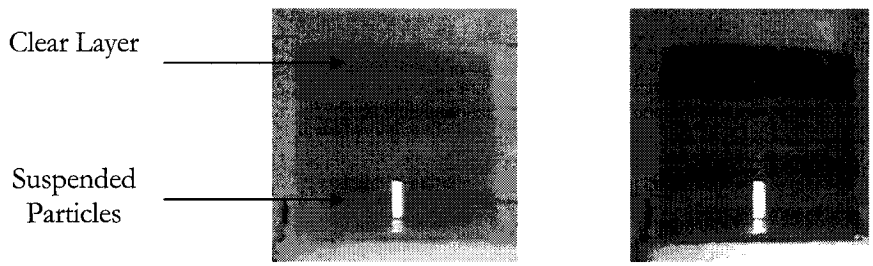

1.5 min 2 min

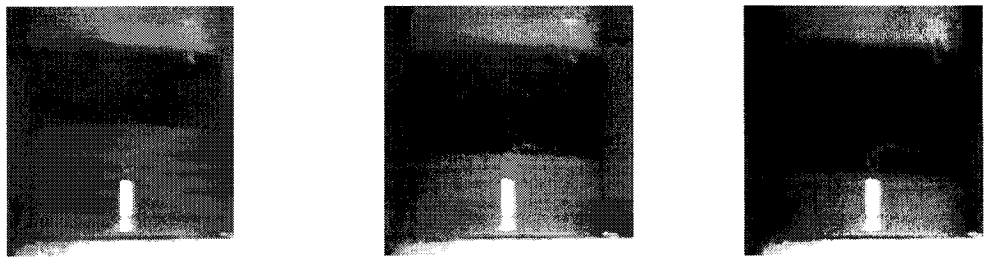

2.5 min 3 min 3.5 min

Figure 50 : Time lapse video frames showing the settling of fine MgO formed during Secondary Bubbling as the temperature was increased from 823 K to 923K in test 3.2.3.

After melting, Ar injection was used to transform the dissolved oxides into MgO. The MgO deposit thickness after melting was approximately 3.5 mm in both baths, shown in Figure 51.

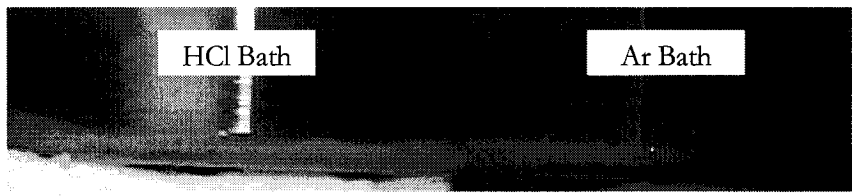

Figure 51 : Deposit in baths after melting and Ar injection.

Prill digestion with a slow feeding rate

5 batches of 2 g of prills were added into each bath. After the two first batches, Secondary Bubbling was observed in the HCl Bath but not in the Ar Bath. Secondary Bubbling was observed in the Ar bath after the 5 batches of prills were added. After prill digestion and Ar injection, the deposit was measured again. A picture of the deposits is shown in Figure 52. The solids generated due to prill digestion in the HCl Bath were finer compared to the Ar Bath and required more time to settle. Two types of deposit were seen in the HCl Bath but not in the Ar Bath. By measuring the two layers of deposit in the HCl bath independently, the heavier (coarser) deposit, that was similar to the deposit formed after melting, seemed to decrease by about 1 mm. In actuality, the heavy deposit did not disappear but blended in with a lighter (finer) deposit that formed during Secondary Bubbling due to the addition

of prills. It was assumed that the heavy deposit remained the same, about 3.5 mm, to which the lighter deposit settled and was thus calculated to be about 2.5 mm. The Ar Bath deposit increased by approximately 1 mm after prills were added and Ar was injected, making the total deposit thickness about 4.5 mm.

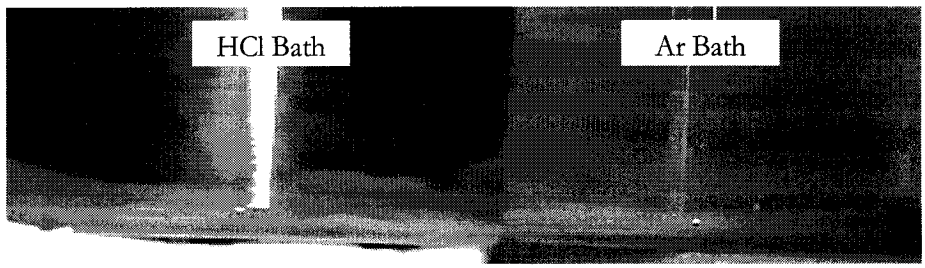

Figure 52 : Deposit after slow feeding rate of prills and Ar injection.

When 10 g of prills were added in one shot, the heavier deposit in the HCl Bath did not increase during prill digestion compared to the deposit during melting and the lighter deposit increased by approximately 5.5 mm, making the total light deposit thickness about 8 mm. The deposit in the Ar bath increased by about 2.5 mm, making the total about 7 mm. These observations are shown in Figure 53.

Figure 53 : Deposits after 10 g of prills fed slowly and 10 g fed in one shot and after Ar injection.

Table 4 summarizes the measured deposit thicknesses throughout the experiments.

Table 4 : Measured deposit thicknesses

	HCl bath heavy deposit	HCl bath light deposit (increase)	Ar Bath deposit (increase)
Melting	~3.5 mm	-	~3.5 mm
Slow feeding rate	~3.5 mm	~2.5 mm	~4.5 mm (~1 mm)
10 g one shot	~3.5 mm	~8 mm (~5.5 mm)	~7 mm (~2.5 mm)

5 INTERPRETATIONS OF RESULTS

5.0 Introduction

The following chapter interprets the results from Chapter 4. It begins with a discussion of the digestion of prills in the molten salt and describes the digestion steps and bubbling behaviour associated with them. The difference between the foam occurring layers during Primary Bubbling and Secondary Bubbling is explained and the results from the gas injection experiments are interpreted including the determination of the presence of dissolved oxides, and their behaviour in the molten salt. The results from the gas composition were found to give insight into the reactions that occurred and oxide precipitation is discussed.

Finally, some possible mechanisms for the precipitation of MgO and for the genesis of MgOHCl in the melt are presented.

5.1 Digestion of MMI Prills

The digestion of prills added onto the surface of the melt can be separated into two steps: the dehydration / hydrolysis step, corresponding to Primary Bubbling, and the dissolving step. The dehydration / hydrolysis step was much faster than the dissolving step, as was noted in section 4.1. The formation of oxides, solid and / or dissolved, occurred during Primary Bubbling. During this first step, the prills did not submerge into the molten salt. For a single prill, the dehydration / hydrolysis step lasted about four seconds and the dissolving step lasted about twenty seconds. Because prill digestion is an endothermic process, the addition of prills onto the surface of the melt caused the melt temperature to drop. Consequently, the activation of the furnace heating elements, in order to return to the set temperature, was noticed, which lead to the observation of Secondary Bubbling.

The melting of the solid charge was seen to appear quite similar to the digestion of prills, in that Primary Bubbling and Secondary Bubbling were observed. The solid charge was dehydrating / hydrolyzing as Primary Bubbling was observed in the partially melted bath. In addition, the formation of dissolved oxides was also taking place as this was confirmed by the latter appearance of Secondary Bubbling.

5.2 Foam Layer on Molten Salt Surface

A foamy layer of electrolyte formed twice when prills were added onto the surface of the molten salt, during Primary Bubbling and Secondary Bubbling, but no foam layer was observed during the Primary Bubbling that was observed throughout melting of the charge. Other observations include:

1. During Primary Bubbling, when prills were added onto the surface of the molten salt, a foam layer during initial stages of Primary Bubbling was observed for about 20 seconds.

2. The Primary Bubbling seen when prills were added to hot electrolyte generated a thicker foam layer as compared to prills added to an electrolyte of lower temperature.

3. The Primary Bubbling seen when prills were added to an electrolyte with a high $MgCl_2$ content generated a thicker foam layer compared to that seen when prills were added to an electrolyte of a lower $MgCl_2$ content.

4. A solid deposit was observed on the walls of the quartz tube after the foam layer of Secondary Bubbling subsided.

The explanations for Primary Bubbling are as follows. The surface of the melt was initially at 550 °C. The first prills that contacted the molten salt were faced with a large temperature gradient and heated rapidly, causing them to flash-off their waters of hydration at a fast rate. However, the temperature of the molten salt on the surface dropped due to the highly endothermic process and the prills that contacted the surface of the molten salt at a later time encountered liquid with less superheat and therefore are heated more slowly, possibly even being encapsulated by frozen electrolyte. The lower heating rate lowered the rate at which the prill was dehydrating / hydrolyzing and hence lowered the rate at which the gas evolved. The smaller rate of gas evolution reduced the foam layer.

The thickness of the foam layer that was observed during Secondary Bubbling depended on the rate of dissolved oxide decomposition. This was clearly seen when comparing the Secondary Bubbling in baths with low and high $MgCl_2$ contents, shown in Figure 48. The

bath with the low $MgCl_2$ had a much smaller foam layer thickness during Secondary Bubbling as compared to the bath with the high $MgCl_2$.

It was also found that the foam layer during Secondary Bubbling produced a solid deposit on the walls, Figure 40. The solid deposit was assumed to be frozen salt loaded with MgO, the MgO particles originating from the decomposition of the dissolved oxide. It was seen that the solid deposit on the reactor walls liquefied when the atmosphere was changed to pure HCl, Figure 41, an indication that MgO present may have been chlorinated.

Lastly, the presence of fine solid particles is known to stabilize foams, thus due to the product of decomposition, it is reasonable to assume that the foam layer was stabilized during Secondary Bubbling.

5.3 Injecting Ar and HCl Into a Molten Salt Containing Oxides

The injection of Ar was seen to decompose the dissolved oxide. Firstly, comparing Figures 37, 38 and 39 shows that prill digestion, without Secondary Bubbling, did not significantly increase the deposit thickness, but the injection of Ar did. Furthermore, after Ar injection, when the temperature was increased, no Secondary Bubbling was observed, indicating there was no dissolved oxide present to decompose upon heating. It can be concluded that reducing the HCl activity in the melt offsets the equilibrium of Reaction (57) to the right.

$$MgOHCl_{(diss)} \rightarrow MgO_{(s)} + HCl_{(g)} \quad (57)$$

The injection of $HCl_{(g)}$ chlorinated the MgO deposit. This was observed by comparing Figures 42 and 43. Reaction (26) presents the overall chlorination reaction.

$$MgO_{(s)} + 2HCl_{(g)} \rightarrow MgCl_{2(l)} + H_2O_{(g)} \quad (26)$$

5.4 Effect of Temperature on Secondary Bubbling

The melting of the solid charge was seen to generate dissolved oxides and in some tests the charge was slowly heated to melting to prevent their decomposition. The temperature was then increased and Secondary Bubbling with the formation of a deposit was

observed. From this, it was concluded that dissolved oxides were present and that increasing the melt temperature decomposed them.

In other tests, prills were added and dissolved into the melt and Secondary Bubbling was prevented by lowering the furnace temperature controller. The temperature was thereafter increased and Secondary Bubbling with a deposit was observed again. From this, it was concluded that prill digestion produced dissolved oxides and that increasing the melt temperature decomposed them.

5.5 Effect of $MgCl_2$ Activity on Secondary Bubbling

Two baths were prepared with different compositions that were to be molten at low temperatures. The melts had to have large differences in $MgCl_2$ content and be molten at low temperature (500 °C). This resulted in the composition of the charges to have different NaCl / $CaCl_2$ ratios, affecting the activity of $MgCl_2$. The charge with the high $MgCl_2$ content had a composition that favoured a reduction in $MgCl_2$ activity, Figure 11. However, the greater content of $MgCl_2$ was sufficient to overcome this effect. The net result was an increase in $MgCl_2$ activity in the bath from 0.0203 with 16 wt.% $MgCl_2$ to 0.146 with 49.04 wt.% $MgCl_2$.

As seen previously, the melting of these two baths produced dissolved oxides. It was found that the bath with low $MgCl_2$ content immediately began Secondary Bubbling once the temperature of the melt was increased, whereas the bath with high $MgCl_2$ content did not. This was an indication that higher $MgCl_2$ content increased the solubility of the dissolved oxide or in other words, pushes the equilibrium in Reaction (59) to the left. Moreover, the melt with low $MgCl_2$ content was closer to saturation with the dissolved oxide after melting.

$$MgOHCl_{(diss)} + HCl_{(g)} \leftrightarrow MgCl_{2(diss)} + H_2O_{(g)} \quad (59)$$

After both melts were cleaned of dissolved oxides by increasing the temperature, 2 g of prills were added to the bath with low $MgCl_2$ content and produced Secondary bubbling, which concluded that the melt was close to saturation with the dissolved oxide after cleaning whereas the bath with high $MgCl_2$ content was not.

Furthermore, when the temperatures of the melts were increased, there was a larger foam layer during Secondary Bubbling in the bath with high $MgCl_2$ content, indicating that there was more dissolved oxide to decompose. These observations follow Savinkova's[41] plot, in Figure 20. It was concluded that Secondary Bubbling was the decomposition of dissolved MgOHCl and that the amount of dissolved MgOHCl present in the melt increased with increasing $MgCl_2$ content and decreased with increasing temperature.

The effect of the activity of $MgCl_2$ has on the activity of MgOHCl can be expressed by the interaction parameter, Equation (66). It has been shown that increasing the mole fraction of $MgCl_2$ increases the amount of MgOHCl present. Therefore, the interaction parameter of the $MgCl_2$ is significant.

$$\ln \gamma_{MgOHCl_{(diss)}} = \ln \gamma^{o}_{MgOHCl_{(diss)}} + \varepsilon \, X_{MgCl_{2\,(l)}} \qquad (66)$$

Where $\gamma_{MgOHCl_{(diss)}}$ activity coefficient of MgOHCl dissolved in the molten salt

$\gamma^{o}_{MgOHCl_{(diss)}}$ activity coefficient at infinite dilution

ε $MgCl_2$ / MgOHCl interaction parameter

$X_{MgCl_{2(l)}}$ mole fraction of $MgCl_2$ in the molten salt

5.6 Identifying the Gas Phase During Secondary Bubbling

Analysis of the off-gas confirmed that during Secondary Bubbling, HCl and H_2O were present. The presence of water was confirmed by the condensation in the gas line from the apparatus. However, HCl was questionable and was confirmed by measuring the acidity of the solutions that scrubbed the off-gases. There were two possible gases originating from the elements in the system that could render the water acidic. They were HCl and Cl_2 gases. *Perry's Chemical Engineers' handbook* gives the solubility at 30 °C for $Cl_{2(g)}$ and $HCl_{(g)}$ as 0.562 wt.% and 67.3 wt.% respectively. The amount of HCl in the condensed water was 66 wt.% at 25 °C. From this information, it was concluded that the gas during Secondary Bubbling was a mixture of HCl and H_2O. The presence of HCl and water were explained by Reactions (57) and (59).

$$MgOHCl_{(diss)} \leftrightarrow MgO_{(s)} + HCl_{(g)} \quad (57)$$

$$MgOHCl_{(diss)} + HCl_{(g)} \leftrightarrow MgCl_{2(diss)} + H_2O_{(g)} \quad (59)$$

The time average concentration of these two species in the off-gas was calculated to be 49 vol.% HCl and 51 vol.% H_2O, assuming that all the mass was collected and that the sample was representative.

The total amount of MgOHCl decomposed during Secondary Bubbling was calculated to be 0.83 ± 0.21 g, equivalent to 0.55 ± 0.14 wt.% $MgOHCl_{(diss)}$ in the 150 g molten salt. This number is in good agreement with Savinkovas's[41] plot, Figure 20, who obtained a value of approximately 1.5 wt.% for a $MgCl_2$-KCl-NaCl molten salt containing 35.8 wt.% $MgCl_2$ at 500°C. The activity of $MgCl_2$ was similar in the present work compared to Savinkova's[41] but a possible reason for the difference was that not all the off-gas was collected, as some of the condensed solution remained in the condenser.

The use of a predominance diagram, also called Kellogg diagram, was thought useful to determine which reactions are occurring in the Mg-O-H-Cl system, if MgOHCl was to decompose. The construction was performed using Fact*Sage*™ and required some assumptions. The activity of the $MgCl_{2(l)}$ and the partial pressure of $Cl_{2(g)}$ were determined using 'equilb' in Fact*Sage*™ with the Fact-Salt solution model. The activities were obtained in a melt that was not hydrolyzed. A hydrolyzed melt was known to reduce the negative behaviour of the $MgCl_2$ activity[38]. The activity of the MgOHCl was estimated by reducing the activity of the solid MgOHCl. The activity was calculated assuming ideal behaviour and the mole fraction was estimated by the mass of condensed sample, calculated above. The predominance diagram presented in Figure 54 shows the possible reactions occurring if the equilibrium is to shift.

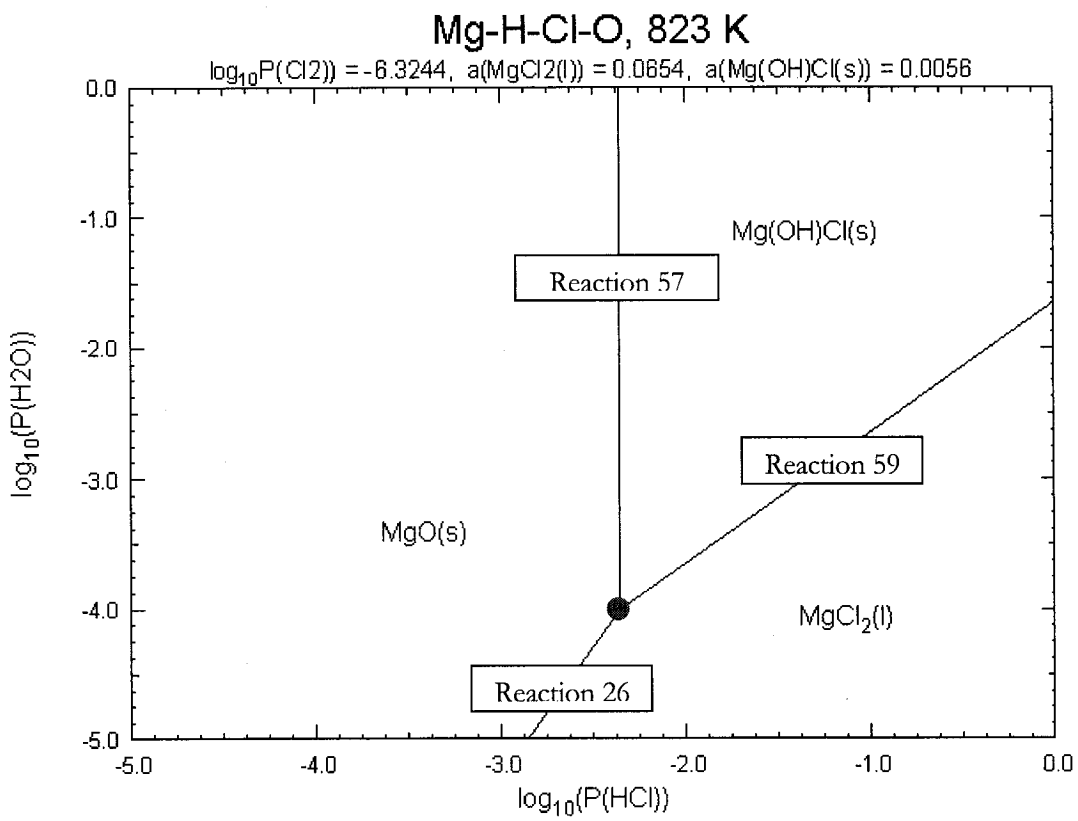

Figure 54 : Predominace diagram when system is at equilibrium at 550 °C.

It was not known if there was a period during Secondary Bubbling when one of the reactions was favoured, i.e. it might be possible that chlorination only occurred at the beginning of the Secondary Bubbling when the $HCl_{(g)}$ was present with the high concentration of dissolved oxides.

The P_{HCl} / P_{H2O} ratio is approximately unity and according to Ficara's thesis[9], p.133, this ratio should prevent any hydrolysis from occurring. From the predominance diagram, this ratio is shown to produce MgOHCl instead of the expected $MgCl_2$, as hydrolysis is not supposed to occur. However, Ficara[9] also neglected the formation of MgOHCl, indicating that the design only avoided the formation of MgO. Keeping this idea in mind, the frozen electrolyte formed on the walls of the quartz crucible, Figure 40, can also be explained by the hydrolysis of the melt, if possible.

5.7 Effect of Atmosphere During Prill Digestion

A very interesting trend was observed in Experiment 3.2.6 when comparing different reactor atmospheres. The MgO deposit formed, when slowly adding 10 g of prills under Ar over a period of 100 seconds, increased by about 1 mm, and by about 2.5 mm when 10 g were added in one shot. Another way to express these results is that feeding 10 g of prills in one shot produced 2.5 times more oxides relative to 10 g fed slowly. Therefore, feeding rate has a significant effect on the production of oxides. Explanations for this observation are presented in the following two paragraphs.

One explanation is that, when 10 g of prills were fed in one shot, the prills supported by the dehydrating prills were hydrated from the water that was flashing off. The hydrated prills then contacted the molten salt and dehydrated in an atmosphere containing more water than the previous dehydrating prills, which led to the formation of more oxides. This also gave the water another chance to hydrolyse the melt, if at all.

Another explanation is that, when 10 g of prills were fed in one shot, the prills supported by the dehydrating prills heated up and dehydrated at a slower rate in a water-rich atmosphere. The slower dehydration rate was because the prills, which were supported by the dehydrating prills, were being heated by the water vapour from the prills below.

The experiment that was run with an HCl atmosphere demonstrated that a bulk HCl atmosphere did not significantly effect the production of oxides during prill digestion. This interpretation was reached as follows. Although the deposit appeared different in size between the HCl atmosphere and the Ar atmosphere test, the increase in the amount of oxides produced were measured relative to each other. It was found that the relative increase between the two feeding methods was the same under different atmospheres.

The variation in MgO particle size, assumed to be the variation Savinkova[41] measured, was very obvious and he explained the variation as follows: the size of the MgO particles depends on the decomposition rate (actually 'super-saturation') of the dissolved MgOHCl.

It was also observed that the furnace heating elements activated after two batches of prills were digested in the bath with the HCl atmosphere. In the bath with the Ar atmosphere, the heating elements were seen to activate only after all five batches were added. The reason for this was that a batch of prills was added only after the previous batch had

completely dissolved. A longer dissolving time was required in the bath with Ar atmosphere compared to the bath with HCl atmosphere. A possible explanation is that, in the case of Ar atmosphere, the prills were fed from the opening of the quartz crucible, and in the case of the HCl atmosphere, prills were fed via a narrow material feeding port. The large opening in the Ar atmosphere bath could have caused more prills to agglomerate and form a prillberg.

In addition, Ar injection was performed in the bath under Ar atmosphere immediately after the 5 batches of prills were digested, resulting in less thermal decomposition of MgOHCl compared to the bath under HCl atmosphere. This result demonstrates that the thermal decomposition of dissolved MgOHCl led to finer MgO particles as opposed to Ar decomposition, which led to coarse MgO particles.

In the HCl Bath, feeding 10 g of prills in one shot produced approximately 2.2 times more oxides relative to feeding the prills slowly. This number is quite close to the Ar Bath (about 2.5 times). If the bulk HCl atmosphere was to significantly suppress hydrolysis during the slow feeding rate, then a larger difference was expected with the two different prill addition rates performed in the present experiment. The ineffectiveness of the HCl atmosphere is further argued as follows. There should be much less oxides produced when feeding 10 g of prills slowly, as the HCl from the atmosphere is more likely to surround the individual prill compared to feeding 10 g in one shot. The difference in oxides produced between the two feeding rates in the HCl bath should be greater compared to the Ar Bath if HCl atmosphere is to have an effect. Because the increase in deposit was quite similar to the Ar, it can be concluded that the HCl atmosphere has as little effect on the production of oxides as does the Ar atmosphere.

Thus a significant finding of the work is that since the dehydration / hydrolysis step has a short duration, it becomes difficult for the HCl atmosphere to suppress the hydrolysis reaction, for obvious reasons, which are not discussed here. In order to suppress the formation of oxides, the $HCl_{(g)}$ must be present at the point of formation of the oxide on an atomic scale.

5.8 Mechanism of Dissolved Oxide Decomposition

The mechanism by which the dissolved oxide decomposed to produce solid MgO and HCl gas is examined in detail in the following paragraph.

The dissolved MgOHCl is considered to be in the form of $MgOH^+ + Cl^-$. The $MgOH^+$ group can further decompose into H^+, Mg_2O^{2+} and O^{2+}, as shown in Reaction (67), following Combes'[40] work on the precipitation of $MgO_{(s)}$ in molten salts. $HCl_{(g)}$ is formed according to Reaction (68) and the formation of $MgO_{(s)}$ proceeds according to Reaction (52).

$$2MgOH^+ + 2Cl^- \rightarrow Mg_2O^{2+} + O^{2+} + 2H^+ + 2Cl^- \quad (67)$$

$$2H^+ + 2Cl^- \rightarrow 2\,HCl_{(g)} \quad (68)$$

$$Mg_2O^{2+} + O^{2+} \rightarrow 2MgO_{(s)} \quad (52)$$

The MgO precipitation deriving from the decomposition reaction can either nucleate homogeneously or grow heterogeneously depending on the Mg_2O^{2+} concentration. Savinkova[41] presented some experimental data illustrating the difference between the types of nucleation occurring during MgOHCl decomposition. He claimed that new crystals will form, i.e. homogeneous nucleation, above a certain limiting value and below the limiting value, MgO will crystallize on the surface of existing particles, i.e. heterogeneous growth.

The intensity of the Secondary Bubbling was concluded to be a function of the rate of MgOHCl decomposition. The intensity was seen to increase when the heating elements were activated and the temperature of the melt increased. A fast increase in temperature would cause the $MgOH^+$ to decompose quickly according to Reaction (67), leading to the rapid evolution of $HCl_{(g)}$, Reaction (68), which in turn causes intense Secondary Bubbling. Savinkova[41] also observed this trend when the temperature was increased in his work.

During the observations of Secondary Bubbling, it was noted that the bubbles were generated on inert particles (see appendix) that were often present in the melt and these observations suggested to the author that a nucleation site was required. This observation implies that the gas is in its dissolved state in the melt. The decomposition of MgOHCl also

meant the electrolyte became saturated with HCl. Once the melt was saturated, Secondary Bubbling was observed.

5.9 Genesis of Oxides Into Molten Salt

It was shown that the digestion of prills in molten salts produced a significant amount of dissolved MgOHCl and small amounts of MgO, see Figures 37, 38, and 39.

The mechanism can be described as follows. It is known that the thermal decomposition of MgOHCl can be slow, as shown by Glasner et al.[29]. Also, the addition to, and the digestion of prills into, a melt was found to reduce the molten salt temperature by approximately 70 °C. The local temperature where a prill was being digested was likely to be even lower as compared to the initial melt temperature. This would have led to less MgOHCl decomposing resulting in more dissolved oxide in the melt. The present results that found that slow feeding, and hence less local undercooling, produced less oxide support the hypothesis and in fact, the design of the Magnola Metallurgie Inc. 'Super-Chlorinator' could be reconsidered in light of this simple discovery for significant improvement in performance.

CONCLUSIONS

The digestion of partially hydrated $MgCl_2$ prills in a molten salt containing $MgCl_2$ produced large quantities of dissolved MgOHCl and small amounts of solid MgO. The formation of solid MgO was due to the decomposition of the dissolved MgOHCl. The decomposition reaction was shown to be a function of temperature and $MgCl_2$ content.

Two types of gas bubbling were associated with the digestion of prills into a molten salt. Primary Bubbling was associated when prills where dehydrating / hydrolyzing. The occurrence of Secondary Bubbling as a function of temperature and $MgCl_2$ activity was an indication that the molten salt was oversaturated or at least saturated with dissolved MgOHCl and that the latter decomposed according to the following reaction:

$$MgOHCl_{(diss)} \rightarrow MgO_{(s)} + HCl_{(g)}$$

The solid MgO product was found to nucleate in two ways, either heterogeneously or homogenously, depending on the rate of MgOHCl decomposition.

The evolution of HCl gas from the above reaction chlorinated the dissolved oxide, producing dissolved $MgCl_2$ and water vapour, according to the following reaction:

$$MgOHCl_{(diss)} + HCl_{(g)} \rightarrow MgCl_{2(diss)} + H_2O_{(g)}$$

The decomposition of dissolved oxides occurred when dry Ar was injected into the melt. Ar reduced the activity of HCl in the melt, offsetting the equilibrium and resulting in the decomposition.

The bulk atmosphere had no significant effect on the rapid dehydration of the partially dehydrated $MgCl_2$ because, even though the bulk atmosphere may have the conditions required to suppress the hydrolysis, the gas evolved by dehydrating the partially dehydrated $MgCl_2$ determined the local HCl partial pressure and hence the local equilibrium.

The removal of insoluble oxides from industrial electrolytes could be accomplished by settling the MgO or by its chlorination. The chlorination of insoluble MgO is now believed to

occur via the dissolved intermediate, MgOHCl. The exact mechanism and kinetics of the chlorination of MgOHCl were beyond the scope of the present work.

Previous workers oversight of the role of this intermediate and the variability in the possible reaction mechanisms has impeded a thorough analysis of the process kinetics and has led to sub-optimal reactor designs.

RECOMMENDATIONS FOR FUTURE WORK

The digestion of prills was performed in melts with a reduced HCl activity. It would be of interest to perform prill digestion experiments were the molten salt has a high HCl activity by injecting HCl prior to feeding the prills. Comparing the deposit thickness would help to determine the role initial HCl plays, if any, in suppressing the hydrolysis of the melt.

It would be of interest to confirm if solid MgOHCl can dissolve directly in the molten salt; even though Savinkova[41] mentioned that it most likely does. This information would indicate whether the hydrolysis occurs in the solid state (prill) or in the liquid state (molten salt).

The off-gas composition determined in the present work was of low accuracy. Accurate measurements of the off-gas would lead to more reliable information about the chlorination of dissolved oxides in the melt.

Measurements of the $MgCl_2$, HCl, and water activities in molten salts, synthetic and industrial, would quantify levels of the saturation of dissolved MgOHCl and allow a complete thermodynamic analysis of the system to be performed.

APPENDIX

INERT PARTICLES IN MOLTEN SALT

Throughout the experimental tests to study prill digestion in a synthetic electrolyte, it was observed that solid black particles were usually present in the melt. These particles were deemed inert as they did not dissolve and were not chlorinated, even after injecting pure HCl gas for 45 minutes (0.75 SLPM).

The black particles were found to originate in the anhydrous $MgCl_2$ ($MgCl_2$) purchased from our supplier, Sigma Aldrich, catalogue number 24,413-9, by leaching a large sample of $MgCl_2$ with distilled water and then filtering by gravity. The filter paper was washed once to remove residual $MgCl_2$ and the black particles collected on the filter were dried and analyzed by energy dispersive x-ray (EDX), Figure 55. Seven other EDX analyses of other particles were similar.

The EDX results showed that the black particles contained the following elements: magnesium and oxygen with traces of zirconium and carbon. Spot analysis at increasing accelerating voltage (not shown here) re-confirmed that zirconium was present. The white spots shown in Figure 55 were also found to contain zirconium.

The carbon peak was always insignificant in each of the 8 EDX measurements and is most likely due to the carbon tape used to hold the samples.

The supplier, Sigma Aldrich, when asked about the origin of these particles responded: *"the black specks are trace amounts of insoluble magnesium and will appear in some batches of this material."* At the present time, there is no clear explanation for this contamination but it is reasoned that if it is to be found in the small expensive batches used in laboratory studies, it is likely to be present, perhaps even in far greater quantities, when $MgCl_2$ is purchased in tonnage for use in commercial magnesium production.

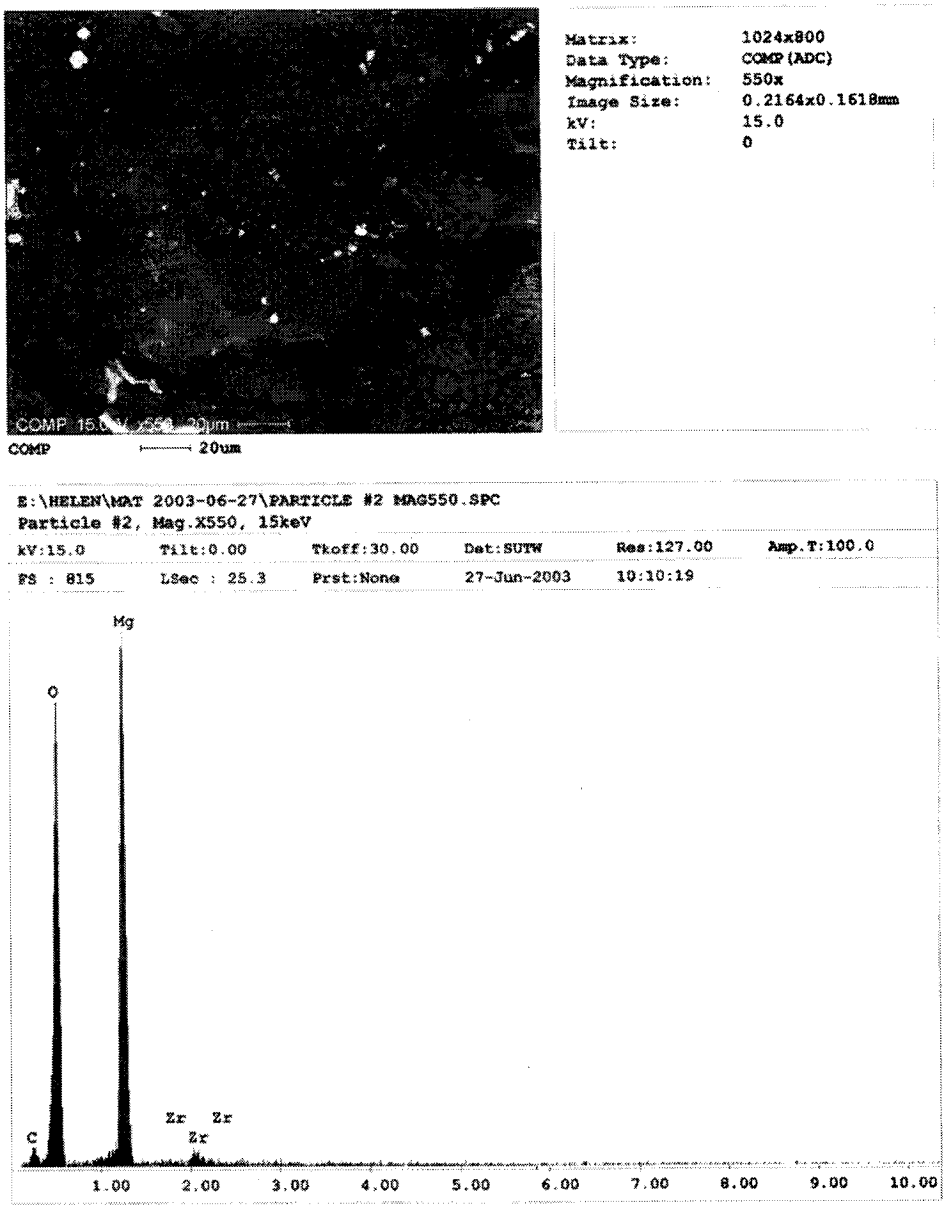

Figure 55 : EDX of black particles present in suppliers anhydrous $MgCl_2$.

THERMODYNAMIC DATA

If $T>T_{max}$, Cp at T_{max} is used for calculation

Compound	C_p (J)	Temp. (K)	Ref.[8]
$MgCO_{3(s)}$	$C_p = 731.32938 + 194820.84T^{-1} - 19273.866T^{-0.5} - 8539074.4T^{-2} - 5.5753758T^{0.5}$	298-1000	128 149
$MgO_{(s)}$	$C_p = 61.109650 - 296.199T^{-0.5} - 621154T^{-2} + 5844612T^{-3}$	298-3098	132 133
$CO_{2(g)}$	$C_p = 103.3446 - 40249.044T^{-2} + 11004.741T^{-1} - 4.74260628E-3T^{1} - 1748.2872T^{-0.5}$	298-1900	128
$CaCO_3 \cdot MgCO_{3(s)}$	$C_p = 273.8 + 2865300T^{-2} - 45578T^{-1} + 1.3125E-2T^{1} + 8.0432E-6T^{2}$	298-3000	149
$CaO_{(s)}$	$C_p = 58.791171 - 133.904T^{-0.5} - 1147146T^{-2} + 1.02978788E8T^{-3}$	298-2845	130 132
$C_{(s)}$	$C_p = 24.778075 - 2883408.3T^{-2} + 9.58723769E-4T - 39.692352T^{-0.5}$	1000-6000	128 149
$CO_{(g)}$	$C_p = 44.086320 + 20893.908T^{-1} - 11633086T^{-2} - 687.27684T^{-0.5}$	1700-6000	128
$Mg_{(g)}$	$C_p = 20.786792$	298-2200	128
$Mg_{(g)}$	$C_p = -392.90224 + 2.30226891E8T^{-2} + 2.06844598E-2T - 924952.21T^{-1}$	2200-5000	128

$MgCl_{2(l)}$	$C_p = 92.048$	660-2500	128
$MgCl_{2(s)}$	$C_p = 54.584343 - 1112119.2T^{-2} + 399.17672T^{-0.5} + 2.14212731E-2T - 2.3566724E-6T^2$	298-2000	128
$Mg_{(l)}$	$C_p = 34.309$	298-2000	128
$Cl_{2(g)}$	$C_p = 20.680767 + 0.19105767T^{-0.5} - 8299.3704T^{-1} + 316713.29T^{-2} + 591.26122T^{-0.5}$	298-1600	128
$O_{2(g)}$	$C_p = 89.681327 - 18682686T^{-2} + 95803.96T^{-1} - 1.44744488E-3T + 4126.5372T^{-0.5}$	1000-4000	128
$HCl_{(g)}$	$C_p = 13.383857 - 623137.74T^{-2} + 5347.3975T^{-1} + 1.73093249E-2T - 3.80334592E-6T^2$	298-1700	128
$H_2O_{(g)}$	$C_p = 25.78164 - 27999.319T^{-2} + 11072618T^{-1} + 1.49497163E-2T - 5.52355895E-7T^2$	298-1100	128
$MgCl_2 \cdot 6H_2O_{(s)}$	$C_p = 315.0552$	295-300	4
$MgCl_2 \cdot 4H_2O_{(s)}$	$C_p = 241.4168$	295-300	4
$MgCl_2 \cdot 2H_2O_{(s)}$	$C_p = 159.2012$	295-300	4
$MgCl_2 \cdot H_2O_{(s)}$	$C_p = 115.2692$	295-300	4
$CaCl_{2(l)}$	$C_p = 102.533$	700-3000	128
$MgOHCl_{(s)}$	$C_p = 56.0656 + 6.054248E-2T$	298-800	1

Ref. 1

"Thermochemical Properties of Inorganic Substances", I. Barin, O. Knacke, and O. Kubaschewski, Springer-Verlag, Berlin, 1977.

Ref. 4

"Selected Values of Chemical Thermodynamic Properties", National Bureau of Standards Series 270, D.D. Wagman et al., U.S. Department of Commerce, Washington, 1968-1971.

Ref. 128

"JANAF Thermochemical Tables", D.R. Stull and H. Prophet, U.S. Department of Commerce, Washington, 1985. Cp Fitted by CRCT, Montreal.

Ref. 130

A.D. Pelton, G. Eriksson and P. Wu, Coupled optimization of thermodynamic and phase diagram data; See also: P. Wu Ph.D. thesis, Ecole Polytechnique, Montreal (1992).

Ref. 132

R.G. Berman and T.H. Brown, Contrib. Miner. Petrol., vol. 89, pp. 168-183 (1985); Ibid, vol. 94, pp. 262 (1986); R.G. Berman, T.H. Brown and H.J. Greenwood, Atomic Energy of Canada Ltd., TR-377, 62 pp. (1985).

Ref. 133

I.Barin, "Thermochemical Data of Pure Substances", VCH, Weinheim, Germany (1989).(Some data may have been modified slightly from values given in this reference in order to conform to phase diagram optimizations.)

Ref. 149

S.K. Saxena, N. Chatterjee, Y. Fei and G. Shen, "Thermodynamic Data on Oxides and Silicates", Springer-Verlag, NY (1993).

REFERENCES

[1] Ullmann's Encyclopaedia of Industrial Chemistry, 5th edition, Vol A15, VCH publisher, New York, 1990, p559.

[2] Kirk-Othmer Encyclopaedia of Chemical Technology, John Wiley and sons Inc., 4th edition, V.15, 1995, pp.622-35.

[3] http://minerals.usgs.gov/minerals/pubs/commodity/magnesium/400498.pdf

[4] http://minerals.usgs.gov/minerals/pubs/commodity/aluminum/050303.pdf

[5] http://minerals.usgs.gov/minerals/pubs/commodity/magnesium/400303.pdf

[6] Meeting with Dr. Avedesian at McGill University on April 4, 2003.

[7] http://www.nrcan.gc.ca/mms/cmy/content/1995/36.pdf

[8] C.W. Bale et al., "Fact*Sage*™ Thermochemical Software and Databases", Center for Research in Computational Thermochemistry Ecole Polytechnique (University de Montréal), www.factsage.com, 2003.

[9] P. Ficara, "The Production of Anhydrous $MgCl_2$", McGill University Thesis, Montreal, Canada, 1996.

[10] http://my.noranda.com/Noranda/magnesium/Magnesium+Overview/Magnesium+Production/Electrolysis.htm

[11] G.P. Demopoulos, "Hydrochemical Processing 306-352", McGill University, Mining and Metallurgical Engineering course notes.

[12] G. J. Kipouros, "Advances in Molten Salt Chemistry", V.6, 1987, Elsevier, Amsterdam.

[13] I. Karakaya, "Electrochemical Determination of Thermodynamic Properties of Magnesium Cell Electrolyte the System $MgCl_2$ – NaCl – $CaCl_2$", McGill University Thesis, Montreal, Canada, 1985.

[14] B.R. Davis, W.T. Thompson, "Thermodynamic Properties of Magnesium Chloride Electrolytes", International Symposium on Light metals 1997 36th annual Conference of Metallurgists of CIM, Sudbury, Ontario, Canada, ISBN 919086-75-6, Aug. 1997, pp.557-66.

[15] H. Bloom, "The Chemistry of Molten Salts", W.A.Benjamin Inc., New York, 1967.

[16] B.R. Sundheim, "Fused Salts", McGraw-Hill book company, Toronto, 1964.

[17] M. Blander, "Some Calculations for a One-Dimensional Salt Mixture", J. Chem. Phys., V.34, Can 56:10794, AN 1962:10794, 1961, pp.697-8.

[18] G. Mamantov, "Molten Salts", Marcel Dekker, New York, 1969, p64.

[19] O.J. Kleppa, F.G. McCarty, "Thermochemistry of Charge – Unsymmetrical Binary Fused Halides Systems. II. Mixtures of Magnesium Chloride with the Alkali Chlorides and with Silver Chloride", J.Phys. Chem., V.70, No.4, ISSN:0022-3654, 1966, pp.1249-1255.

[20] I. Karakaya, W.T. Thompson, "A Thermodynamic Study of the System $MgCl_2$ – NaCl – $CaCl_2$", Canadian Metallurgical Quarterly, ISSN 0008-4433, V.25, No.4, 1986, pp.307-17.

[21] Kh. L. Streletes, "Electrolytic Production of Magnesium", translated by J. Schmorak, Israel Program for Scientific Translation, Keterpress Entreprises, Jerusalem, 1977.

[22] N. Kanari & I. Gaballah, "Chlorination and Carbochlorination of MgO", ISSN 1073-5615, V.30B, No3, 1999, pp.383-391.

[23] T.L Inyushkina, L.P. Petukova, V.T. Kornilova, "Solubility of MgO in Alkali Metal Chloride Melts", Russian Journal of inorganic Chemistry, V.20, No.4, 1975, pp.594-595.

[24] H.Mediaas, J.E. Vindstad, T. Oestvold, "Solubility of MgO in $MgCl_2$-NaCl-NaF Melts", Light Metals (Warrendale, Pennsylvania), ISSN:0147-0809, CAN 124:243586, AN 1996:178815, Caplus, 1996, pp.1129-37.

[25] P. Ficara, E. Chin, T. Walker, D. Laroche, E. Palumbo, C. Celik, M. Avedesian, "Magnola : A Novel Commercial Process for the Primary Production of Magnesium", CIM Bulletin V.91, No.1019, 1998, p.75.

[26] K.K. Kelley, "Energy Requirements and Equilibria in the Dehydration, Hydrolysis, and Decomposition of Magnesium Chloride", U.S. Department of the Interior Bureau of Mines, 1945.

[27] W. Moldenhauer, "The Action of Oxygen and Water on Magnesium Chloride", Ztschr.anorg.allgem.Chem., vol.51, 1906, pp.369-390.

[28] Rolando Lastra Quintero, "On the Thermodynamic Properties of Hydrates and Ammines of Magnesium Chloride", McGill University Thesis, Montreal, Canada, 1981.

[29] A. Glasner, I. Mayer, "The Thermal Hydrolysis of Metal Chlorides.III. Magnesium Chloride", Bull. Research Council Isreal, 10A, 1961, pp.17-24.

[30] Y.E.Vil'nyanskii, E.I. Savinkova, "Solid Solutions of MgOHCl in Magnesium Chloride", Journal of Applied Chemistry of U.S.S.R., V.26, No.8, Can 49:38354, 1953, pp.735-9.

[31] P. K. Dutt, R. M. Kava, D. J. Mehta, "Thermal Decomposition of Magnesium Chloride Hexahydrate", Indian J.Technol, CAN 77:55857, V.10, No.1, 1972, pp.41-2.

[32] F.H. Herbstein, M. Kapon, A. Weissman, "X-ray Diffraction as a Toll for Studying Stoichiometry and Kinetics of Solid State Thermal Decomposition Reactions. Application to the Thermal Decomposition of Bischofite $MgCl_2 \cdot 6H_2O$", Israel journal of Chemistry, V.22, 1982, pp.207-13.

[33] A. K. Galwey, G. M. Laverty, "The Thermal Decomposition of Magnesium Chloride Dihydrate", Thermochimica Acta, ISSN:0040-0631, V.138, No.1, 1989, pp.115-27.

[34] A.I. Orekhova, R.P. Lelekova, E.I. Savinkova, "Equilibrium in the Hydrolysis of Magnesium Chloride, Containing NaCl, in an Atmosphere of HCl and H_2O", Sov.Non-ferrous Met. Res., V.8, No.1, 1980, pp.40-1.

[35] A.B. Ivanov, N.M. Zuev, "Equilibria of Magnesium Chloride Hydrolysis in an Electrolyte", Zhurnal Prikladnoi Khimii, V.41, No.8, 1968, pp.1693-98.

[36] D.Laroche, B.R.Davis, K.Watson, P.Ficara, "Oxide Speciation in Magnesium Chloride Based Fused Salts", Light Metals 1999: Gateway to the 21st Century, Proceedings of the International Symposium on Light Metals, Quebec City, Qc, Canada, Aug.22-26, 1999, Coden:69BGK2, CAN 135:8079, An 2001:311795, Caplus, pp.103-9.

[37] J.E. Vindstad, H. Mediaas, T. Ostvold, "Hydrolysis of $MgCl_2$-Containing Melts", Act Chemica Scandinavica, ISSN 0904-213X, V.51, No.12, 1997, pp.1192-1200.

[38] E.I. Savinkova, R.P. Lelekova, "Equilibrium of Magnesium Chloride Hydrolysis in Chloride Melts", Zhurnal Prikladnoi Khimii, V.51, No.7, 1978, pp.1453-6.

[39] S. Boghosian, Aa. Godo, H. Mediaas, W. Ravio, T. Ostvold, "Oxide Complexes in Alkali-Alkaline-Earth Chloride Melts", Acta Chemica Scandinavica, V.45, 1991, pp.145-157.

[40] R. Combes, F. Andrade, A.Barros, H. Ferreira, "Dissociation and Solubility Variation vs pO^{2-} of some Alkaline-Earth Oxides in Molten NaCl-KCl (at 1000K)", Eletrochimica Acta., V.25, Pergamon Press Ltd., 1980, pp.371-374.

[41] E. I. Savinkova, R. P. Lelekova, V.L. Brayalovskaya, "Crystallization of MgO in a Hydrolyzed $MgCl_2$ - KCl – NaCl Melt", Zhurnal Prikladnoi Khimii, V.50, No.10, 1977, pp2155-57.

[42] Savinkova, E. I.; Lelekova, R. P.; Brayalovskaya, V. L.; Nikitina, S. A. "Determination of Carnallite (MgO,MgOHCl) Hydrolysis Products by Alkalimetric Titration." Deposited Doc. 1976, VINITI 1127-76, 7 pp.

[43] M.Lamy, "Mechanism of MgO Chlorination by HCl in a Molten Salt", McGill University Thesis, 2001.

[44] T.L, Lukmanova, E.A. Savinkova, Ya.E. Vil'nyanskii, "Chlorination of Hydrolyzed Products from Molten Carnallite", Izvestiya Vysshikh Uchebnykh Zavedenii, Tsvetnaya Metallurgiya, ISSN:0021-3438, Vol. 8, No. 6, 1965, pp. 63-8.

[45] M.Kreuh, "Conversion of MgOHCl to MgO", Research Project report, McGill University, Department of Materials Engineering, Ralph Harris, Montreal, Canada, April 2002.

[46] M.Nadler, "Procedé de Dehydration de Chloride de Magnesium Hydraté", Fr. 1476331, 1967.

[47] Chemglass Inc., 3861 N.Mill road, Vineland, New Jersey, USA, 08360, telephone # 1-800-843-1794.

[48] I.J. Roumeliotis, "Desulfurization of Inco Semi-Blister Copper", Master's Thesis McGill University, Montreal Canada, August 1998, p.42.